

พฤติกรรมด้านอุทกพลศาสตร์ของนวัตกรรมถังสัมผัสดอกอากาศแบบไร้แผ่นกั้น



นางสาวแพรวพุกุล ศิลธรรม

จุฬาลงกรณ์มหาวิทยาลัย

CHULALONGKORN UNIVERSITY

วิทยานิพนธ์นี้เป็นส่วนหนึ่งของการศึกษาตามหลักสูตรปริญญาวิศวกรรมศาสตรมหาบัณฑิต

สาขาวิชาวิศวกรรมเคมี ภาควิชาวิศวกรรมเคมี

คณะวิศวกรรมศาสตร์ จุฬาลงกรณ์มหาวิทยาลัย

ปีการศึกษา 2556

ลิขสิทธิ์ของจุฬาลงกรณ์มหาวิทยาลัย

บทคัดย่อและแฟ้มข้อมูลฉบับเต็มของวิทยานิพนธ์ตั้งแต่ปีการศึกษา 2554 ที่ให้บริการในคลังปัญญาจุฬาฯ (CUIR)

เป็นแฟ้มข้อมูลของนิสิตเจ้าของวิทยานิพนธ์ ที่ส่งผ่านทางบัณฑิตวิทยาลัย

The abstract and full text of theses from the academic year 2011 in Chulalongkorn University Intellectual Repository (CUIR) are the thesis authors' files submitted through the University Graduate School.

HYDRODYNAMIC BEHAVIOR AND GAS-LIQUID MASS TRANSFER OF NOVEL
NON-BAFFLED AIRLIFT CONTACTOR

Miss Praewpakun Sintharm



จุฬาลงกรณ์มหาวิทยาลัย

CHULALONGKORN UNIVERSITY

A Thesis Submitted in Partial Fulfillment of the Requirements
for the Degree of Master of Engineering Program in Chemical Engineering

Department of Chemical Engineering

Faculty of Engineering

Chulalongkorn University

Academic Year 2013

Copyright of Chulalongkorn University

Thesis Title	HYDRODYNAMIC BEHAVIOR AND GAS-LIQUID MASS TRANSFER OF NOVEL NON-BAFFLED AIRLIFT CONTACTOR
By	Miss Praewpakun Sintharm
Field of Study	Chemical Engineering
Thesis Advisor	Associate Professor Prasert Pavasant, Ph.D.

Accepted by the Faculty of Engineering, Chulalongkorn University in Partial
Fulfillment of the Requirements for the Master's Degree

.....Dean of the Faculty of Engineering
(Professor Bundhit Eua-arporn, Ph.D.)

THESIS COMMITTEE

.....Chairman
(Associate Professor Tharathon Mongkhonsi, Ph.D.)

.....Thesis Advisor
(Associate Professor Prasert Pavasant, Ph.D.)

.....Examiner
(Associate Professor Siriporn Damrongsakkul, Ph.D.)

.....External Examiner
(Nawin Viriya-empikul, D.Eng.)

แพรวพกุล ศิลธรรม : พฤติกรรมด้านอุทกพลศาสตร์ของนวัตกรรมถังสัมผัสอากาศยกแบบไร้แผ่นกั้น. (HYDRODYNAMIC BEHAVIOR AND GAS-LIQUID MASS TRANSFER OF NOVEL NON-BAFFLED AIRLIFT CONTACTOR) อ.ที่ปรึกษาวิทยานิพนธ์หลัก: รศ. ดร.ประเสริฐ ภูวสันต์, 122 หน้า.

งานวิจัยนี้ศึกษาพฤติกรรมทางอุทกพลศาสตร์และการถ่ายเทมวลสารของนวัตกรรมถังสัมผัสอากาศยกแบบไร้แผ่นกั้นระหว่างส่วนของเหลวไหลขึ้นและส่วนของเหลวไหลลงที่มีการไหลวนแบบภายใน ถึงที่ศึกษามี 2 รูปแบบ คือ แบบแบนและแบบกรวย โดยแบบแบนศึกษาที่ความกว้างของถังเท่ากับ 20, 30, 40 และ 50 เซนติเมตร และแบบกรวยที่มุม 30° , 45° และ 53° ตัวแปรที่ศึกษา คือ อัตราการให้อากาศและระดับความสูงของน้ำก่อนให้อากาศ (สูง 40, 50, 60 เซนติเมตร และที่ความสูงเท่ากับปริมาตร 100 ลิตร) จากผลการศึกษาพบว่า เมื่ออัตราการให้อากาศเพิ่มมากขึ้นจะส่งผลให้ค่าทางอุทกพลศาสตร์ ซึ่งได้แก่ ปริมาณก๊าซในระบบ การกระจายตัวของขนาดฟองอากาศ ความเร็วของของเหลวไหลลง และการถ่ายเทมวลสาร มีค่าเพิ่มมากขึ้น สำหรับพื้นที่ของของเหลวไหลขึ้นและพื้นที่ของของเหลวไหลลงจะไม่แปรผันตามอัตราการให้อากาศและระดับน้ำก่อนให้อากาศ แต่จะแปรผันตามความกว้างของถังสำหรับถังแบบแบน ในขณะที่ถังแบบกรวยจะแปรผันตามมุมของกรวย การกระจายตัวของขนาดฟองอากาศจะแสดงผลได้เฉพาะในถังแบบแบนเพราะวิธีการวัดขนาดฟองอากาศด้วยการถ่ายภาพไม่สามารถใช้ได้ในถังแบบกรวย ที่อัตราการให้อากาศต่ำ (น้อยกว่า 0.4 เซนติเมตรต่อวินาที) ฟองอากาศจะมีขนาดเล็ก (เส้นผ่านศูนย์กลางประมาณ 0.3-0.4 เซนติเมตร) ลักษณะการกระจายตัวของขนาดฟองอากาศเป็นแบบทวิฐานนิยม เมื่ออัตราการให้อากาศสูง (มากกว่า 1 เซนติเมตรต่อวินาที) ฟองอากาศจะมีขนาดใหญ่ (เส้นผ่านศูนย์กลางประมาณ 0.5-0.6 เซนติเมตร) และมีลักษณะการกระจายตัวแบบฐานนิยมกว้าง เส้นผ่านศูนย์กลางเฉลี่ยของขนาดฟองอากาศประมาณ 0.2-0.8 เซนติเมตร ปริมาณก๊าซในระบบและสัมประสิทธิ์การถ่ายเทมวลสารของถังแบบแบนจะมีค่าเพิ่มมากขึ้นตามความกว้างของถังจากความกว้าง 30 เซนติเมตร ไปยัง 50 เซนติเมตร แต่ที่ถังกว้าง 20 เซนติเมตร ค่าต่างๆ จะมีค่าสูงเทียบเท่ากับค่าของถังกว้าง 50 เซนติเมตรและมีค่าสูงที่สุดเมื่ออัตราการให้อากาศเท่ากับ 0.6 เซนติเมตรต่อวินาที โดยค่าสูงสุดของปริมาณก๊าซในส่วนของเหลวไหลขึ้น ปริมาณก๊าซในส่วนของเหลวไหลลง ปริมาณก๊าซรวมในระบบและสัมประสิทธิ์การถ่ายเทมวลสารมีค่าเท่ากับ 0.10, 0.075, 0.08 และ 0.014 ต่อวินาที ตามลำดับ นอกจากนี้ในถังกรวย พบว่า ค่าปริมาณก๊าซในส่วนของเหลวไหลขึ้น ปริมาณก๊าซในส่วนของเหลวไหลลง ปริมาณก๊าซรวมในระบบและสัมประสิทธิ์การถ่ายเทมวลสารจะมีค่าลดลงเมื่อมุมกรวยเพิ่มมากขึ้น ค่าสูงสุดของปริมาณก๊าซในส่วนของเหลวไหลขึ้น ปริมาณก๊าซในส่วนของเหลวไหลลง และปริมาณก๊าซรวมในระบบเท่ากับ 0.09, 0.06 และ 0.07 ตามลำดับ ส่วนสัมประสิทธิ์การถ่ายเทมวลสารของถังชนิดกรวยจะมีค่าใกล้เคียงกันในทุกสภาวะการทดลองและจะมีค่าเพิ่มมากขึ้นเมื่ออัตราการให้อากาศเพิ่มขึ้น สำหรับความสูงของระดับน้ำก่อนให้อากาศจะส่งผลเฉพาะค่าความเร็วของของเหลวไหลลงเท่านั้น นั่นคือ เมื่อความสูงของระดับน้ำก่อนให้อากาศเพิ่มขึ้นจะส่งผลให้ความเร็วของของเหลวไหลลงเพิ่มขึ้น ซึ่งความเร็วของของเหลวไหลลงสูงสุดสำหรับถังแบบแบนและกรวยเท่ากับ 27 และ 24 เซนติเมตรต่อวินาที ตามลำดับ

ภาควิชา วิศวกรรมเคมี

ลายมือชื่อนิสิต

สาขาวิชา วิศวกรรมเคมี

ลายมือชื่อ อ.ที่ปรึกษาวิทยานิพนธ์หลัก

ปีการศึกษา 2556

5470316621 : MAJOR CHEMICAL ENGINEERING

KEYWORDS: HYDRODYNAMIC / MASS TRANSFER / AIRLIFT CONTACTOR / FLAT PANEL / CONE

PRAEWPAKUN SINTHARM: HYDRODYNAMIC BEHAVIOR AND GAS-LIQUID MASS TRANSFER OF NOVEL NON-BAFFLED AIRLIFT CONTACTOR. ADVISOR: ASSOC. PROF. PRASERT PAVASANT, Ph.D., 122 pp.

This work purposed to study hydrodynamic behavior and gas-liquid mass transfer of novel non-baffle airlift contactors in which the fluid cyclic flow pattern was induced without the need of physical partition between riser and downcomer. Two geometries were examined, i.e. flat panel and cone bottom cylindrical airlifts. The flat panel of various widths, i.e. at 20, 30, 40, and 50 cm and the cone of various angles of bottom cone, i.e. at 30° , 45° and 53° were employed as a model study. The parameters for analysis were aeration rate and unaerated liquid height (40, 50, 60 cm and at volume 100 L). Results showed that most hydrodynamic parameters, i.e. riser gas-holdup, downcomer gas-holdup, overall gas-holdup, bubble size, downcomer liquid velocity and mass transfer ($k_L a$) increased with aeration rate. Riser and downcomer cross sectional area did not depend on air flow rate and unaerated liquid height, but did depend on the width of contactor for flat panel and angle of cone bottom for flat plate and cone geometries, respectively. Bubbles size distribution could only be observed in flat panel configuration as the employed photographic technique could not be used accurately with the cone bottom airlift. At low u_{sg} (<0.4 cm/s), bubble sizes were small (0.3-0.4 cm) and presented in bimodal distribution. The high air flow rate ($u_{sg} > 1$ cm/s) bubble sizes were large (0.5-0.6 cm) and with a broader distribution. Bubble Sauter mean diameter was within the range of 0.2-0.8 cm. Flat panel showed that riser gas-holdup, downcomer gas-holdup, overall gas-holdup and $k_L a$ increased with the width of contactor from 30 to 50 cm, whereas the contactor with the width of 20 cm exhibited similar behavior with those of 50 cm. The maximum values of riser gas-holdup, downcomer gas-holdup, overall gas-holdup and $k_L a$ were 0.10, 0.075, 0.08 and 0.014 1/s, respectively. On the other hand, it was demonstrated that riser gas-holdup, downcomer gas-holdup and overall gas-holdup from the cone geometry decreased when the angle of bottom increased. The maximum values of riser gas-holdup, downcomer gas-holdup and overall gas-holdup were 0.09, 0.06 and 0.07. The $k_L a$ of the cone geometry only depended on air flow rate and not on other design parameters. The unaerated liquid height had strong effect on downcomer liquid velocity. The maximum of downcomer liquid velocity in the flat panel and cone geometries were 27 and 24 cm/s, respectively.

Department: Chemical Engineering

Student's Signature

Field of Study: Chemical Engineering

Advisor's Signature

Academic Year: 2013

ACKNOWLEDGEMENTS

My thesis was finished and completed because of assistance from many people. Firstly, I would like to express appreciations to Associate Professor Dr. Prasert Pavasant who is the best advisor. He gives me to opportunity to do novel project that provide new acknowledgements for my life. I am extremely grateful to him for his suggestions, good support and his concentration onto my work.

I would like to thank my thesis committee: Associate Professor Dr. Tharathon Mongkhonsi, Associate Professor Dr. Siriporn Damrongsakkul and Dr. Nawin Viriya-empikul for their suggestions and useful knowledges.

I would like to appreciations the financial supports from PTT Research and Technology Institute.

Special thanks to people in safety and environment lab group at chemical engineering faculty at Chulalongkorn University, Miss Watadta Ritcharoen and Mr. Puchong Sri ouam for assistances and suggestions. Wonderful friends, Miss Sudarat Phuklang, Miss Titimat Sukhsawatsak, Miss Hathaichanok Rodrakhee, Miss Patthama Sang and Mr. Eakkachai Khongkasem for friendship, helping me setup experiments and going back home with me at night. Last, thanks for their smiles and laughs that make me happy all times.

Most of all, I would like to acknowledge my parents and my sister for everything that support me in master degree learning. They give encouragement, inspiration, understanding and believing in me. All of them make me to finish this thesis. Finally, thanks for their precious love and good things in my life.

CONTENTS

	Page
THAI ABSTRACT	iv
ENGLISH ABSTRACT	v
ACKNOWLEDGEMENTS	vi
CONTENTS	vii
LIST OF FIGURES	x
LIST OF TABLES	xiv
CHAPTER I INTRODUCTION.....	1
1.1 Motivations.....	1
1.2 Objectives.....	1
1.3 Scopes of this work.....	1
CHAPTER II BACKGROUNDS & LITERATURE REVIEW	2
2.1 Airlift contactors.....	2
2.1.1 Types of airlift contactors	3
2.1.2 Advantages of airlift contactors	3
2.2 Gas-liquid hydrodynamics and mass transfer	4
2.2.1 Hydrodynamics behavior.....	4
2.2.1.1 Gas holdup.....	4
2.2.1.2 Liquid velocity.....	6
2.2.2 Gas-liquid mass transfer	7
CHAPTER III MATERIALS AND METHODS	13
3.1 Summary of scope and methodology	13
3.2 Experimental setup	14
3.2.1 Various designs angle of cone and width of flat panel.....	14
3.2.2 Determination of virtual riser and downcomer cross-section area.....	14
3.2.3 Effect of liquid height	15
3.3 Measurements.....	15
3.3.1 Bubble size.....	15

	Page
3.3.2 Gas holdup.....	16
3.3.3 Liquid velocity.....	16
3.3.4 Overall volumetric gas-liquid mass transfer coefficient	17
3.4 Calculations.....	18
3.4.1 Riser and downcomer cross section area.....	18
3.4.2 Bubble size and distribution.....	19
3.4.3 Gas holdup.....	19
3.4.4 Liquid velocity	22
3.4.5 Overall volumetric gas-liquid mass transfer coefficient	23
3.4.6 Unit of aeration.....	23
CHAPTER IV RESULTS AND DISCUSSION	32
4.1 Characteristics of novel non-baffled flat panel airlift contactors (NB-FP-ALCs) .	32
4.2 Effect of width of contactor (w) and unaerated liquid height (h) on the performance of NB-FP-ALCs	32
4.2.1 Riser and downcomer cross-sectional area.....	33
4.2.2 Bubble size distributions and bubble size diameters	33
4.2.3 Riser, downcomer and overall gas-holdups.....	34
4.2.4 Downcomer liquid velocity.....	36
4.2.5 Overall gas-liquid volumetric mass transfer.....	37
4.3 Characteristics of non-baffled cone airlift contactors (NB-C-ALCs).....	38
4.4 Effect of the angle of bottom (B) and unaerated liquid height (h) on the performance of NB-C-ALCs	39
4.4.1 Riser and downcomer cross-sectional area.....	39
4.4.2 Riser, downcomer and overall gas-holdup.....	40
4.4.3 Downcomer liquid velocity.....	40
4.4.4 Overall gas-liquid volumetric mass transfer.....	41
4.5 Empirical models for hydrodynamic and gas-liquid mass transfer in NB-FP-ALCs and NB-C-ALCs	41

	Page
CHAPTER V CONCLUSIONS & RECOMMENDATIONS	66
5.1 Conclusions	66
5.2 Contributions	66
5.3 Recommendations.....	67
REFERENCES	68
VITA.....	122



จุฬาลงกรณ์มหาวิทยาลัย
CHULALONGKORN UNIVERSITY

LIST OF FIGURES

	Page
Figure 2.1 Configurations of pneumatic reactors: (a) bubble column and (b) airlift contactor	9
Figure 2.2 The type of airlift reactors: (a) internal loop airlift contactor (b) external loop airlift contactor	9
Figure 3.1 Outline of experiments and analysis in this work.....	13
Figure 3. 2 Schematic of novel non-baffled flat panel airlift contactors.....	26
Figure 3.3 Novel non-baffled flat panel airlift contactors.....	27
Figure 3.4 Schematic of circular columns with cone bottom airlift contactors (a) angle of bottom 30° (b) angle of bottom 45° (c) angle of bottom 53°	28
Figure 3.5 circular columns with cone bottom airlift contactors (a) angle of bottom 30° (b) angle of bottom 45° (c) angle of bottom 53°	29
Figure 3. 6 Schematic diagram of experiments	30
Figure 3.7 Example of finding flow directions in airlift contactor.....	31
Figure 3.8 Example of photographs of bubbles from photographic technique	31
Figure 4.1 Flow directions in NB-FP-ALCs	43
Figure 4.2 Flow directions diagram in NB-FP-ALCs at width of contactor 50 cm with unaerated liquid height 60 cm	44
Figure 4.3 Area of riser in NB-FP-ALCs with different widths and unaerated liquid heights.....	45
Figure 4.4 Area of downcomer in NB-FP-ALCs with different widths and unaerated liquid heights	45
Figure 4.5 Downcomer to riser cross sectional area ratios in NB-FP-ALCs with different widths and unaerated liquid heights.....	46
Figure 4.6 Frequency distribution of bubble sizes in NB-FP-ALCs width 20 cm at unaerated liquid height 40 cm	46
Figure 4.7 Frequency distribution of bubble sizes in NB-FP-ALCs width 20 cm at unaerated liquid height 50 cm	47

	Page
Figure 4.8 Frequency distribution of bubble sizes in NB-FP-ALCs width 20 cm at unaerated liquid height 60 cm	47
Figure 4.9 Frequency distribution of bubble sizes in NB-FP-ALCs width 30 cm at unaerated liquid height 40 cm	48
Figure 4.10 Frequency distribution of bubble sizes in NB-FP-ALCs width 30 cm at unaerated liquid height 50 cm	48
Figure 4.11 Frequency distribution of bubble sizes in NB-FP-ALCs width 30 cm at unaerated liquid height 60 cm	49
Figure 4.12 Frequency distribution of bubble sizes in NB-FP-ALCs width 40 cm at unaerated liquid height 37 cm	49
Figure 4.13 Frequency distribution of bubble sizes in NB-FP-ALCs width 40 cm at unaerated liquid height 40 cm	50
Figure 4.14 Frequency distribution of bubble sizes in NB-FP-ALCs width 40 cm at unaerated liquid height 50 cm	50
Figure 4.15 Frequency distribution of bubble sizes in NB-FP-ALCs width 40 cm at unaerated liquid height 60 cm	51
Figure 4.16 Frequency distribution of bubble sizes in NB-FP-ALCs width 50 cm at unaerated liquid height 35 cm	51
Figure 4.17 Frequency distribution of bubble sizes in NB-FP-ALCs width 50 cm at unaerated liquid height 40 cm	52
Figure 4.18 Frequency distribution of bubble sizes in NB-FP-ALCs width 50 cm at unaerated liquid height 50 cm	52
Figure 4.19 Frequency distribution of bubble sizes in NB-FP-ALCs width 50 cm at unaerated liquid height 60 cm	53
Figure 4.20 Frequency distribution of bubble sizes in NB-FP-ALCs at air flow rate 0.30 - 0.38 vvm with different widths of contactor and various unaerated liquid heights.....	53
Figure 4.21 Average bubble diameter (d_{Bs}) in NB-FP-ALCs with different widths and unaerated liquid heights	54
Figure 4.22 Section in NB-FP-ALCs	55

	Page
Figure 4.23 Gas-holdup in riser of NB-FP-ALCs with different widths and unaerated liquid heights	56
Figure 4.24 Gas-holdup in downcomer of NB-FP-ALCs with different widths and unaerated liquid heights	56
Figure 4.25 Overall gas-holdup in NB-FP-ALCs with different widths and unaerated liquid heights	57
Figure 4.26 Downcomer liquid velocity in NB-FP-ALCs with different widths and unaerated liquid heights	57
Figure 4.27 $k_L a$ in NB-FP-ALCs with different widths and unaerated liquid heights	58
Figure 4.28 Specific interfacial area (a) in NB-FP-ALCs with different widths and unaerated liquid heights	58
Figure 4.29 Overall gas-liquid mass transfer coefficient (k_L) in NB-FP-ALCs with different width of contactors and unaerated liquid heights	59
Figure 4.30 Flow directions in NB-C-ALCs	60
Figure 4.31 Flow directions diagram of NB-C-ALCs at the angle of bottom 30° with unaerated liquid height 50 cm and air flow rate 0.15 vvm	61
Figure 4.32 Area of riser in NB-C-ALCs with different the angles of bottom and unaerated liquid heights	62
Figure 4.33 Area of downcomer in NB-C-ALCs with different the angles of bottom and unaerated liquid heights	62
Figure 4.34 A_d/A_r ratio in NB-C-ALCs with different the angles of bottom and unaerated liquid heights	63
Figure 4.35 Riser gas-holdup in NB-C-ALCs with different the angles of bottom and unaerated liquid heights	63
Figure 4.36 Downcomer gas-holdup in NB-C-ALCs with different the angles of bottom and unaerated liquid heights	64
Figure 4.37 Overall gas-holdup in NB-C-ALCs with different the angles of bottom and unaerated liquid heights	64
Figure 4.38 Downcomer liquid velocity in NB-C-ALCs with different the angles of bottom and unaerated liquid heights	65

Figure 4.39 $k_L a$ in NB-C-ALCs with different the angles of bottom and unaerated liquid heights..... 65



LIST OF TABLES

	Page
Table 2. 1 Literature review	10
Table 3.1 Volume of flat panel at different unaerated liquid heights	25
Table 3.2 Volume of cone at different unaerated liquid heights.....	25
Table 5.1 Summary the hydrodynamic and mass transfer in airlift contactors	67



CHAPTER I

INTRODUCTION

1.1 Motivations

Airlift reactors are one type of pneumatic reactors which have several advantages over other types of pneumatic reactors such as simple construction, low energy requirement, low shear, good recirculation and uniform flow pattern. These make airlift reactors widely applied in many industries e.g. chemical, water treatment, pharmaceuticals, fermentation particularly in biotechnologies for cell culture cultivation.

Typical airlifts employ either draft tube or separation plate installed inside the column to physically separate riser from downcomer. This extra partitioning component has generated some drawbacks such as the installation, cleaning, maintenance, not to mention the higher cost of construction. Due to these problems, a novel airlift system “Non-baffled airlift contactor” has been developed at the Department of Chemical Engineering, Faculty of Engineering, Chulalongkorn University. This novel system was designed such that a pattern cyclic movement of fluid can be induced without having to install the draft tube or separating plate. Preliminary examination indicates that this configuration works quite well as airlift system. This work aims to study the hydrodynamics and mass transfer of this novel contactor to generate necessary design information for such system.

1.2 Objectives

The objective of this work is to investigate hydrodynamics (gas holdup and liquid velocity) and mass transfer characteristics of novel non-baffled airlift contactors.

1.3 Scopes of this work

- The cone and flat panel airlift contactors are examined in this work.
- The air flow rate is controlled at 0.1 to 0.3 vvm (gas volume flow per unit of liquid volume per minute).
- Only gas-liquid systems are examined where water is liquid phase and air is the gas phase.
- Experiments are performed with outdoor conditions.

CHAPTER II

BACKGROUNDS & LITERATURE REVIEW

2.1 Airlift contactors

Airlift contactors cover a wide range of gas-liquid or gas-liquid-solid pneumatic contacting devices characterized by fluid circulation in defined cyclic pattern (Chisti, 1989). Airlift contactors do not have mechanically agitated device, mixing in airlift system arise from pneumatically agitated by a stream of air or gas that is usually injected at the bottom of contactors. Airlift contactors have fix flow patterns of fluid circulation that are different from bubble columns (another type of pneumatic contactors) which have random flow of fluid in system (show in figure 2.1(a)). Airlift contactors comprise three sections with different flow patterns as described below: (Schematic flow directions shown in Figure 2.1(b))

Riser: Gas is injected in this section, and therefore contains the highest gas content. The fluid density in this section is lower than other section, which makes fluid move up to the top of riser by gas lift momentum transfer and the buoyant force due to the different fluid density between riser and downcomer.

Gas-liquid separator: The section locates at the top of riser and downcomer. Fluid from riser enters into this section and spends some time in separator after that it leaves to downcomer. Some of the gas bubbles disengage from the fluid at the top of the contactor. Design of this section could have gas residence time in this section longer than times required for the gas bubble disengagement (Chisti, 1989).

Downcomer: As most gas bubbles in fluid leaves from separator the density of fluid becomes higher and flows downward in the downcomer section and recirculates back to the riser again along with fresh air/gas bubbles at the bottom of the contactor.

Apparently the various fixed flow patterns in the airlift are induced from the difference of fluid densities in each section and result in a circulation pattern in the system, this characteristic of airlift reactor is not found in other types of pneumatic contactors.

2.1.1 Types of airlift contactors

There are two types of airlift contactors, internal loop and external loop (as shown in Figure 2.2).

(1) Internal loop airlift contactors (ILALR) contain riser and downcomer in a single column, each section separate by installation of draft tube in the cylindrical column or by tightly fitting vertical baffle in rectangular contactors.

(2) External loop airlift contactors (ELALR) consist of two or more columns for riser and downcomer, and these are connected by horizontal conduits at the top and bottom sections.

2.1.2 Advantages of airlift contactors

Airlift contactors have been widely applied in biotechnology and multiphase chemical reactions particularly those that do not require high mass transfer rate (Lu *et al.*, 2000). Some of advantages of airlift over are another kind of contactors (bubble columns and stirred tanks), are listed below (Choi *et al.*, 1996, Luo *et al.*, 2011, Chisti, 1989) :

- Simple construction
- Low power consumption
- Good mixing and circulation
- Homogeneous distribution of hydrodynamic shear
- Relatively high mass transfer efficiency
- Reducing contamination of seals
- Low capital cost
- Low shear stress
- Well defined flow pattern
- Controllable liquid circulation rate
- Mild and uniform mixing
- Better suited to suspending solid

2.2 Gas-liquid hydrodynamics and mass transfer

The important variables that indicate behavior of airlift contactors are gas holdup, liquid velocity and gas-liquid mass transfer. The relationships between the various variables are necessary for design and scale up of airlift system. Details of hydrodynamic and gas-liquid mass transfer are discussed below.

2.2.1 Hydrodynamics behavior

2.2.1.1 Gas holdup

The essential parameter for design airlift contactors is the volume fraction of the gas-phase in the gas-liquid that is known as the gas void fraction or the gas holdup. In generally, the gas hold up in riser is higher than downcomer. The gas hold up can be used to indicate the potential mass transfer in reactors, whereby the large gas hold up indicates the large gas-liquid interfacial area (provided similar bubble sizes). Moreover, the difference in gas hold up between riser and downcomer indicates the driving force of liquid circulation in system. The overall gas holdup (\mathcal{E}) is the ratio between the volume of gas phase and the total volume of contactor which can be expressed as:

$$\mathcal{E} = \frac{V_G}{V_G + V_L} \quad 2.1$$

where: V_G is the gas volume

V_L is the liquid volume.

The gas holdups are different in each parts of airlift contactors (riser, gas-liquid separator and downcomer). In general, gas holdups are described using three quantities, i.e. overall gas holdup, riser gas holdup and downcomer gas hold up, they can be correlated as follows:

$$\mathcal{E} = \frac{A_r \mathcal{E}_r + A_d \mathcal{E}_d}{A_r + A_d} \quad 2.2$$

where: \mathcal{E}_r is the riser gas holdup

\mathcal{E}_d is the downcomer gas holdup

A_r is the riser cross sectional area

A_d is the downcomer cross sectional area.

The overall gas holdup cannot be determined directly, they can be determined from the volume expansion method where

$$\epsilon_o = 1 - \frac{h_u}{h_A} \quad 2.3$$

where: ϵ_o is the overall gas holdup

h_u is the unaerated liquid height

h_A is the dispersed liquid height.

Riser and downcomer gas holdups can be determined from the pressure drop measured from the two side-ports of the column where

$$\epsilon_G = 1 - \frac{\Delta Z}{\Delta H} \quad 2.4$$

where: ΔZ is the pressure difference of defined liquid level

ΔH is a distance of liquid level in the airlift column.

Table 2.1 summarizes literature of hydrodynamics and mass transfer in ELALR and ILALR in various conditions.

In summary, literatures conclude that increasing the superficial gas velocity (u_{sg}) increased gas holdup. The geometric design of airlift contactors had significant influence on gas holdup, i.e. gas holdup decreased with an increase in downcomer and riser cross section area (A_d/A_r) at the same superficial gas velocity (Lu *et al.*, 2000, Luo *et al.*, 2011, Korpijarvi *et al.*, 1999). This was because a change in the ratio of A_d/A_r changed the liquid and gas resident time in each part of reactor. A small diameter of draft tube (large A_d/A_r), although induced high riser liquid velocity, imposed high flow resistances and allowed a short time for gas bubbles in riser. Thus low liquid circulation velocity was resulted and this generally let to low, gas holdup in downcomer.

As for the large scale airlift, the gas hold up normally increases with an increase in the superficial gas velocity for all scale reactors (Masry *et al.*, 1998, (Juraščík *et al.*, 2006). Scale influence on gas holdup were investigated by Blazej *et al.* (2004). They found the gas holdup driving force ($\epsilon_r - \epsilon_d$) was important only for lower gas flow rate but high gas flow rate, the circulation velocity was governed by friction of contactor wall. To provide higher circulation velocities (shorter mixing times) and a better distribution of the gas phase (higher gas hold-up), it was suitable

to use larger contactor volumes to avoid unfavourable influences of the gas hold-up reduction due to wall friction.

2.2.1.2 Liquid velocity

Liquid velocity is one of the important parameters for the design of airlift system. This parameter, describes both liquid velocities in riser and downcomer. Liquid velocity can indicate momentum transfer from the gas input to the system and difference fluid densities between riser and downcomer that forces the fluid in the riser to move up and move down in downcomer and induce the liquid circulation in system. Liquid velocity is measured in terms of linear liquid velocity defined as:

$$v_i = \frac{L_i}{t} \quad 2.5$$

where: v_i is liquid velocity

L_i is the liquid path length

t is times for liquid movement.

i is riser or downcomer

Generally, rate of gas input to airlift system is can be related to superficial liquid velocity (u_L) calculated based on the empty column area. The superficial liquid velocity and actual liquid velocity in riser and downcomer can be related as:

$$v_r = \frac{u_{L,r}}{1 - \epsilon_r} \quad 2.6$$

$$v_d = \frac{u_{L,d}}{1 - \epsilon_d} \quad 2.7$$

where: v_r is actual linear liquid velocities in riser

v_d is actual linear liquid velocities in downcomer

$u_{L,r}$ is superficial liquid velocities in riser

$u_{L,d}$ is superficial liquid velocities in downcomer

The relationship between the riser and downcomer of superficial liquid velocities can be formulated as follows:

$$u_{L,r}A_r = u_{L,d}A_d \quad 2.8$$

Literatures (shown in Table 2.1) suggest that an increase in superficial gas velocity increases the liquid velocity (Freitas *et al.*, 1999, Kochbeck & Hempel, 1994, Šimčík *et al.*, 2011). Flow regime has significant effects on liquid velocity. It was reported that liquid velocity in downcomer increased rapidly in the homogenous flow regime, while only slightly increased in the heterogeneous flow regime (Blažej *et al.*, 2004, Luo *et al.*, 2011). Because the high superficial gas velocity in heterogeneous created high friction loss, this turned to reduce liquid velocity. Another reason was that the heterogeneous flow regime contained more large bubbles that could not move down in downcomer due to their high terminal velocity.

At the same superficial gas velocity, the riser liquid velocity increased with an increase in the ratio between downcomer and riser cross section area (A_d/A_r). This was because a smaller riser area normally induced a faster liquid velocity in riser, however, this ended up with a much lower gas holdup and lower downcomer liquid velocity (Wongsuchoto & Pavasant, 2004, Kochbeck & Hempel, 1994). As an overall observation, the circulation rate also decreased with an increase in A_d/A_r . Heijnen *et al.* (1997) concluded that a higher liquid velocity was obtained from the larger scale of contactor because of the lower wall friction as a result of lower wall to volume ratio.

2.2.2 Gas-liquid mass transfer

Gas-liquid mass transfer is among the most important factors for in the design of bioreactors. Generally, the two-film theory is used for describe mass transfer between the two phases. The mechanisms of gas transfer to liquid can be described into four steps:

1. the gas transported from inside the bubble to gas film
2. the gas transferred from the gas film to the gas-liquid interface
3. the gas transferred from the gas-liquid interface to the liquid film
4. the transport in the bulk liquid

The mass transfer resistance on the gas side is much lower than that in the liquid side, and the mass transfer resistance is only controlled by the resistance of the liquid film.

The volumetric mass transfer coefficient ($k_L a$) is the rate of gas transfer through the gas-liquid interface per unit liquid volume and per unit driving force. The $k_L a$ combine two quantities, k_L is a gas-liquid mass transfer coefficient and a is specific surface area. The k_L is related to the gas side and liquid side mass transfer coefficient K_g and K_L through the Henry's law constant (He):

$$\frac{1}{k} = \frac{1}{K_L} + \frac{1}{HeK_G} \quad 2.9$$

For oxygen, K_G is larger than K_L so that we can neglect the second term of the right side of Equation 2.9 and reduces $k_L \approx K_L$. In fact k_L and a are difficult to determine separately, and they are more common to be evaluated by:

$$\frac{dC_L}{dt} = k_L a (C_L^* - C_L) - r_{O_2} \quad 2.10$$

where: $k_L a$ is the overall volumetric gas-liquid mass transfer coefficient

C_L is dissolved oxygen concentration

C_L^* is dissolved oxygen concentration in equilibrium with partial pressure of oxygen in air

r_{O_2} is the rate of oxygen used per unit mass

In the system without reactions, r_{O_2} disappeared and Equation 2.9 became

$$\frac{dC_L}{dt} = k_L a (C_L^* - C_L) \quad 2.11$$

From the literatures review, the volumetric oxygen mass transfer coefficient increased with an increase in superficial gas velocity. When A_d/A_r increased $k_L a$ decreased because liquid in riser moved quite fast and there were less contacting time between gas bubbles and liquid and therefore lower energy transfer (Hsiun & Wu, 1995, Littlejohns & Daugulis, 2009).

Masry *et al.* (1998) investigated the three external loop airlift contactors different ratios of downcomer to riser area (A_d/A_r) (i.e. A_d/A_r 0.25 implies the smaller reactor, A_d/A_r 0.44 implies the medium reactor and A_d/A_r 1 implies the larger reactor). The volumetric gas-liquid mass transfer coefficient ($k_L a$) was found to decrease as the reactor was scaled-up and liquid circulation velocity increased. Increasing A_d/A_r increased the riser liquid velocity, shortened the time the bubbles spent in the riser thus decreases the gas hold-up in the riser. This in effect decreased the interfacial

area available for mass transfer and hence lowered the volumetric gas-liquid mass transfer coefficient.

For scale up of internal-loop airlift reactors, Jurascik *et al.*(2006) found that $k_L a$ increased with increasing superficial gas velocity in all scale reactors (12, 40 and 195 L).

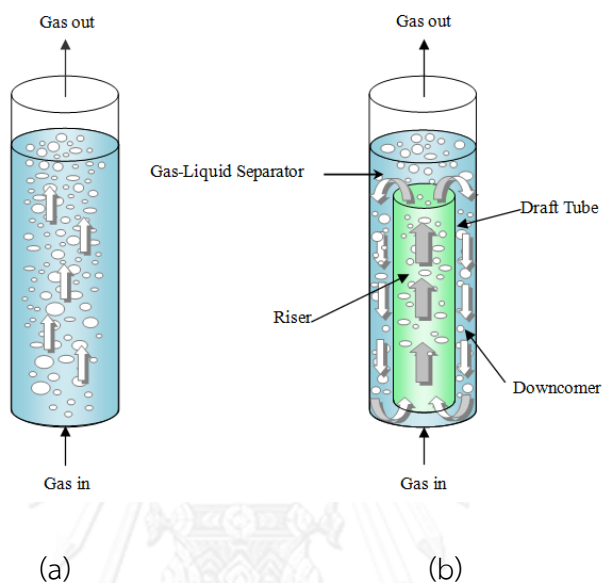


Figure 2.1 Configurations of pneumatic reactors: (a) bubble column and (b) airlift contactor (Krichnavaruk *et al.*, 2005)

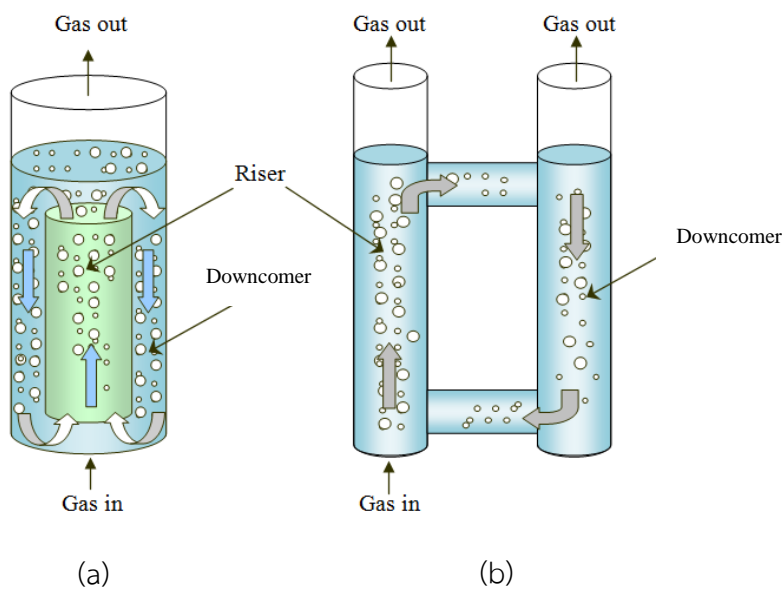


Figure 2.2 The type of airlift reactors: (a) internal loop airlift contactor (b) external loop airlift contactor (Krichnavaruk *et al.*, 2005)

Table 2. 1 Literature review

Author (year)	Type of contactors	Details	volume (L)	h (m)	D (m)	L _c (m)	A _g /A _l (-)	u _{sp} (cm/s)	V _r (cm/s)	V _d (cm/s)	riser gas holdup (-)	downcomer gas holdup (-)	overall gas holdup (-)	k ₀ (1/s)		
Korpajarvi et al. (1999)	ILALR	-	15	1.25	-	-	0.592	1-6	-	-	0.040-0.135	-	-	-	-	
			15	1.25	-	-	1.225	1-6	-	-	0.047-0.140	-	-	-	-	
			15	1.25	-	-	2.703	1-6	-	-	0.030-0.100	-	-	-	-	
			15	1.25	-	-	7.143	1-6	-	-	0.016-0.065	-	-	-	-	
Freitas et al. (1999)	ELALR	-	60	1.28	-	-	0.10	3-17	12-19	-	0.08-0.21	-	-	-	-	
			60	2.07	-	-	4.25	3-17	30-48	-	0.05-0.23	-	-	-	-	
Wu et al. (1992)	ILALR	-	15	1.13	-	-	3.000	0.3-6.0	-	-	-	-	-	-	0.0075-0.0045	
			15	1.13	-	-	1.642	0.3-6.0	-	-	-	-	-	-	0.0085-0.0044	
			15	1.13	-	-	1.087	0.3-6.0	-	-	-	-	-	-	0.0090-0.0042	
			15	1.13	-	-	0.563	0.3-6.0	-	-	-	-	-	-	0.0095-0.0037	
Kockbeck et al. (1994)	ILALR,	-	56	1.90	-	-	0.060	1-7	2.5-6.0	-	-	-	-	-	-	
			56	1.90	-	-	0.057	1-7	3.5-6.5	-	-	-	-	-	-	
			56	1.90	-	-	0.101	1-7	6.0-13.5	-	-	-	-	-	-	-
			56	1.90	-	-	0.156	1-7	10.0-19.5	-	-	-	-	-	-	-
Kawalec and Holowacz (1998)	ILALR	-	49	0.52	-	-	0.72	0.6-8	18-52	-	0.023-0.142	-	-	-	0.003-0.050	
			91	0.95	-	-	0.72	0.6-8	-	-	-	0.008-0.120	0.017-0.110	-	-	
			105	1.10	-	-	0.72	0.6-8	30-55	-	30-55	-	-	-	0.003-0.040	
			172	1.80	-	-	0.72	0.6-8	0.6-8	-	-	-	0.007-0.100	-	0.003-0.033	
Littelojohms et al.(2009)	ILALR	-	11	0.76	0.14	-	1.96	0.03-0.54	-	-	-	-	-	0.001-0.005		
			11	0.76	0.14	-	1.96	0.03-0.54	-	-	-	-	-	-	0.01-0.04	
Simcik et al. (2011)	ILALR	Shot draft tube	50	-	-	-	2.29	1-7.5	0.4-0.88	0.1-0.2	0.006-0.102	0-0.065	-	-		
			50	-	-	-	1.63	1-7.5	0.35-0.7	0.24-0.45	0.02-0.11	0-0.08	-	-		
			50	-	-	-	2.29	1-7.5	0.42-0.9	0.11-0.23	0.01-0.058	-	-	-		

Table 2.1 Literature review (cont.)

Author (year)	Type of contactors	Details	volume (L)	h (m)	D (m)	L _c (m)	A _g /A _c (-)	u _{gs} (cm/s)	v _g (cm/s)	v _{lr} (cm/s)	riser gas holdup (-)	downcomer gas holdup (-)	overall gas holdup (-)	k _{ga} (1/s)	
Ceri and Badino (2010)	IL/ALR	-	2	0.327	-	-	1.68	0.01-0.11	-	-	-	-	-	0.008-0.069	
		-	5	0.450	-	-	1.78	0.01-0.11	-	-	-	-	-	0.010-0.061	
		-	10	0.550	-	-	1.84	0.01-0.11	-	-	-	-	-	0.010-0.072	
Choi et al. (1996)	BB	BB	110	1.64	-	-	1	1-8	-	-	-	-	0.038-0.016	-	
		Draft tube sparged	-	-	-	-	-	-	-	-	-	-	-	-	-
		ALR	110	1.64	-	-	1	1-8	-	-	-	-	0.038-0.0158	-	
Luo et al. (2011)	IL/ALR (Different Spargers)	ALR with gas injection in outer tube	110	1.64	-	-	1	1-8	-	-	-	-	0.038-0.0154	-	
		2-orifice	-	1.3	0.284	-	9.34	0.07-0.281	-	0.092-0.165	0.003-0.01	0.0019-0.006	0.0028-0.0085	0.0005-0.0017	
		4-orifice	-	1.3	0.284	-	9.34	0.07-0.281	-	0.11-0.195	0.0044-0.0122	0.0025-0.007	0.0038-0.011	0.0007-0.0022	
Lu et al. (2000)	IL/ALR	O-ring	-	1.3	0.284	-	9.34	0.07-0.281	-	0.1-0.178	0.0038-0.011	0.002-0.0068	0.003-0.0098	0.0006-0.0021	
		Modified square ALR	-	-	-	-	1.43	2-10	-	-	-	-	0.04-0.18	-	
		Modified square ALR	-	-	-	-	7.25	2-10	-	-	-	-	0.04-0.16	-	
		Round ALR	-	-	-	-	1.43	2-10	-	-	-	-	0.028-0.16	-	
		Round ALR	-	-	-	7.25	2-10	-	-	-	-	0.028-0.15	-		

CHAPTER III

MATERIALS AND METHODS

3.1 Summary of scope and methodology

Experiments in this work could be described using the following diagram. Detail of each section was delineated in this chapter.

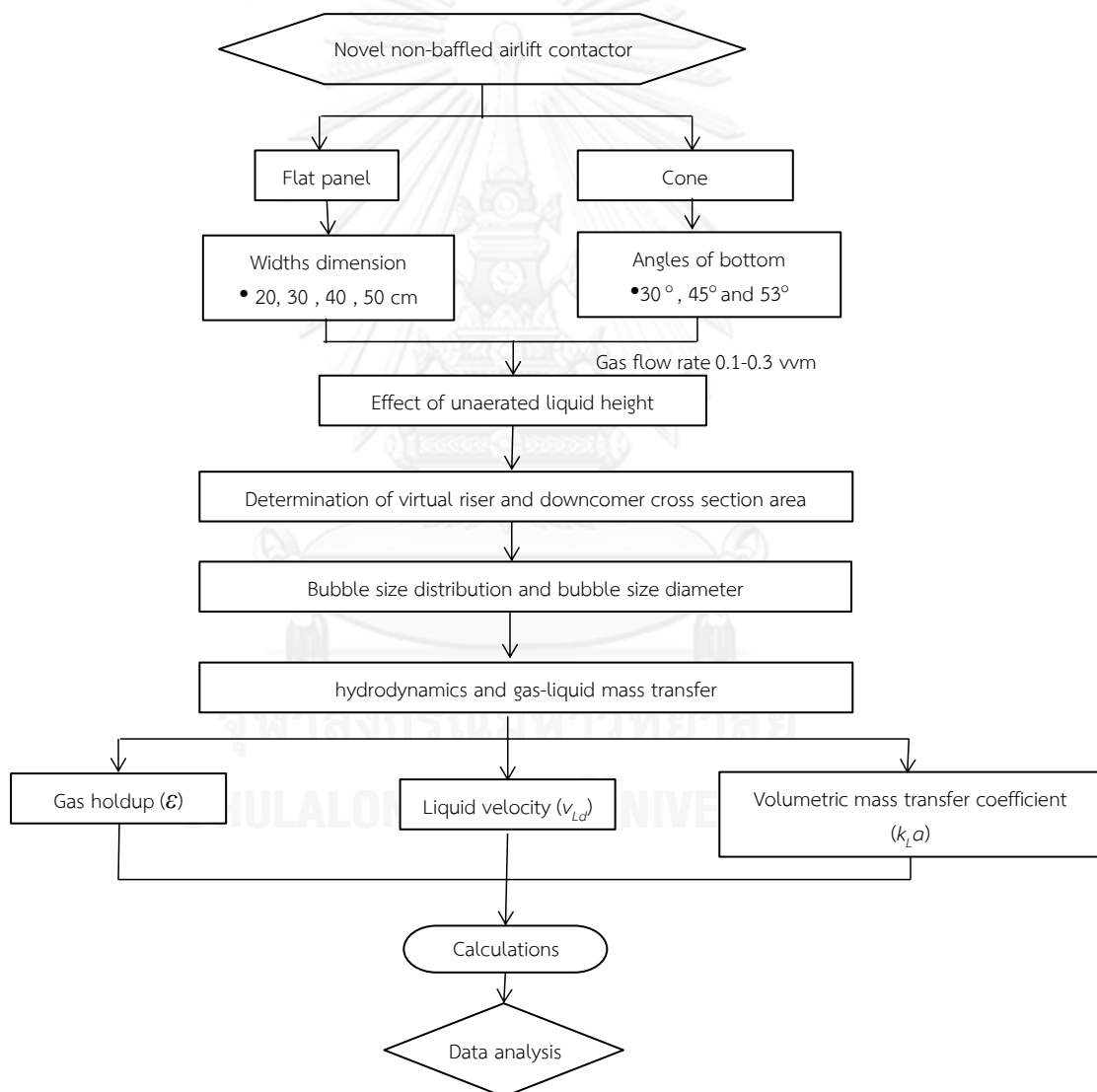


Figure 3.1 Outline of experiments and analysis in this work

3.2 Experimental setup

The large scale internal-loop airlift contactor was used in this work. The airlift system was operated as a two phase system (liquid and gas), where the liquid phase was water supply and the gas phase was ambient air. The liquid was filled in the airlift contactors and the gas was supplied by air pump. The shape of airlift contactors in this work were flat panels and cones, flat panels were made of fiber with the dimension of: length 100 cm, height 80 cm and varied widths (Figure 3.2 and 3.3). The cones shape airlifts were made of acrylic with the height of 80 cm and varied angle (Figure 3.4 - 3.5). For all experiments, air was dispersed by porous spargers installed along the length of flat panel and at the middle of cone. Gas flow rate was controlled in range 0.1 to 0.3 vvm (gas volume flow per unit of liquid volume per minute) and regulated by rotameters. The experiments could be setup divided into 3 parts, i.e. (i) various designs of airlift contactors, (ii) determination of virtual riser and downcomer cross-section area, (iii) effect of liquid height.

3.2.1 Various designs angle of cone and width of flat panel

Hydrodynamics and mass transfer of large scale airlift contactor was being investigated in this section. Flat panel airlift contactors were varied in width dimension (20, 30, 40 and 50 cm) whilst the operation of cones airlifts were subject to the angle at the bottom of the contactor from 30° to 45° and 53° .

3.2.2 Determination of virtual riser and downcomer cross-section area

As the airlift had no solid partition to indicate the riser and downcomer area, the sizes of riser and downcomer were variable. It was the purpose of this section to propose a method employed to determine the 'virtual' cross sectional area of riser and downcomer. This boundary between riser and downcomer was important for the calculation of hydrodynamics and mass transfer in the system. The liquid flow directions were observed by directions of light rope as follows:

- Set equipment as displayed in Figure 3.6
- Turn on the air at a desired flow rate to the water-filled airlift contactors, wait until the system operates at steady state (no further changed in fluid movement)

- Inject pole with a light rope and analyze the characteristics of the light rope directions. If the rope flow up show that, this point is defined in riser zone if the rope flow down, this point is downcomer
- Repeat experiments at various height
- Estimate the distances of riser and calculate area of riser of each type of contactor with Equations 3.1 and 3.3
- Calculate downcomer area by Equations 3.2 and 3.5
- Repeat experiment, change the air flow rate from 0.1 to 0.3 vvm

Example of finding flow direction by light rope is shown in Figure 3.7.

3.2.3 Effect of liquid height

Liquid height posed the hydrostatic pressure in the system which could affect both hydrodynamic and mass transfer behaviors in contactor. This section aimed to investigate such relationships where the unaerated liquid height is varied from 40, 50, 60 cm and height at 100 L (fill water 100 L in contactor and measure water height from bottom of contactor). Experiments can be described step by step as follows:

- Fill water at different heights of contactor (40, 50, 60 cm and the height at 100 L in volume)
- Measure gas holdup, liquid velocity and gas-liquid mass transfer
- Repeat the experiments with gas supply from 0.1 to 0.3 vvm

Volumes of contactors at different unaerated liquid heights are shown in Table 3.1-3.2.

3.3 Measurements

3.3.1 Bubble size

The bubble size measurement was used by photographic technique. Bubbles were photographed by digital camera (Canon EOS 60D) at different air flow rate and unaerated liquid height. The real sizes of bubbles were based on scale attached to a board that dips in the contactor. The steps are:

1. Fill water into contactor at desired level of unaerated liquid height
2. Attach scale to a board and dips in the contactor at position that want to photograph the bubble
3. Turn on the air at a desired flow rate
4. Focus camera on scale and photograph the bubble
5. Calculate bubble size from Equation 3.6 to 3.7
6. Repeat Steps 4 to 6 by varying air flow rate from 0.1 to 0.3 vvm
7. Repeat Step 7 by varying the unaerated liquid height from 40 to 60 cm and height at 100 L

3.3.2 Gas holdup

The U-tube water manometer was used to measure the pressure differences between the two measuring ports at the side of the reactor. This information will be used to estimate the gas holdup. The experimental steps are as follows:

1. Set equipment as displayed in Figure 3.6
2. Measure the liquid level before and after dispersing gas into airlift and calculate overall gas-holdup from Equation 3.12
3. Disperse gas in contactor and measure pressure difference at the two different vertical points in the riser of airlift via U-tube manometer
4. Calculate riser gas holdup from Equation 3.20
5. Repeat Steps 2 to 4 by varying air flow rate from 0.1 to 0.3 vvm and the unaerated liquid height from 40 to 60 cm and height at 100 L
6. Repeat Steps 5, change the measuring ports to downcomer side
7. Calculate downcomer gas holdup from Equation 3.25

3.3.3 Liquid velocity

The liquid velocity of downcomer in airlift system was measured by the color tracer injection method as described below:

1. Set equipment as displayed in Figure 3.6
2. Fix vertical distances for the color tracer to move (10 cm)
3. Fix point in downcomer zone for measurement and dip equipment of tracer injection
4. Turn on the air at a desired flow rate and then inject the color tracer at fixed point
5. Measure time for the tracer to move between two fixed vertical distances
6. Calculate downcomer liquid velocity from Equation 3.27
7. Repeat Steps 2 to 5 by varying air flow rate from 0.1 to 0.3 vvm
8. Repeat Step 7 by varying the unaerated liquid height from 40 to 60 cm and height at 100 L

3.3.4 Overall volumetric gas-liquid mass transfer coefficient

Dynamic method was used for investigate mass transfer coefficient that could be estimated from dissolved oxygen concentration in the system with the dissolved oxygen (DO) meter. The steps are:

1. Set equipment as Figure 3.6
2. Calibrate DO meter
3. Purge nitrogen to remove dissolved oxygen in airlift until DO reaches zero% air saturation
4. Turn off nitrogen valve and turn on air rotameter at defined flow rate
5. Collect data on %saturation of DO until it reaches 100% saturation and temperature
6. Calculate $k_L a$ from Equation 3.28
7. Repeat Steps 2 to 5 by varying air flow rate from 0.1 to 0.3 vvm
8. Repeat Step 9 by varying the unaerated liquid height from 40 to 60 cm and height at 100 L

3.4 Calculations

3.4.1 Riser and downcomer cross section area

The estimate of the riser and downcomer cross section area depended on the size of riser obtained from experiment. The shape of riser was assumed to be ring cylinder for the circle column (with cone bottom) airlift and rectangular cylinder for the flat panel airlift.

For circular column with cone bottom airlift, the riser cross section area is

$$A_r = \pi R_r^2 \quad 3.1$$

R_r was obtained from the experiment, and the downcomer cross sectional area (A_d) can be calculate from

$$A_d = \text{Area of column} - \text{Area of riser} \quad 3.2$$

For flat panel airlift; the riser cross section area is

$$A_r = W_r \times L \quad 3.3$$

The width of riser (W_r) was known from the experiment whereas the width of downcomer (W_d) is estimated from:

$$W_d = \text{width of reactor} - W_r \quad 3.4$$

and the downcomer cross section area is

$$A_d = W_d \times L \quad 3.5$$

where A = cross section area (cm^2)

R = radius (cm)

W = width of section (cm)

L = length of contactor (cm)

and the subscript

r = riser

d = downcomer.

3.4.2 Bubble size and distribution

The bubbles in liquid were various shapes. In this work, bubble shape was assumed to be like ellipsoidal. The diameter of equivalent size (d_B) of ellipsoidal bubble was estimated by volume consideration basis, the major and minor axes of ellipse in two dimensions were measured as show in Figure 3.8. The diameter of equivalent size of individual bubble is express as:

$$d_B = (p^2 q)^{1/3} \quad 3.6$$

where d_B = diameter of equivalent size (cm)

p = length of major axis of bubble (cm)

q = length of minor axis of bubble (cm).

From this experiment, bubbles were photographed images about 30 at the same condition. The individual bubble diameter can be calculated by equation 3.6 so that the number of bubbles usually reported in term of “Sauter mean diameter (d_{Bs})”, using the following formula:

$$d_{Bs} = \frac{\sum_i n_i d_{Bi}^3}{\sum_i n_i d_{Bi}^2} \quad 3.7$$

where n_i = the number of bubbles with diameter (d_{Bi})

3.4.3 Gas holdup

The riser and downcomer gas holdups were volumetric gas fraction in each section. The overall gas holdup could be calculated from the volume expansion which was measured from the difference between aerated and unaerated liquid heights. The definition of gas holdup is

$$\epsilon = \frac{V_G}{V_G + V_L} \quad 3.8$$

The volume of gas could not be measured directly, so that we defined V_A (volume in system when aeration) as the total volume of gas phase plus volume of liquid phase.

Then

$$\mathcal{E} = \frac{V_A - V_L}{V_A} \quad 3.9$$

$$\mathcal{E} = 1 - \frac{V_L}{V_A} \quad 3.10$$

$$\mathcal{E} = 1 - \frac{h_u A}{h_A A} \quad 3.11$$

$$\mathcal{E} = 1 - \frac{h_u}{h_A} \quad 3.12$$

where \mathcal{E} = overall gas holdup

h = liquid height (cm)

V = volume (cm³)

subscript L = liquid

G = gas

A = aerated

u = unaerated.

The U-tube manometer was employed to measure the downcomer gas holdup where.

$$\Delta P_{reactor} = \Delta P_{manometer} \quad 3.13$$

$$\rho_L g \Delta H = \rho_G g \Delta Z \quad 3.14$$

$$(\rho_L \mathcal{E}_L + \rho_G \mathcal{E}_G) g \Delta H = \rho_L g \Delta Z \quad 3.15$$

Neglecting the wall friction loss and $\rho_L \gg \rho_G$, the gas holdup can be calculated from equations:

$$\rho_L \epsilon_L g \Delta H = \rho_L g \Delta Z \quad 3.16$$

$$\epsilon_L = \frac{\Delta Z}{\Delta H} \quad 3.17$$

since

$$\epsilon_L = 1 - \epsilon_G \quad 3.18$$

so

$$1 - \epsilon_G = \frac{\Delta Z}{\Delta H} \quad 3.19$$

finally,

$$\epsilon_G = 1 - \frac{\Delta Z}{\Delta H} \quad 3.20$$

where ΔP = pressure difference of defined liquid level in contactor ($\text{g/cm} \cdot \text{s}^2$)

ΔH = height of defined liquid level in contactor (cm)

ΔZ = height of liquid level in U-tube manometer (cm)

ρ = density (g/cm^3)

g = gravitational acceleration (cm/s^2)

subscript L = liquid

G = gas.

The riser gas holdup is calculated from following equation

$$\epsilon_r = \frac{V_{Gr}}{V_{Gr} + V_{Lr}} \quad 3.21$$

$$\epsilon_r = \frac{V_{GT} - V_{Gd}}{V_{GT} - V_{Gd} + V_{LT} - V_{Ld}} \quad 3.22$$

$$\epsilon_r = \frac{\epsilon_0 V_T - \epsilon_d V_d}{V_T - V_d} \quad 3.23$$

$$\epsilon_r = \frac{\epsilon_o - \epsilon_d(V_d/V_T)}{1 - (V_d/V_T)} \quad 3.24$$

$$\epsilon_r = \frac{\epsilon_o - \epsilon_d[A_d h / (A_d + A_r) h]}{1 - [A_d h / (A_d + A_r) h]} \quad 3.25$$

where ϵ = gas holdup (-)

A = area (cm²)

V = volume (cm³)

h = liquid height (cm)

subscript o = overall

r = riser

d = downcomer

T = total.

3.4.4 Liquid velocity

The liquid velocities in riser and downcomer were estimated by the color tracer injection method where the time in which the tracer used to move at fixed vertical distances was used for the calculation:

$$v_r = \frac{L_r}{t_r} \quad 3.26$$

$$v_d = \frac{L_d}{t_d} \quad 3.27$$

where v = liquid velocity (cm/s)

L = fixed vertical distances (cm)

t = time for the tracer used for moving (s).

subscript r = riser

d = downcomer.

3.4.5 Overall volumetric gas-liquid mass transfer coefficient

The overall volumetric gas-liquid mass transfer coefficient ($k_L a$) was determined using the dynamic method. In this method, the solution was freed of oxygen by nitrogen purge, and as the aeration was supplied, the time profile of dissolved oxygen concentration in the system was measured and recorded. The $k_L a$ can be calculated from:

$$\ln \frac{(c^* - c_0)}{(c^* - c_L)} = k_L a t \quad 3.28$$

where c^* = final oxygen concentration (mg/L)

c_0 = initial oxygen concentration (mg/L)

c_L = oxygen concentration in liquid phases (mg/L)

$k_L a$ = overall volumetric mass transfer coefficient (1/s)

t = time to reach final oxygen concentration (s).

When the bubble size and overall gas holdup were known, they could calculate $k_L a$ in terms of liquid phase mass transfer coefficient (k_L) and specific gas-liquid interfacial area (a) separately. The specific gas-liquid interfacial area is expressed as:

$$a = \frac{6\epsilon_0}{(1 - \epsilon_0)d_{Bs}} \quad 3.29$$

where a = the specific gas-liquid interfacial area (cm^2/cm^3)

3.4.6 Unit of aeration

The unit of aeration in this work was reported in both vvm and u_{sg} . They can be calculated from:

- vvm (volume per volume per minute)

$$vvm = \frac{\text{air flow rate (L/min)}}{\text{volume of liquid in system (L)}} \quad 3.30$$

- u_{sg} : superficial gas velocity (cm/s)

$$u_{sg} = \frac{\text{air flow rate (L/ min)}}{A_r \text{ (cm}^2\text{)}} \quad 3.30$$

where A_r = area of riser (cm²)



Table 3.1 Volume of flat panel at different unaerated liquid heights

Width 20 cm		width 30 cm		width 40 cm		width 50 cm	
liquid height cm	volume (L) fiber	liquid height cm	volume (L) fiber	liquid height cm	volume (L) fiber	liquid height cm	volume (L) fiber
40	74	40	100	37	100	35	100
50	100	50	129	40	120	40	118
60	123	60	162	50	160	50	169
				60	200	60	223

Table 3.2 Volume of cone at different unaerated liquid heights

Angle 30°		Angle 45°		Angle 53°	
liquid height cm	volume (L) acrylic	liquid height cm	volume (L) acrylic	liquid height cm	volume (L) acrylic
34	100	40	100	40	45
40	135	50	125	50	78
50	230	60	200	53	100
60	310			60	125

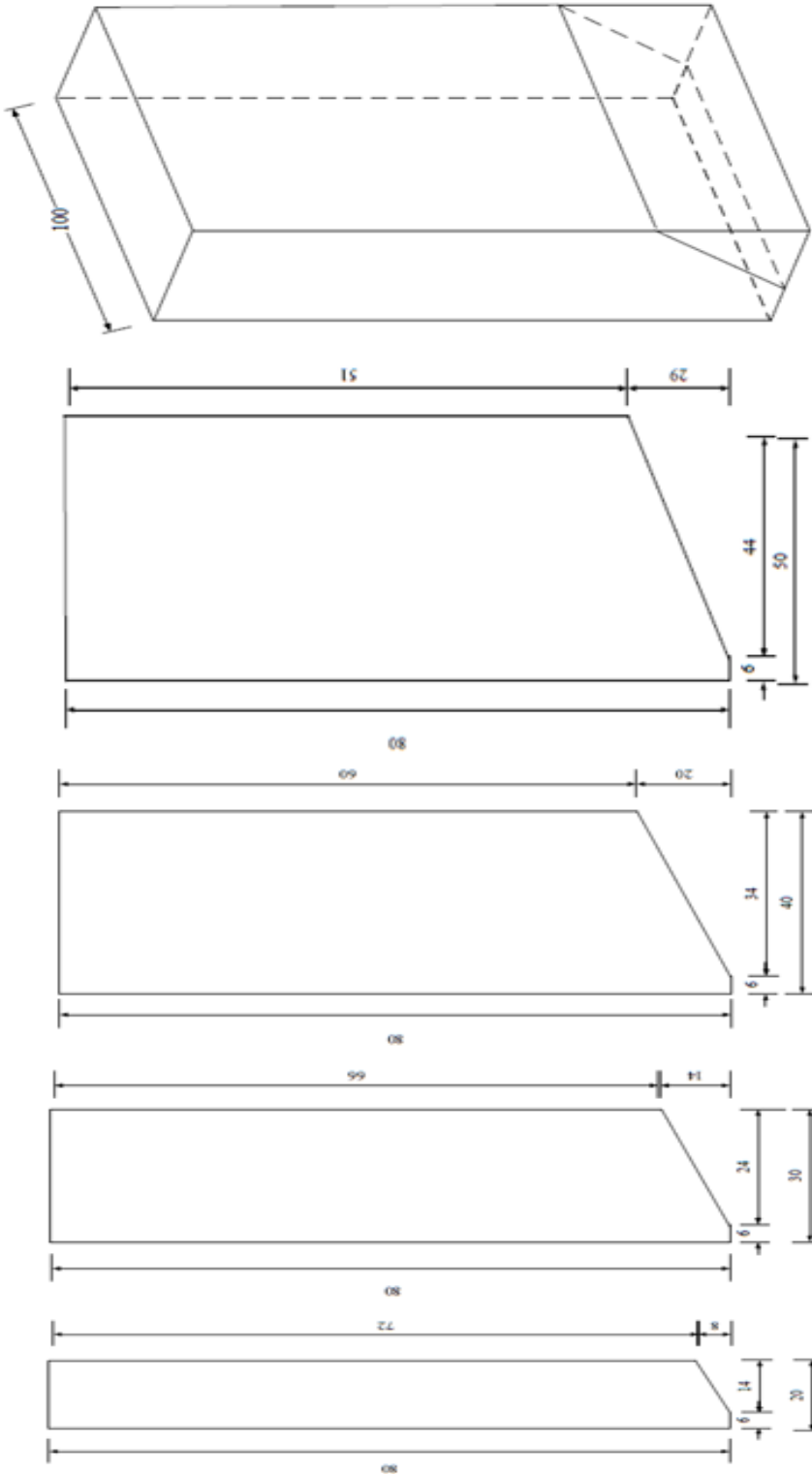


Figure 3. 2 Schematic of novel non-baffled flat panel airlift contactors

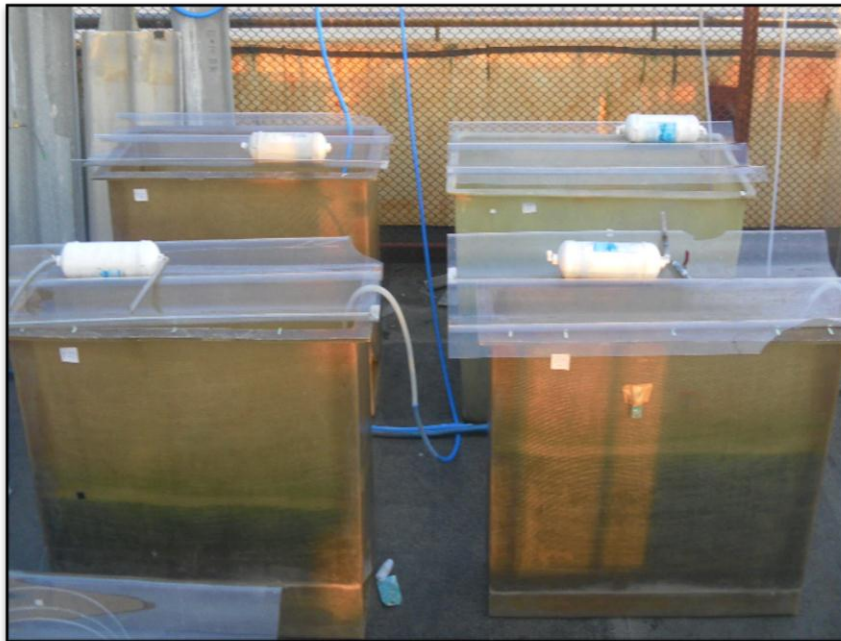


Figure 3.3 Novel non-baffled flat panel airlift contactors

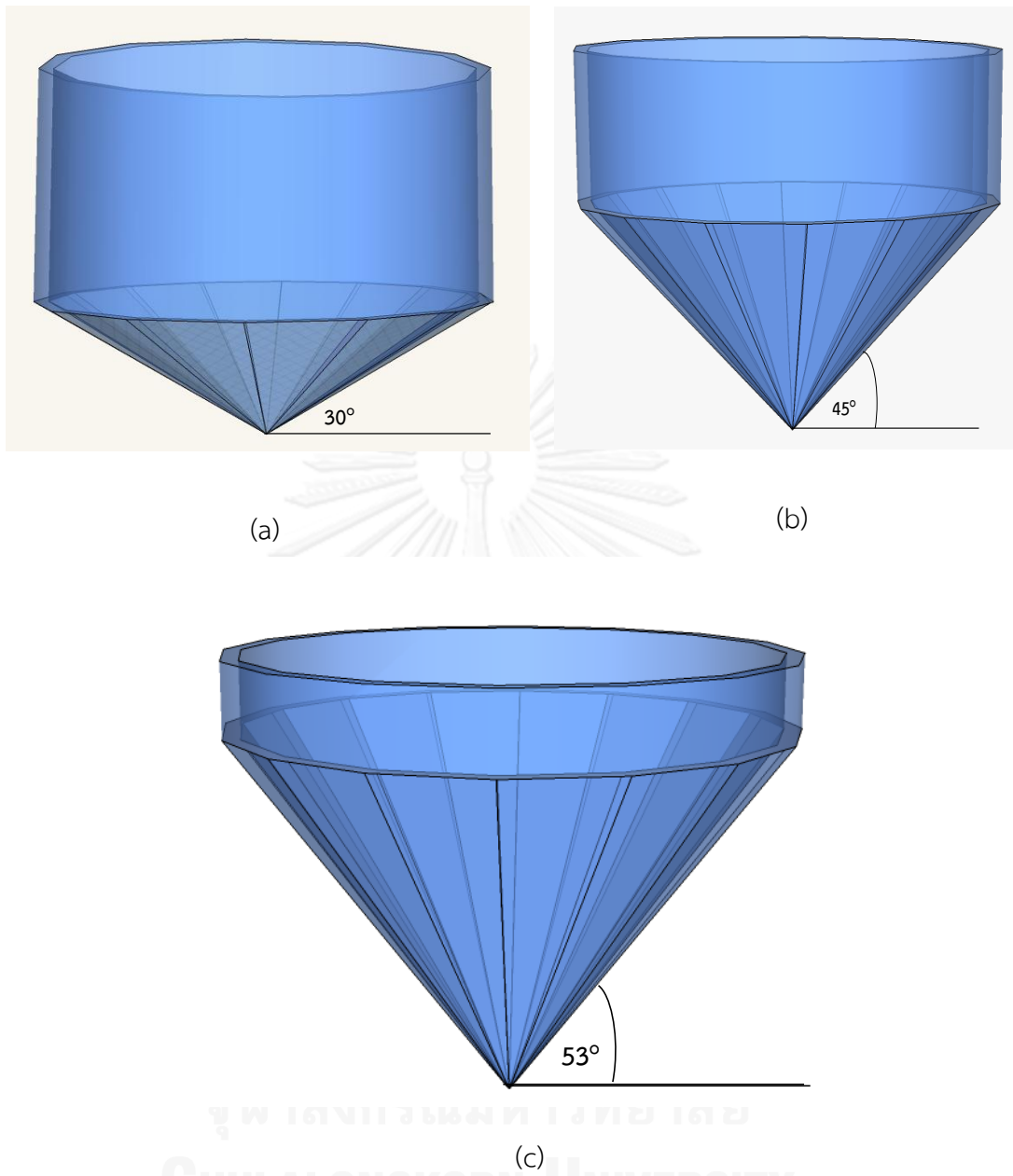


Figure 3.4 Schematic of circular columns with cone bottom airlift contactors (a) angle of bottom 30° (b) angle of bottom 45° (c) angle of bottom 53°



(a)

(b)



(c)

Figure 3.5 circular columns with cone bottom airlift contactors (a) angle of bottom 30° (b) angle of bottom 45° (c) angle of bottom 53°

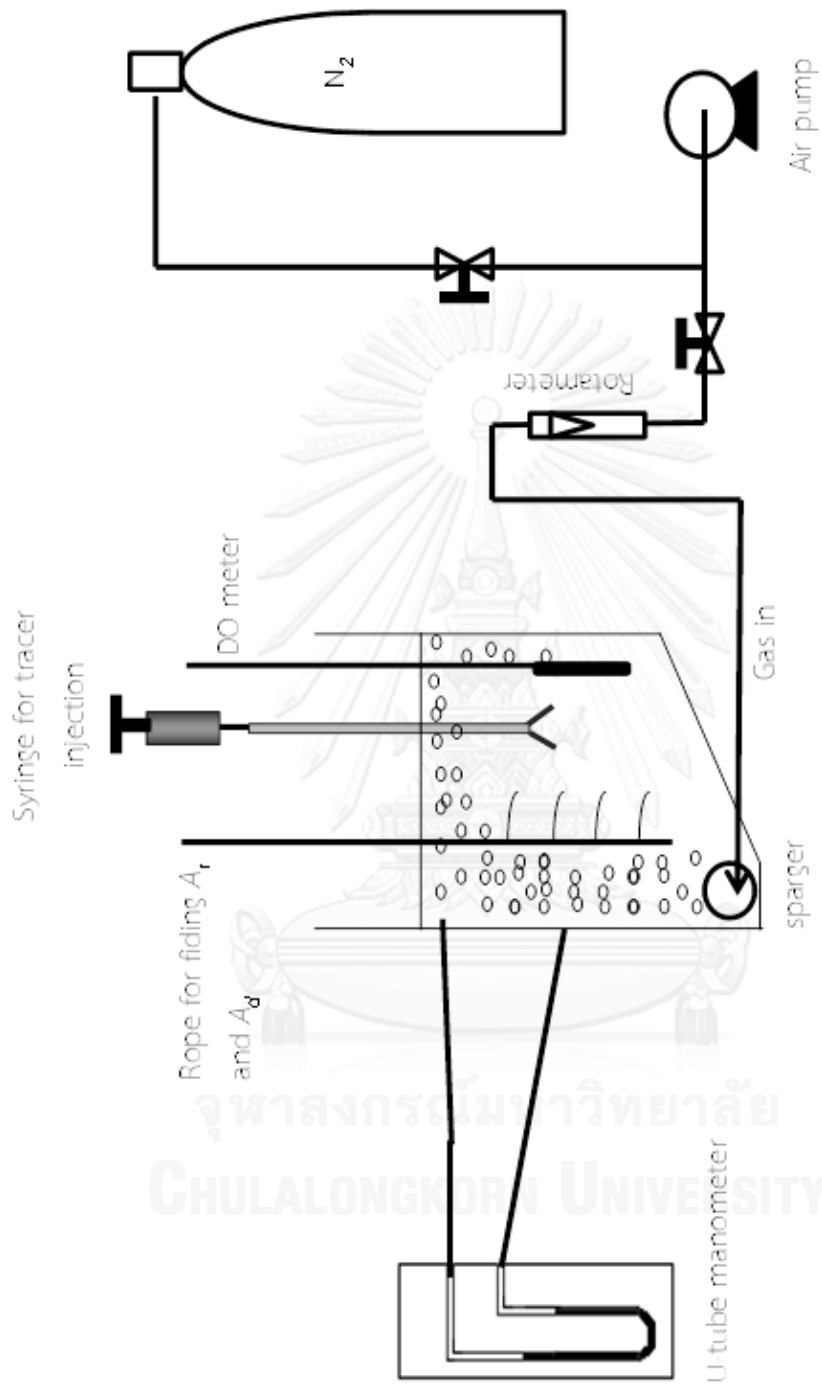


Figure 3. 6 Schematic diagram of experiments

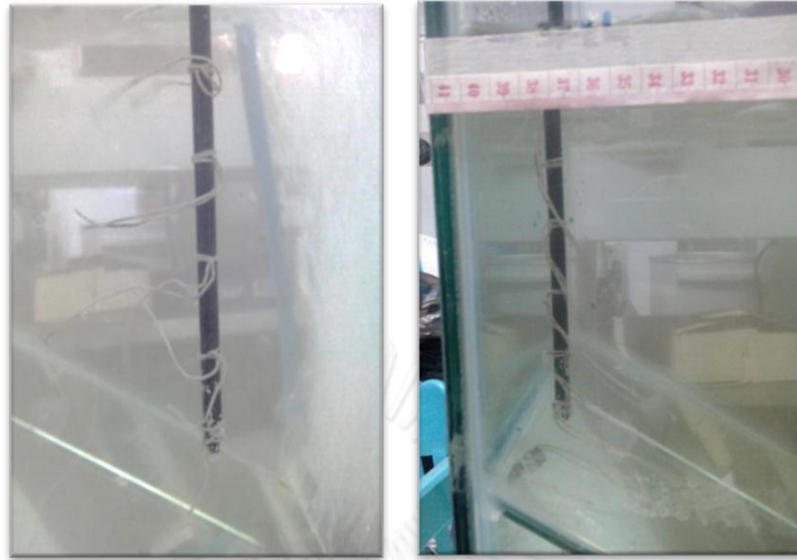


Figure 3.7 Example of finding flow directions in airlift contactor

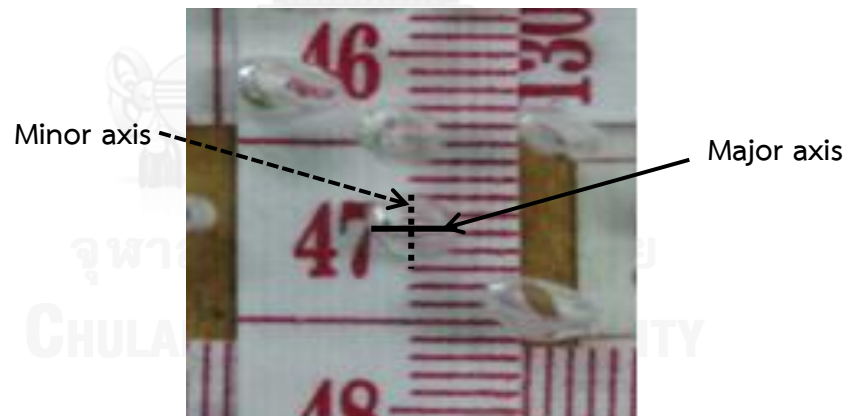


Figure 3.8 Example of photographs of bubbles from photographic technique

CHAPTER IV

RESULTS AND DISCUSSION

4.1 Characteristics of novel non-baffled flat panel airlift contactors (NB-FP-ALCs)

NB-FP-ALCs has a flat geometry. Unlike other airlift system, NB-FP-ALC does not have a partition or a draft tube that separates riser and downcomer, but still can induce a cyclic movement pattern of the fluid within the contactor. This design reduces dead zone which is a common problem found in typical gas-liquid contactors such as bubble column and cylindrical airlift contactors. Particularly in cell suspension systems, the existence of dead zone might allow all precipitation and prevent effective growth. Therefore, this inclined plane supports the well-defined movement of solid particles from downcomer to riser. The movement and directions of liquid in NB-FP-ALC are shown in Figure 4.1.

4.2 Effect of width of contactor (w) and unaerated liquid height (h) on the performance of NB-FP-ALCs

This part describes the effect of width of contactors and unaerated liquid heights on riser cross-sectional area (A_r), downcomer cross-sectional area (A_d), bubble size distributions, riser gas-holdup (\mathcal{E}_r), downcomer gas-holdup (\mathcal{E}_d), overall gas-holdup (\mathcal{E}_o), downcomer liquid velocity (v_{Ld}) and the overall gas-liquid volumetric mass transfer coefficient ($k_L a$). The unit of aeration in this work is reported in both vvm (volume per volume per minute) and u_{sg} : superficial gas velocity (cm/s). For flat panel systems, the fluid flow was rather well defined as riser and downcomer. The results were therefore discussed in terms of u_{sg} . In the later stage of this chapter, the discussion in large cylindrical systems was done using vvm as the fluid flow pattern became more difficult to define. It is noted that raw data used in this chapter are given in Appendix B.

4.2.1 Riser and downcomer cross-sectional area

As the flat panel airlift systems used in the work did not have a physical partition to separate riser and downcomer, it was difficult to distinguish between riser and downcomer sections. In other words, A_r and A_d were visually unknown. To determine the riser and downcomer area, a simple pole with a light rope attached to it was inserted into the system and the flow direction of the rope would indicate the fluid flow direction. By repeatedly inserting this rope into the various locations in the contactor, the overall fluid flow direction in the system could be defined, i.e. A_r and A_d could be virtually located. Figure 4.2 shows an example of a flow direction diagram in NB-FP-ALC where the direction of liquid at each specific location could be identified. A_r and A_d can then be calculated from the widths of riser and downcomer in this diagram and then multiplied by the length of contactor (100 cm). It is noted that overall flow direction diagram are given in Appendix A.

Figure 4.3 demonstrates that most A_r were constant and did not depend on u_{sg} and liquid height (h), but rather depended on the contactor width. Increasing the width of the contactor from 30 to 50 cm saw an increase in A_r . This might be because there was less horizontal force being imposed on the riser in the contactor with larger width (from the liquid back-flow from downcomer). Hence, the riser could expand due particularly to the expansion of the bubble. However, the riser was quite wide in the contactor with 20 cm width which could be due to a more turbulent condition in such reactor which allowed the mixing between liquid in riser and downcomer. It is therefore more difficult to accurately define the riser and downcomer in such system.

Figure 4.4 illustrates that u_{sg} and h did not have strong impact on A_d , but rather, A_d seemed to increase when the width of contactor increased ($W_{50} > W_{40} > W_{30} > W_{20}$ cm). Figure 4.5 shows how A_d/A_r changed with the air flow rate and also the reactor dimension. It was interesting to observe that most A_d/A_r were more or less constant, regardless of the air flow, and took the value between 1-2.5; the highest occurred at the width of 40 cm and the lowest at 20 cm.

4.2.2 Bubble size distributions and bubble size diameters

Bubble size distributions are shown in Figures 4.6-4.20. Common observations could be summarized. Small bubbles were usually found in the system operated with low aeration rate, i.e. at $u_{sg} < 0.4$ cm/s, the bubble size was in the range of 0.3-0.4 cm.

As the supply of air increased, bubble size increased steadily and there might also exhibit two major bubble sizes (bimodal distribution). At this low u_{sg} range, the system was in a homogeneous regime, gas holdup and turbulence were low thus bubble breakup and coalescence were negligible. The bubble size distribution was mainly determined by the gas distributor and liquid properties. At large aeration, i.e. $u_{sg} > 1$ cm/s, bubble size seemed to reach a maximum size of 0.5-0.6 cm. Bubble size increased due primarily to the coalescence of small bubbles and therefore when the system was supplied with a large quantity of gas bubbles, chances of the two bubbles being combined with each other became quite high and this led to a formation of larger bubbles. And due to the same reason, at high aeration rate, the distribution of bubble size became broader than that at lower aeration rate. These findings were supported well by the report of Deng *et al.*(2010). At this high aeration condition, bubble coalescence was finally balanced by bubble breakup and the bubble size remained at their equilibrium. It is noted that the bubble size distribution only varied with u_{sg} and did not depend on h , the finding in agreement with that of Lau *et al.* (2013).

Bubble Sauter mean diameters (d_{Bs}) was 0.2-0.8 cm as shown in Figure 4.21. The d_{Bs} slightly increased when u_{sg} increased as discussed above. It was also found that d_{Bs} did not depend on h but increased with the width of the contactor. d_{Bs} at w 50 and 40 cm were similar and had a value of more than that at w 30 and 20 cm, respectively. The results also illustrate that d_{Bs} took a similar trend with A_d/A_r meaning that a system with small riser would lead to a larger bubble size. This agreed well with the report of Ruen-ngam *et al.*(2008). Who described that turbulence in system with smaller riser was stronger than larger riser and promoted bubble coalescence.

4.2.3 Riser, downcomer and overall gas-holdups

Gas holdup for this experiment had to be measured with the volume expansion method as the manometer could not be installed effectively as the height of the contactor was not adequate for the installation of the manometer. As described in previous sections, liquid flow in NB-FP-ALCs could be well classified into four directions, i.e. upflow, downflow, and cross-sectional flows (right and left) as illustrated in Figure 4.2. These four flow sections can be graphically described as shown in Figure 4.22.

Overall gas-holdup ($\epsilon_{overall}$) can be mathematically described as shown in Equations 4.1-4.2:

$$V_{overall} \epsilon_{overall} = \epsilon_r V_r + \epsilon_{rd} V_{rd} + \epsilon_{dr} V_{dr} + \epsilon_d V_d \quad 4.1$$

$$\epsilon_{overall} = \frac{\epsilon_r V_r + \epsilon_{rd} V_{rd} + \epsilon_{dr} V_{dr} + \epsilon_d V_d}{V_{overall}} \quad 4.2$$

where

$$V_{overall} = V_r + V_{rd} + V_{dr} + V_d \quad 4.3$$

$$V_r = \frac{1}{2} \times w_r \times (h_r + h_1) \times L \quad 4.4$$

$$V_{rd} = w_{rd} \times h_2 \times L \quad 4.5$$

$$V_{dr} = \frac{1}{2} \times w_{rd} \times (h_1 - h_2 + h_3) \times L \quad 4.6$$

$$V_d = \frac{1}{2} \times w_d \times (h_2 + h_3 + h_d) \times L \quad 4.7$$

Assumptions for calculations:

Assumption 1 $\epsilon_1 = \epsilon_d$
gas-holdup of Section rd was equal downcomer gas-holdup

Assumption 2 $\epsilon_2 = 0$

Section dr did not have bubbles

With these two assumptions, Equation 4.2 becomes:

$$\epsilon_{overall} = \frac{\epsilon_r V_r + \epsilon_{rd} V_{rd} + \epsilon_d V_d}{V_{overall}} \quad 4.8$$

Figures 4.23-4.25 show that riser, downcomer and overall gas-holdups increased with air flow rate. Increasing air flow rate into system caused more gas to enter the system, and this led to a larger quantity of gas being retained in the contactor, and a higher gas holdup was observed. This agreed well with the report of Luo *et al.* (2011) and Kilonzo *et al.* (2007). In addition, Wongsuchoto (2002) described that high air flow rate promoted high bubble breakage, and small bubbles from this breakage would move more slowly than large bubbles. Therefore gas bubbles stayed a longer time in the contactor, and thus, the gas holdups were high. The riser gas-holdup was higher than the downcomer gas-holdup because aeration was supplied to the riser directly. The bubbles disengaged at the top of contactor, and thus, there was a lower gas content in the downcomer. The riser gas-holdup was in the range of 0–0.08 while the downcomer and the overall gas-holdups were 0–0.06.

The riser, downcomer and overall gas-holdups produced a similar trend with the aeration rate. When u_{sg} was less than 0.3 cm/s, it became quite difficult to distinguish between gas-holdups in the various sections in the contactor. The difference became more pronounced at higher u_{sg} than 0.3 cm/s, where the width of the contactor had a slight impact on gas-holdup. Increasing the width of the contactor from 30 to 50 cm saw an increase in the riser, downcomer and overall gas-holdups. This could be because A_r became larger with the width of the contactor and this larger A_r could accumulate a larger quantity of gas bubbles. However, the gas-holdup of the contactor with 20 cm width was more or less equal to that of the 50 cm width contactor. In fact, the highest gas holdup was observed in the 20 cm width contactor at the unaerated liquid height of 40 cm. (u_{sg} 0.6 cm/s). This could be due to the inherit small A_c/A_r in the 20 cm width contactor (large A_r) which rendered the behavior of the system closer to that of bubble column which could retain more gas bubble than the airlift system.

4.2.4 Downcomer liquid velocity

Downcomer liquid velocity increased with aeration rate and unaerated liquid height as shown in Figure 4.26. Increasing aeration rate supplied more energy to the system and therefore the fluid moved faster as a result whereas increasing height allowed more time for the energy to be transferred to the system which also enhanced the fluid velocity. In addition, the friction loss due to the circulating of liquid at the top and the bottom of the airlift was relatively small in the system with higher level of

liquid height, and this led to a faster liquid flow. Similar findings were also reported elsewhere (Wongsuchoto, 2002).

The effect of the width of contactor was not so clear. Generally, liquid velocity was fastest when the contactor width was 40 cm and lowest at 50 cm. This could be because contactors with 40 cm width had relatively high A_d/A_r which promoted a larger hydrostatic pressure difference which then resulted in a high liquid velocity. At the width of 50 cm, the system behavior was very similar to that with the width of 40 cm. However, there was more space for the liquid to move (larger cross sectional area) which led to a slower movement of fluid and a slightly slower liquid flow was observed.

4.2.5 Overall gas-liquid volumetric mass transfer

Figure 4.27 shows that the overall gas-liquid volumetric mass transfer coefficient ($k_L a$) increased with air flow rate. This was not uncommon as supplying more air to the system resulted in a generation of a larger quantity of air bubbles which enhanced the gas-liquid mass transfer area and also mass transfer rate. Within the aeration rate employed in this work, an almost linear relationship between $k_L a$ and aeration rate both in terms of flow rate and superficial velocity was observed. However, in terms of air flow rate (v_m), there was no difference between the contactor configuration on $k_L a$, and this became clearer when the air flow rate was converted to superficial velocity using the riser area obtained from Section 4.2.1. This is described below.

Increasing the width of the contactor from 30 to 50 cm saw an increase in $k_L a$. However, $k_L a$ was also quite high in the contactor with the width of 20 cm which is in more or less the same level with that of 50 cm. The highest $k_L a$ was obtained from the contactor of 20 cm in width and 40 cm in liquid height at u_{sg} of 0.6 cm/s. When comparing Figure 4.27 with the overall gas holdup (Figure 4.25) and riser gas holdup (Figure 4.23), there seemed to be a very close relationship between $k_L a$ and the gas holdup (both overall and riser gas holdups). This suggested that the gas-liquid mass transfer area (a) might play an important role in setting the mass transfer rate between the two phases. Particularly in the contactor with the width of 20 cm, previous results indicated that bubbles in such system had the smallest sauter mean diameter and therefore a high mass transfer area was obtained. The specific interfacial area (a) for the various airlift configurations is shown in Figure 4.28 whereas the mass transfer coefficient (k_L) is reported in Figure 4.29. This reveals that k_L was

almost constant, in the range of 1.5-2.5 cm/s, regardless of the system configuration and aerate rate, and hence, $k_L a$ followed closely the trend of a .

In airlift systems, Wongsuchoto (2002) demonstrated that k_L depended on properties of substance, and the differences between the density of gas and liquid which promoted the natural movement of the fluid, i.e. $Sh = f(Gr, Sc)$. And in this work, such relationship can be formulated as:

$$Sh = 0.149Gr^{0.565} \quad 4.9$$

However, it was observed that k_L was found to be quite low when the unaerated liquid height was lower than 40 cm. This could be that, at this liquid height, the fluid velocity (both air bubbles and liquid) was still not fully developed and therefore Reynold's number also exerted some effect on the mass transfer rate. This low velocity exerted adverse effect on the mass transfer resistance leading to a low mass transfer rate.

4.3 Characteristics of non-baffled cone airlift contactors (NB-C-ALCs)

NB-C-ALCs has cylindrical with cone bottom geometry. The contactor was designed to have various angles of the cone bottom (30° , 45° and 53°) to investigate the effect of this design on the system performance. Similar to NB-FP-ALCs, NB-C-ALCs was not equipped with the partition to separate between riser and downcomer, but the cyclic movement was induced by fitting air porous sparger at some specific location, in this case, at the center of the cone bottom. The movement and directions of liquid in NB-C-ALCs are shown in Figure 4.30. During the operation, bubbles swarmed at the center of the column making it a riser. A large quantity of bubbles disengaged at the liquid surface whilst some small ones re-entered, moving downward on the side of the column, which makes this a downcomer. All NB-C-ALCs employed here have a diameter of 100 cm which is large enough to allow most bubbles to disengage, leaving very few bubbles remaining in the downcomer. Due to the size of the system, it was not possible for the visual measurement of bubble sizes and its distribution.

4.4 Effect of the angle of bottom (B) and unaerated liquid height (h) on the performance of NB-C-ALCs

This part describes the effect of the angle of the cone bottom and unaerated liquid heights on riser cross-sectional area (A_r), downcomer cross-sectional area (A_d), riser gas-holdup (ϵ_r), downcomer gas-holdup (ϵ_d), overall gas-holdup (ϵ_o), downcomer liquid velocity (v_{Ld}) and the overall gas-liquid volumetric mass transfer coefficient ($k_L a$). The unit of aeration in this work is reported in both vvm and u_{sg} , and the raw data are given in Appendix B.

4.4.1 Riser and downcomer cross-sectional area

The same method for the determination of riser and downcomer cross-sectional area with NB-FP-ALCs was applied for this cone bottom airlift where the example of the flow direction diagram is shown in Figure 4.31. It is worth nothing here that, since each airlift contactor has different bottom angle, they did not have the same volume at the same liquid height. NB-C-ALC with 30° cone bottom had a larger volume of liquid than NB-C-ALC with 45° and NB-C-ALC 53° when they were operated at the same height. In other words, the liquid height in NB-C-ALC with 30° cone bottom would be lower than that with 45° and 53° if they were operated at the same liquid volume.

Figure 4.32 shows that A_r was constant for each contactor configuration in the range of 120-1,500 cm^2 , independent of aeration rate. The A_r of angle of bottom 30° was slightly greater than that at 45° and clearly greater than 53° . This is because the 30° cone bottom airlift had a greater quantity of water when compared with the others at the same height, a higher aeration rate had to be supplied to give it the same specific aeration rate (vvm). Therefore it was not unexpected that this 30° system would accommodate more bubbles and a larger riser was obtained.

In the cone bottom airlift, unlike the flat panel, liquid always flowed upwards and downwards, and there was a very small area where a horizontal flow was observed. Hence, the whole area was therefore consisted of riser and downcomer, In other words, A_d could be estimated from the subtraction of A_r from the total area of the contactor. Hence, since A_r did not depend on the air flow rate, A_d also did not depend on air flow rate, and in most cases, A_d was larger than A_r as shown in Figure 4.33. A_d increased with unaerated liquid height but Figure 4.34 shows that A_d/A_r did

not change with the air flow rate and unaerated liquid height. A_d/A_r was typically in the range of 2-55.

4.4.2 Riser, downcomer and overall gas-holdup

Calculations of riser, downcomer and overall gas-holdup were similar with NB-FP-ALCs in Section 4.2.3. Figures 4.35-4.37 show how riser, downcomer and overall gas-holdup increased with air flow rate, which could be described using similar reasons with those given in Section 4.2.3.

At the same operating liquid height, riser gas holdup was often found to be large in the systems with 30° and 45° as a large aeration rate needed to be supplied to compensate the large volume of the contactor. In addition, these systems were operated with smaller A_d/A_r which promoted the high residence time of gas bubbles. This ended up with a large riser gas holdup than that at 53° .

An increase in liquid height also gave a positive effect on the riser gas holdup due primarily to two major reasons. First an increase in liquid height meant that there was a larger quantity of water in the system and therefore a larger aeration was supplied. This gave rise to the gas holdup. Secondly, a higher liquid height allowed bubbles to stay longer in the system leading to a larger gas holdup. Similar description can be given to the overall gas holdup as illustrated in Figure 4.37.

4.4.3 Downcomer liquid velocity

Figure 4.38 shows that downcomer liquid velocity generally increased with air flow rate. There was a few exception, e.g. at 30° and a liquid height of 60 cm where the velocity stayed constant in the range of 17-18 cm/s at low air flow rate range (0.04-0.20 vvm) and increased with air flow rate at high air flow rate range (>0.2 vvm). The angle of bottom did not have a significant effect on downcomer liquid velocity. Additionally, downcomer liquid velocity depended on unaerated liquid height. The downcomer liquid velocity was the largest at 30° h 60 cm whereas the lowest at 30° h 34 cm. This was mainly due to a longer contact time which allowed more energy transfer from gas bubbles to liquid. This exerted a positive effect on liquid velocity. Also a greater liquid height often saw an increase in riser gas holdup which enhanced the difference between the hydrostatic pressure in riser and downcomer, and promoting a faster liquid movement. This reason was supported by Bentifraouine *et al.* (1997).

4.4.4 Overall gas-liquid volumetric mass transfer

Figure 4.39 demonstrates that $k_L a$ depended significantly and solely on air flow rate. When more air was added into system, the chance for mass transfer between gas and liquid increased. In addition, a high air flow rate caused more turbulence within the system which positively affected the mass transfer rate. No information on bubble size could be drawn from this experiment with the setup employed in this work, and therefore it was not possible at this stage to find the relationship between k_L and a . The angle of the cone bottom and the unaerated liquid height did not show strong impact on $k_L a$.

4.5 Empirical models for hydrodynamic and gas-liquid mass transfer in NB-FP-ALCs and NB-C-ALCs

For flat panel airlift

Relationship between overall gas-holdup and u_{sg} and width of contactor and unaerated liquid height

$$\mathcal{E}_o = \frac{0.06 u_{sg}^{0.49} h^{0.25}}{W^{0.52}} \quad 4.10$$

Relationship between downcomer liquid velocity and u_{sg} and width of contactor and unaerated liquid height

$$V_{Ld} = \frac{20.49 u_{sg}^{0.23} h^{0.12}}{W^{0.08}} \quad 4.11$$

Relationship between $k_L a$ and u_{sg} and width of contactor and unaerated liquid height

$$k_L a = \frac{0.25 u_{sg}^{0.54}}{W^{0.27} h^{0.58}} \quad 4.12$$

Relationship between a and u_{sg} and width of contactor and unaerated liquid height

$$a = 0.56 u_{sg}^{1.39} W^{0.09} \quad 4.13$$

From prediction, the a did not depend on unaerated liquid height.

Relationship between k_L and u_{sg} and width of contactor and unaerated liquid height

$$k_L = 0.02u_{sg}^{0.99} \quad 4.14$$

From prediction, the k_L did not depend on width of contactor and unaerated liquid height.

For cone shape airlift

Relationship between overall gas-holdup and u_{sg} and the angle at the bottom of the contactor and unaerated liquid height

$$\mathcal{E}_o = \frac{0.003u_{sg}^{0.23} B^{0.59}}{h^{0.05}} \quad 4.15$$

Relationship between downcomer liquid velocity and u_{sg} and the angle at the bottom of the contactor and unaerated liquid height

$$V_{Ld} = \frac{1.18u_{sg}^{0.08} h^{1.08}}{B^{0.46}} \quad 4.16$$

Relationship between $k_L a$ and u_{sg} and the angle at the bottom of the contactor and unaerated liquid height

$$k_L a = \frac{0.003u_{sg}^{2.23} B^{1.03}}{h^{0.98}} \quad 4.17$$

The comparison between the predicted hydrodynamics and mass transfer from Eq.4.10-4.17 and the experimental values are shown in Appendix C.

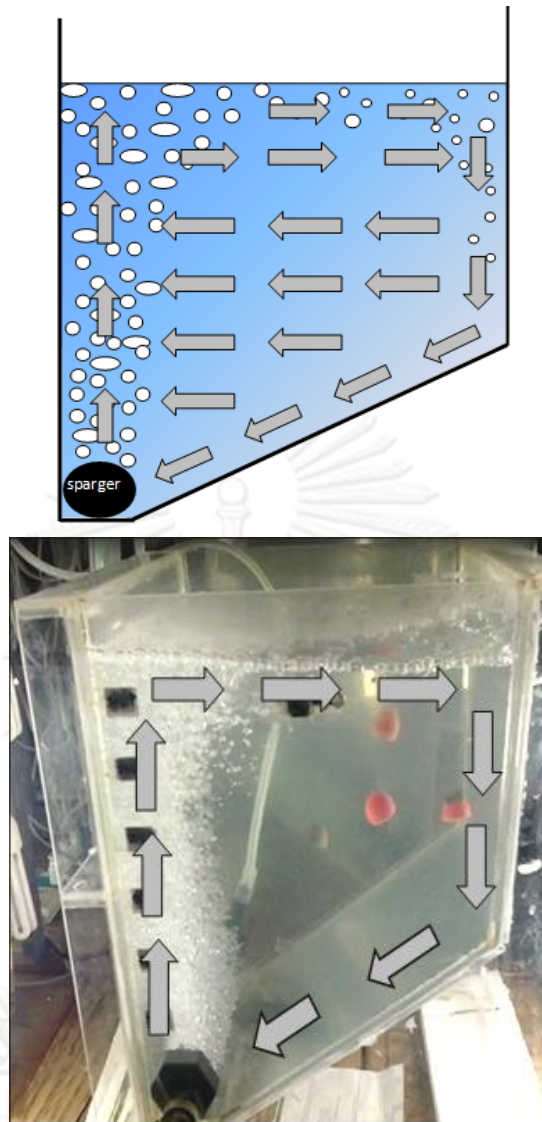


Figure 4.1 Flow directions in NB-FP-ALCs

h \ w	3	6	9	12	15	18	21	24	27	30	33	36	39	42	45	48	50
3	↑	→	→	→	→	→	→	→	→	→	→	→	→	→	→	↓	↓
6	↑	↑	→	→	→	→	→	→	→	→	→	→	↓	↓	↓	↓	↓
9	↑	↑	→	→	→	→	→	→	→	→	→	→	↓	↓	↓	↓	↓
12	↑	↑	→	→	→	→	→	→	→	↓	↓	↓	↓	↓	↓	↓	↓
15	↑	↑	↑	↑	←	←	←	←	←	↓	↓	↓	↓	↓	↓	↓	↓
18	↑	↑	↑	↑	←	←	←	←	←	↓	↓	↓	↓	↓	↓	↓	↓
21	↑	↑	↑	←	←	←	←	←	←	↓	↓	↓	↓	↓	↓	↓	↓
24	↑	↑	↑	←	←	←	←	←	←	↓	↓	↓	↓	↓	↓	↓	↓
27	↑	↑	↑	←	←	←	←	←	←	←	↓	↓	↓	↓	↓	↓	↓
30	↑	↑	↑	←	←	←	←	←	←	←	↓	↓	↓	↓	←	↓	↓
33	↑	↑	↑	←	←	←	←	←	←	←	←	↓	↓	↓	←	←	↓
36	↑	↑	↑	←	←	←	←	←	←	←	←	←	←	←	←	←	↓
39	↑	↑	↑	←	←	←	←	←	←	←	←	←	←	←	←	←	↓
42	↑	↑	↑	←	←	←	←	←	←	←	←	←	←	←	←	←	
45	↑	↑	↑	←	←	←	←	←	←	←	←	←	←	←	←	←	
48	↑	↑	↑	←	←	←	←	←	←	←	←	←	←	←	←	←	
50	↑	↑	↑	←	←	←	←	←	←	←	←	←	←	←	←	←	
54	↑	↑	↑	←	←	←	←	←	←	←	←	←	←	←	←	←	
57	↑	↑	↑	←	←	←	←	←	←	←	←	←	←	←	←	←	
60	↑	↑	↑														



Figure 4.2 Flow directions diagram in NB-FP-ALC at width of contactor 50 cm with unaerated liquid height 60 cm

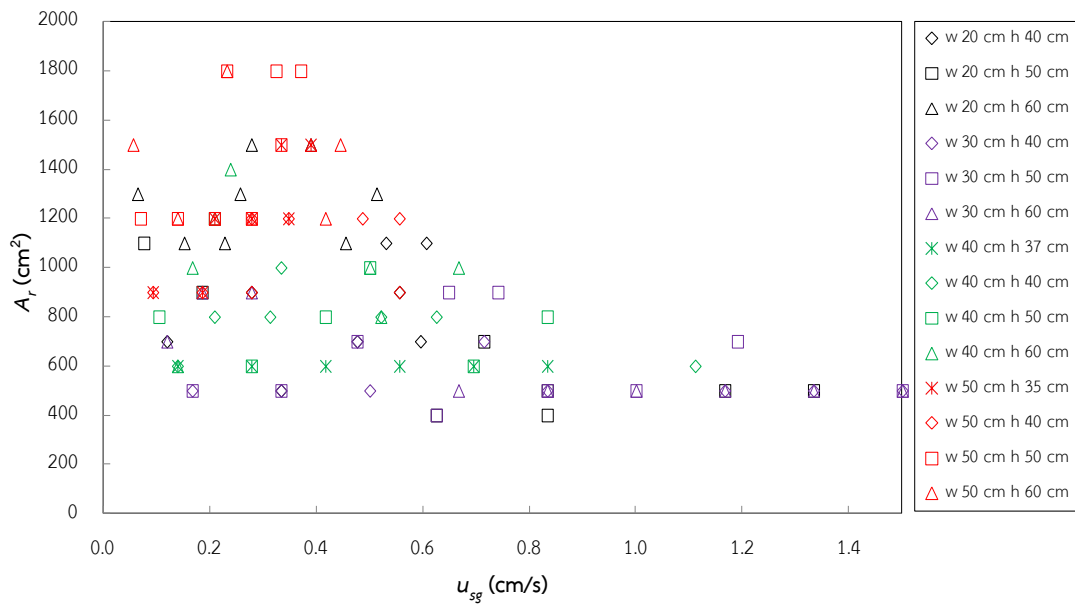


Figure 4.3 Area of riser in NB-FP-ALCs with different widths and unaerated liquid heights

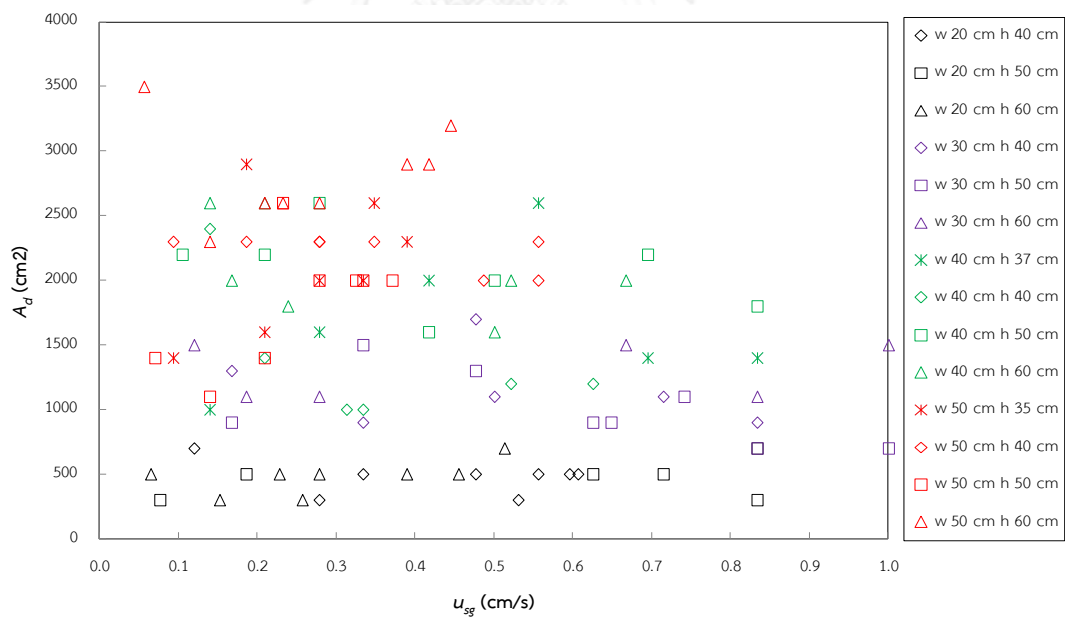


Figure 4.4 Area of downcomer in NB-FP-ALCs with different widths and unaerated liquid heights

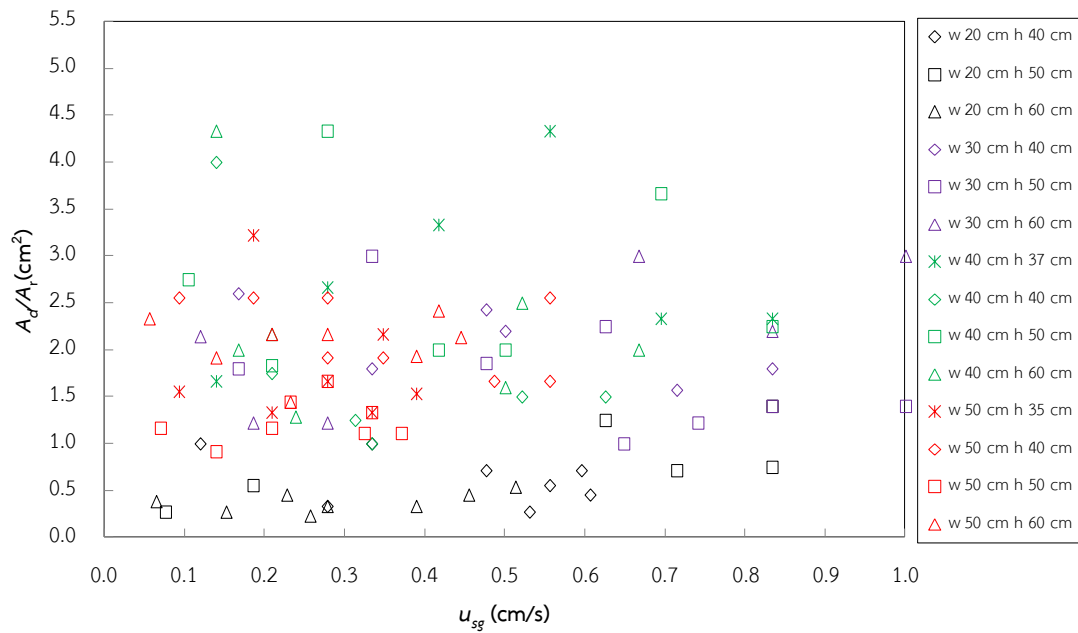


Figure 4.5 Downcomer to riser cross sectional area ratios in NB-FP-ALCs with different widths and un-aerated liquid heights

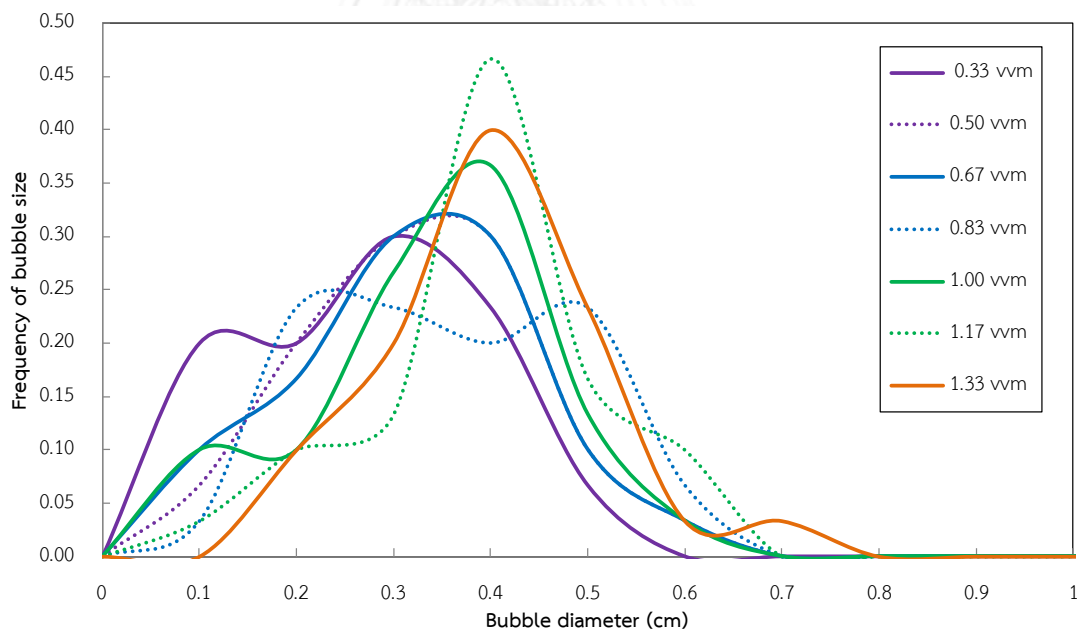


Figure 4.6 Frequency distribution of bubble sizes in NB-FP-ALCs width 20 cm at un-aerated liquid height 40 cm

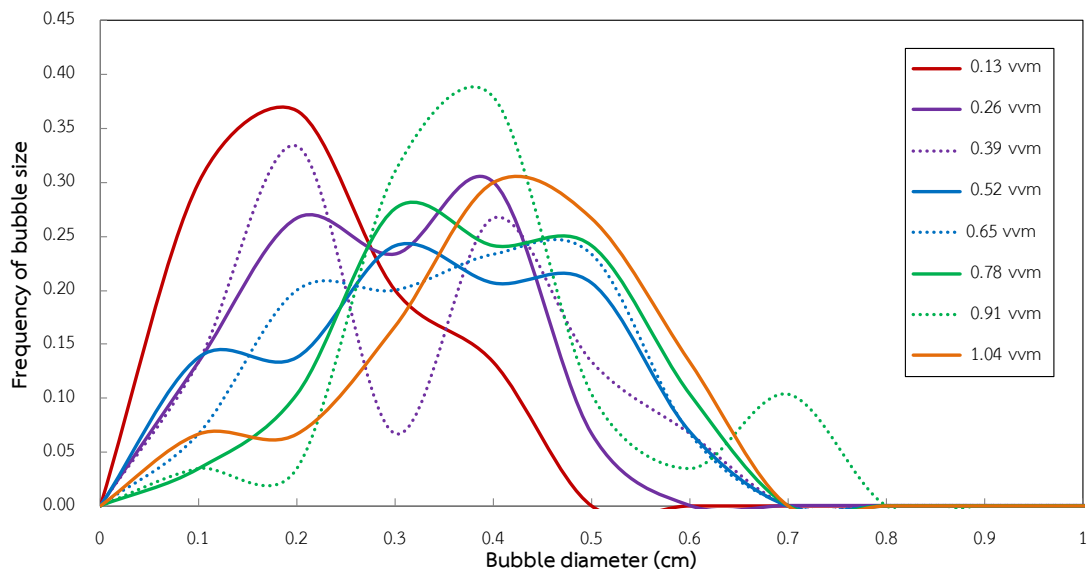


Figure 4.7 Frequency distribution of bubble sizes in NB-FP-ALCs width 20 cm at unaerated liquid height 50 cm

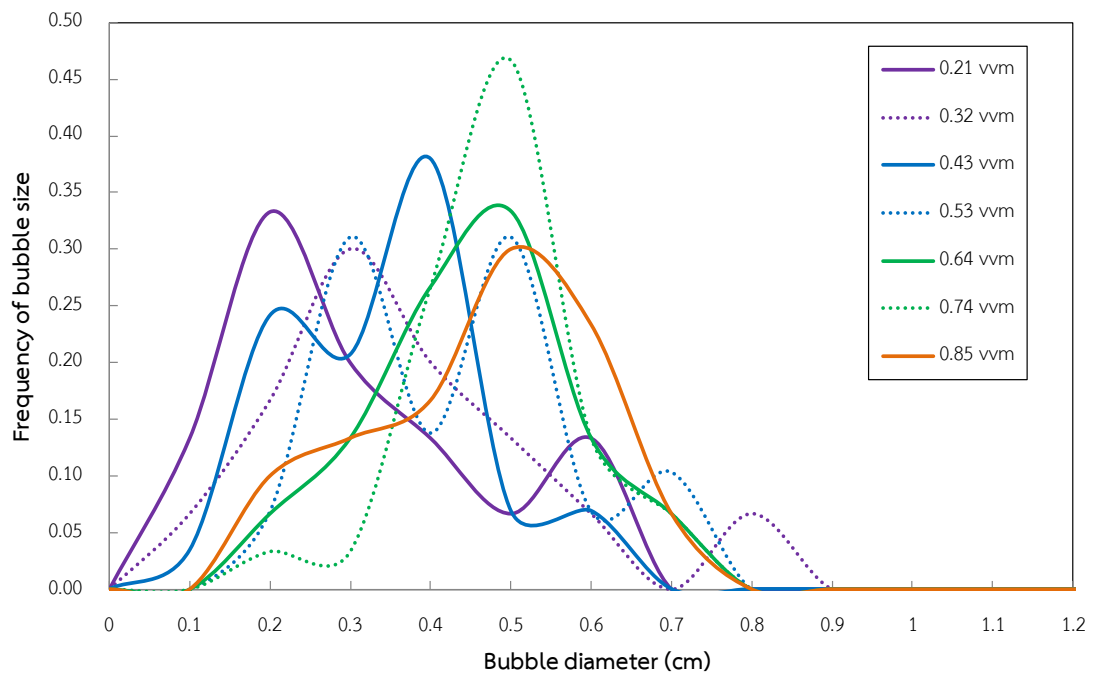


Figure 4.8 Frequency distribution of bubble sizes in NB-FP-ALCs width 20 cm at unaerated liquid height 60 cm

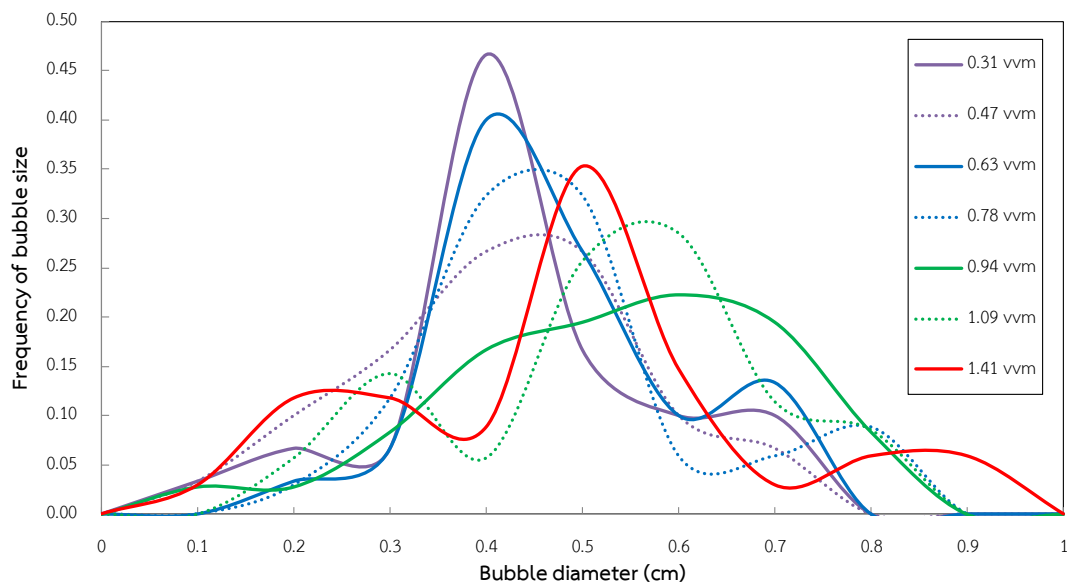


Figure 4.9 Frequency distribution of bubble sizes in NB-FP-ALCs width 30 cm at unaerated liquid height 40 cm

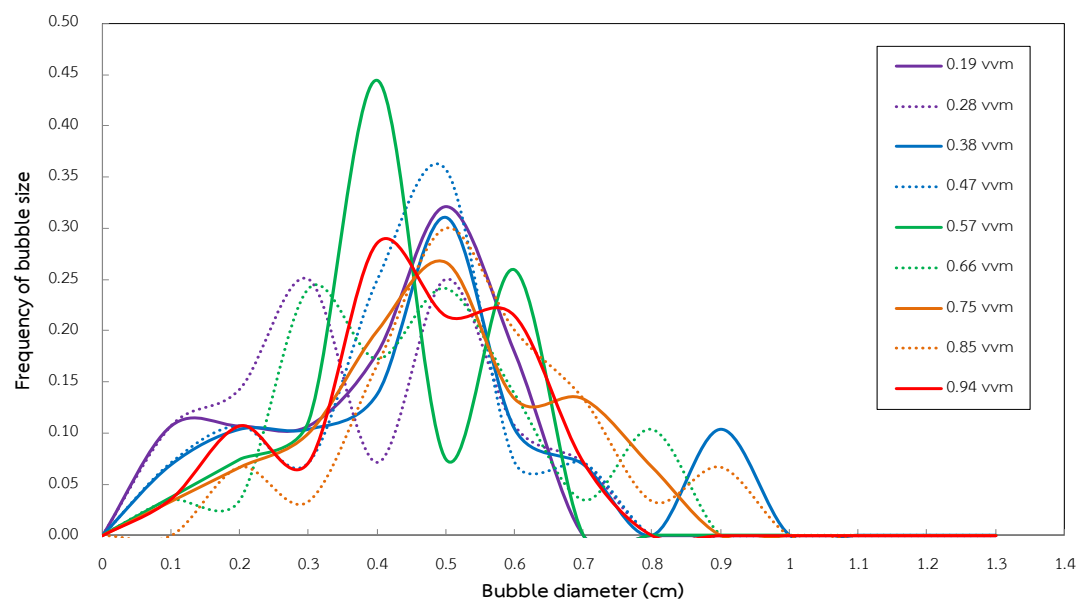


Figure 4.10 Frequency distribution of bubble sizes in NB-FP-ALCs width 30 cm at unaerated liquid height 50 cm

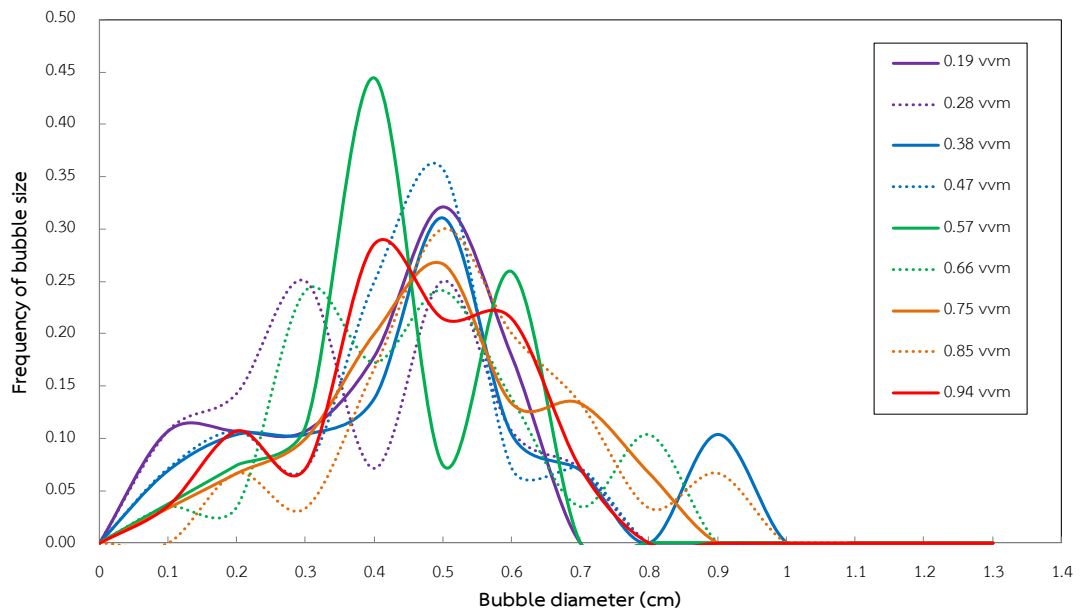


Figure 4.11 Frequency distribution of bubble sizes in NB-FP-ALCs width 30 cm at unaerated liquid height 60 cm

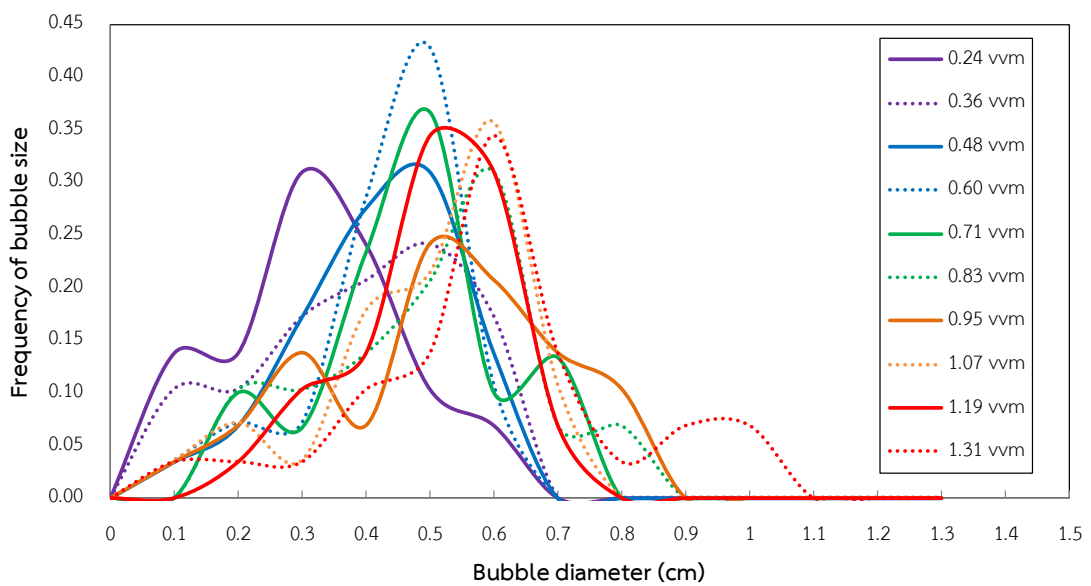


Figure 4.12 Frequency distribution of bubble sizes in NB-FP-ALCs width 40 cm at unaerated liquid height 37 cm

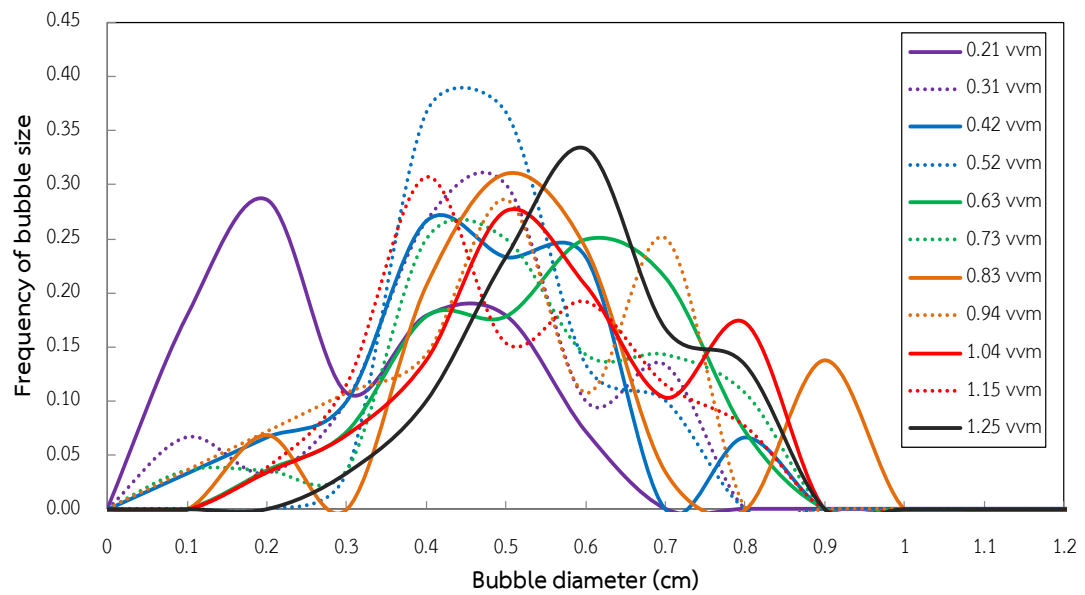


Figure 4.13 Frequency distribution of bubble sizes in NB-FP-ALCs width 40 cm at unaerated liquid height 40 cm

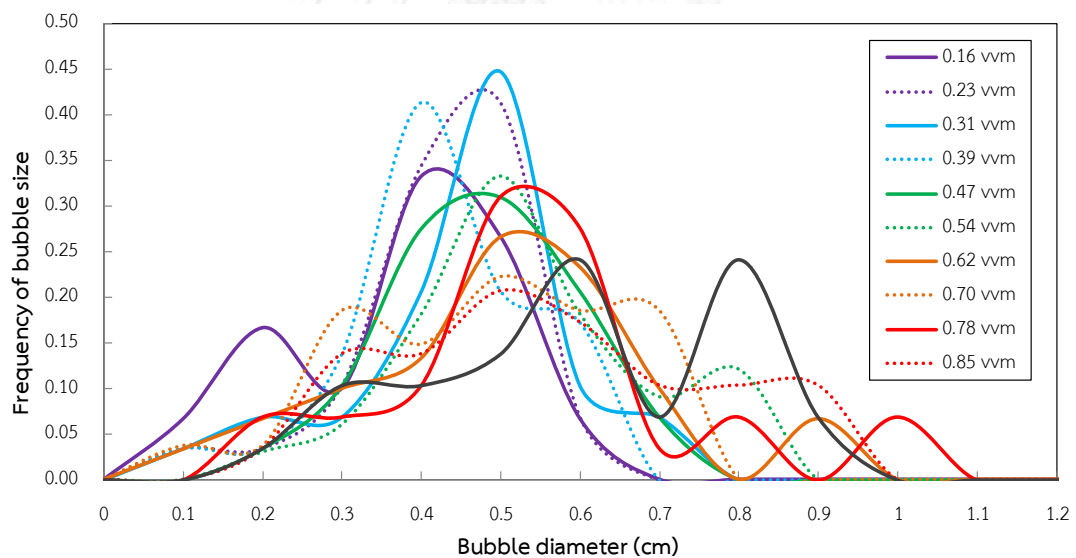


Figure 4.14 Frequency distribution of bubble sizes in NB-FP-ALCs width 40 cm at unaerated liquid height 50 cm

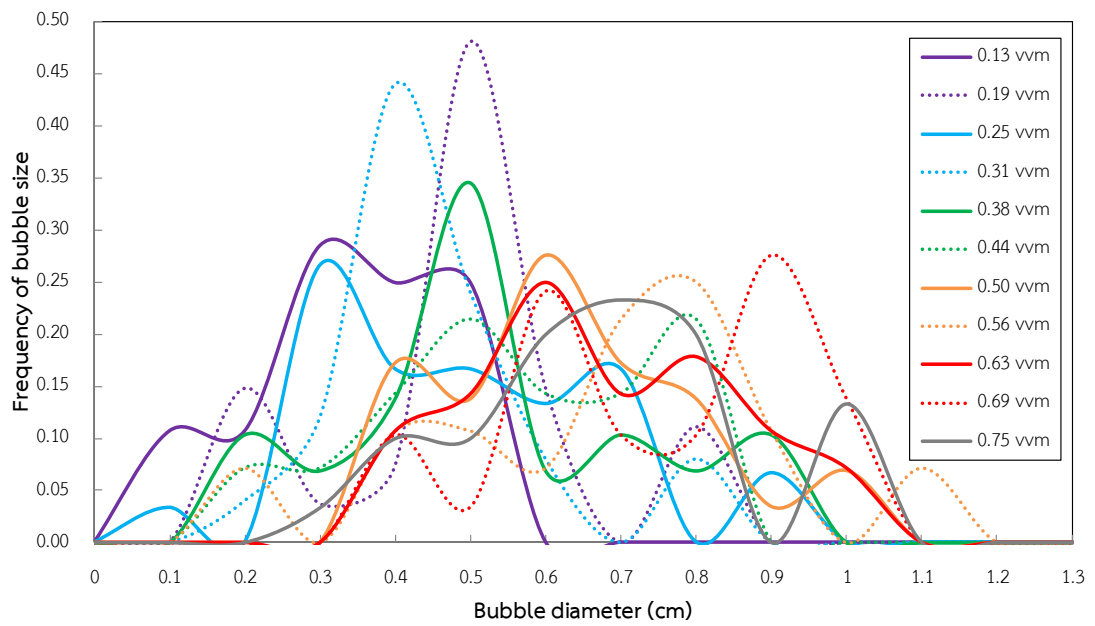


Figure 4.15 Frequency distribution of bubble sizes in NB-FP-ALCs width 40 cm at unaerated liquid height 60 cm

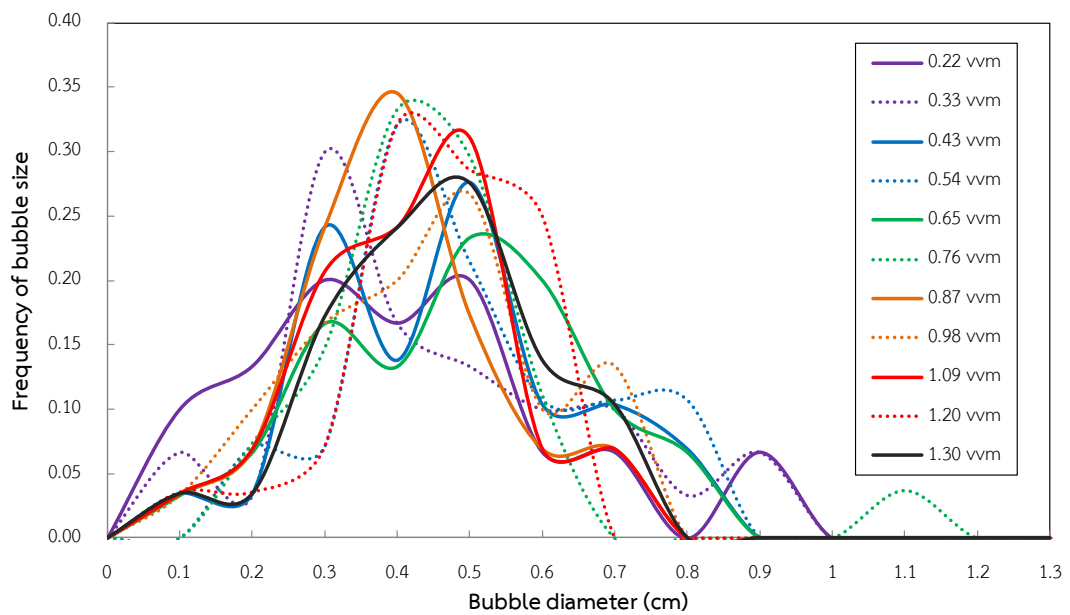


Figure 4.16 Frequency distribution of bubble sizes in NB-FP-ALCs width 50 cm at unaerated liquid height 35 cm

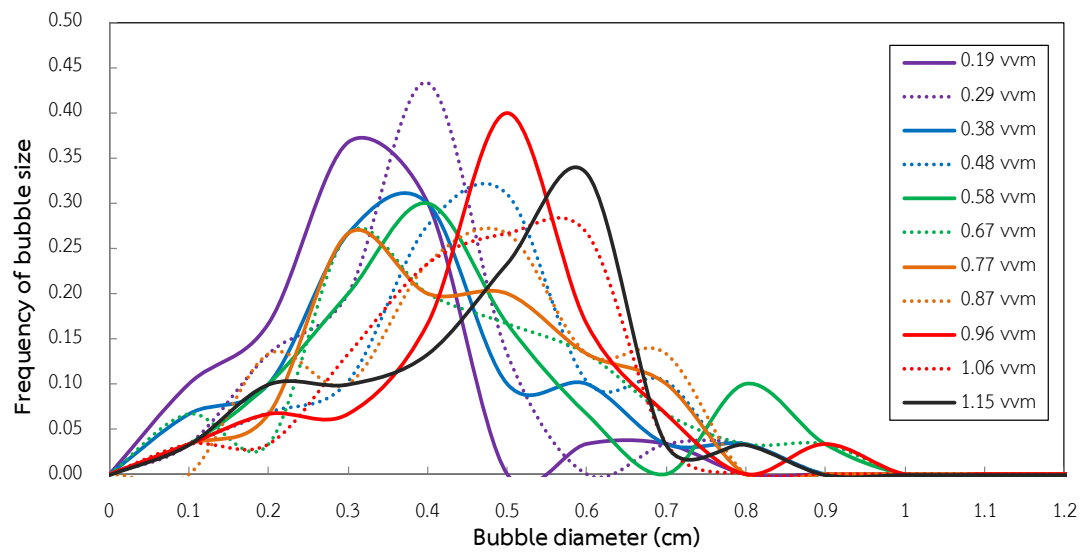


Figure 4.17 Frequency distribution of bubble sizes in NB-FP-ALCs width 50 cm at unaerated liquid height 40 cm

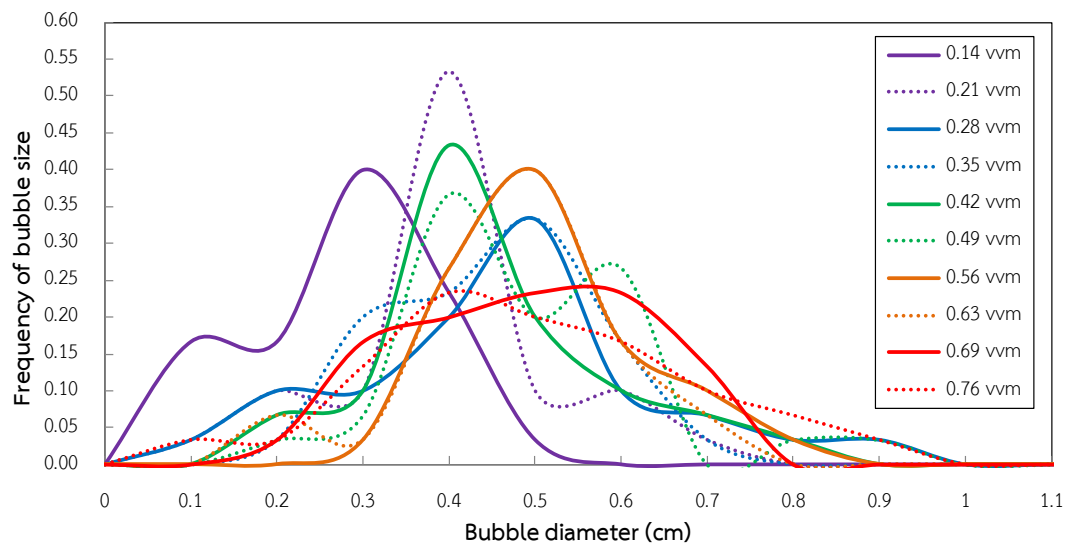


Figure 4.18 Frequency distribution of bubble sizes in NB-FP-ALCs width 50 cm at unaerated liquid height 50 cm

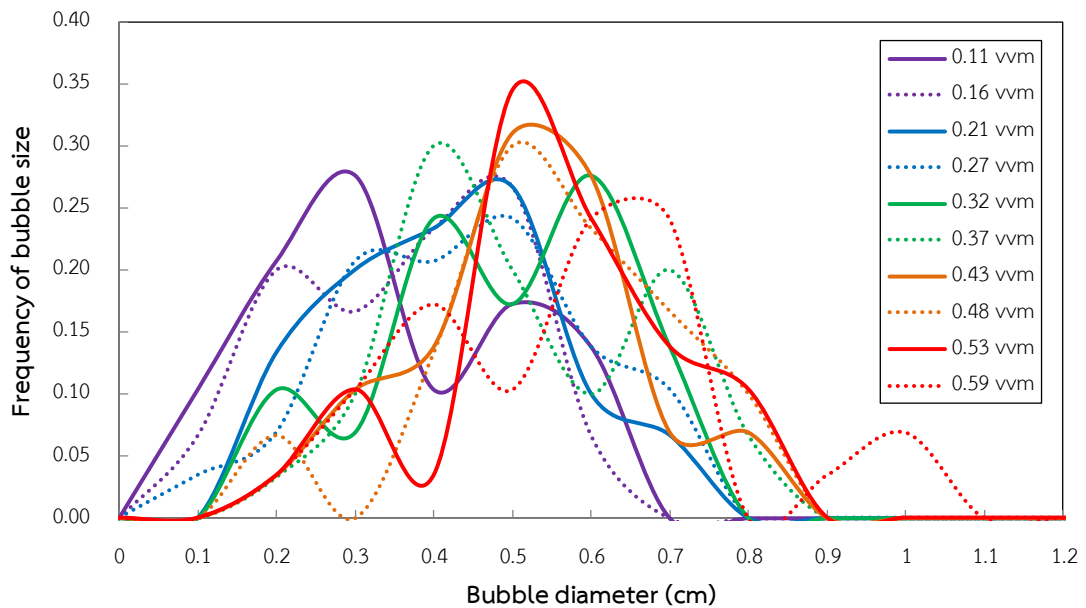


Figure 4.19 Frequency distribution of bubble sizes in NB-FP-ALCs width 50 cm at unaerated liquid height 60 cm

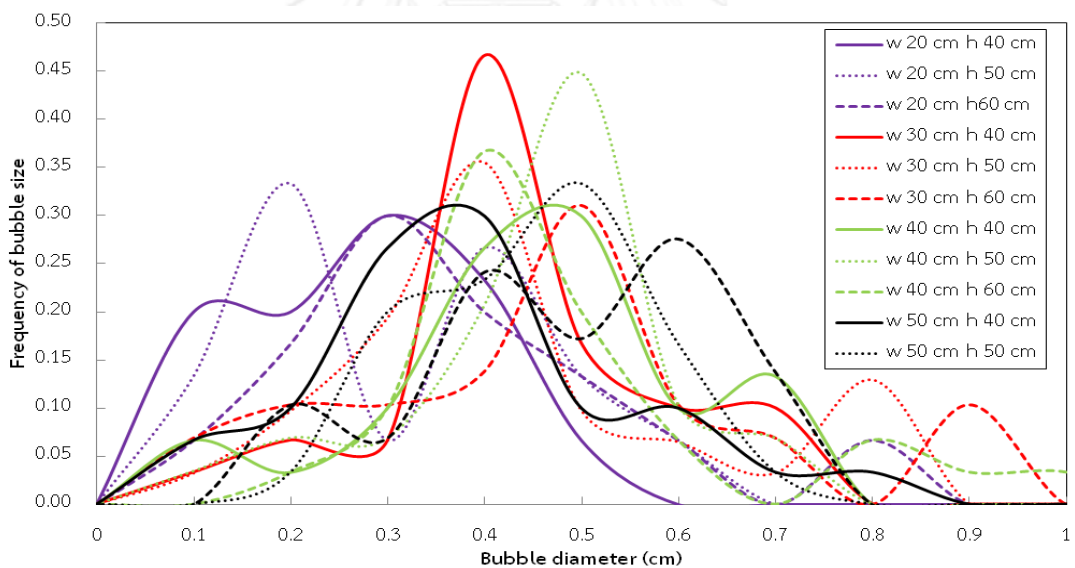


Figure 4.20 Frequency distribution of bubble sizes in NB-FP-ALCs at air flow rate 0.30 - 0.38 vvm with different widths of contactor and various unaerated liquid heights

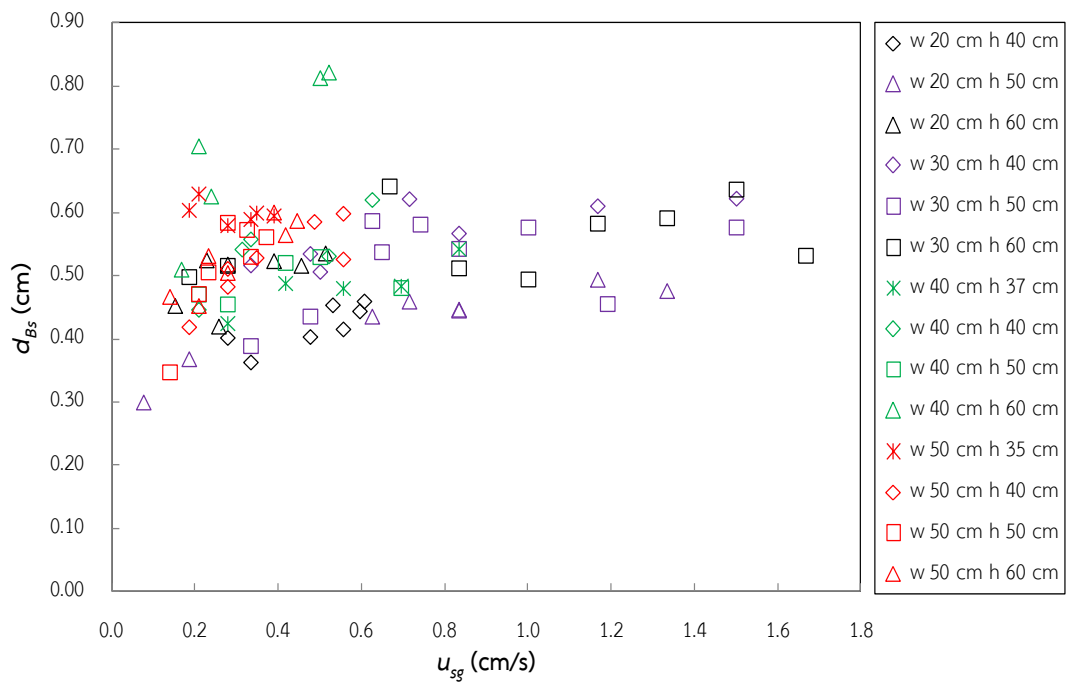


Figure 4.21 Average bubble diameter (d_{Bs}) in NB-FP-ALCs with different widths and unaerated liquid heights

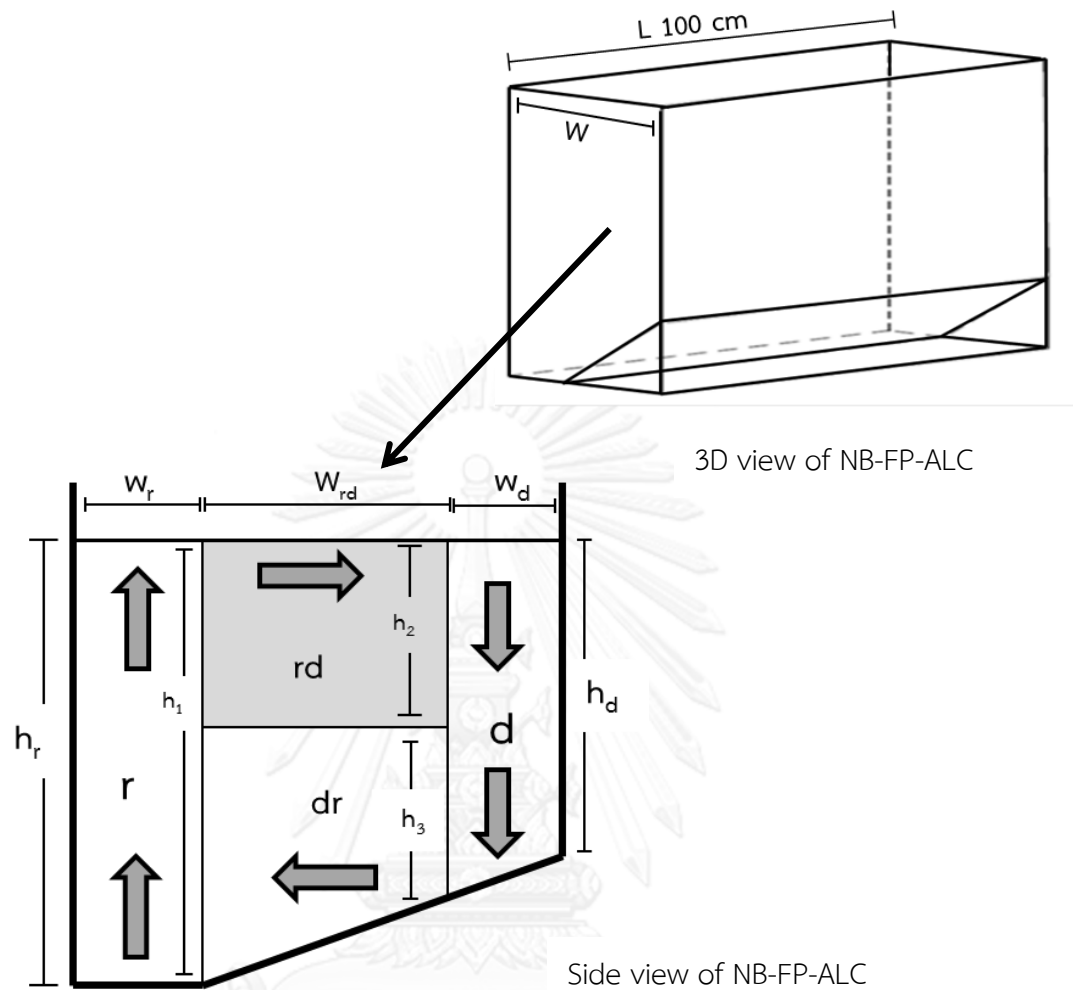


Figure 4.22 Section in NB-FP-ALC

For a definite V = volume (cm^3)

W = width of section (cm)

L = length of contactor (cm)

h = unaerated liquid height (cm)

subscript r = riser

d = downcomer

rd = rd cross flow (\rightarrow)

dr = dr cross flow (\leftarrow)

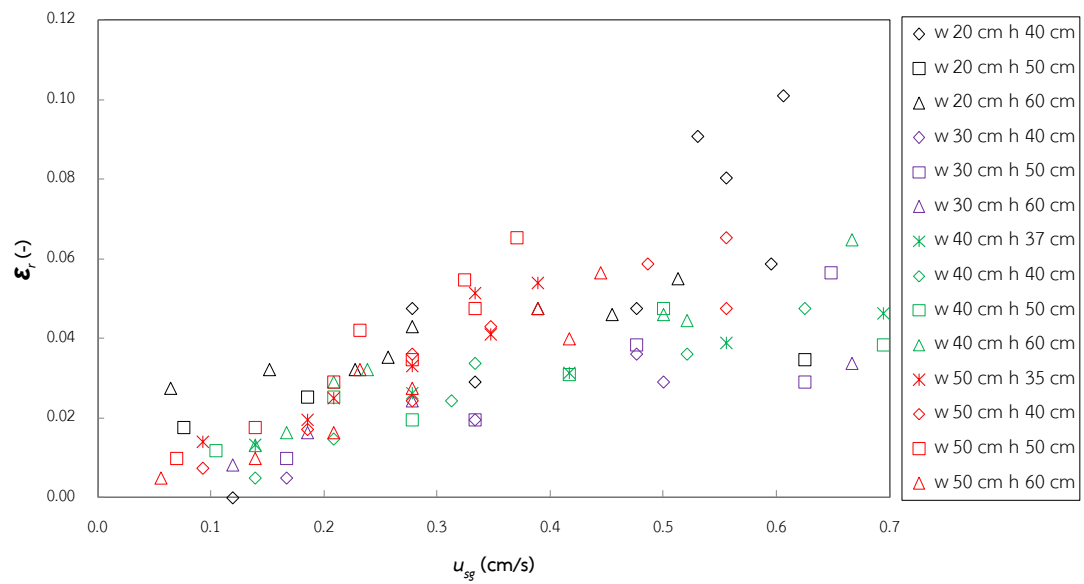


Figure 4.23 Gas-holdup in riser of NB-FP-ALCs with different widths and unaerated liquid heights

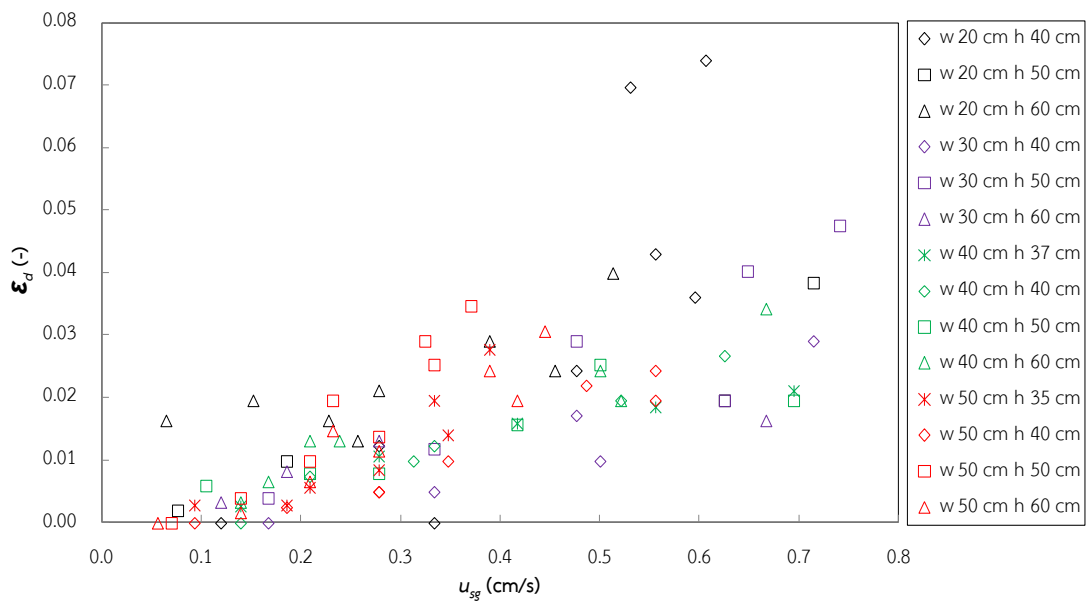


Figure 4.24 Gas-holdup in downcomer of NB-FP-ALCs with different widths and unaerated liquid heights

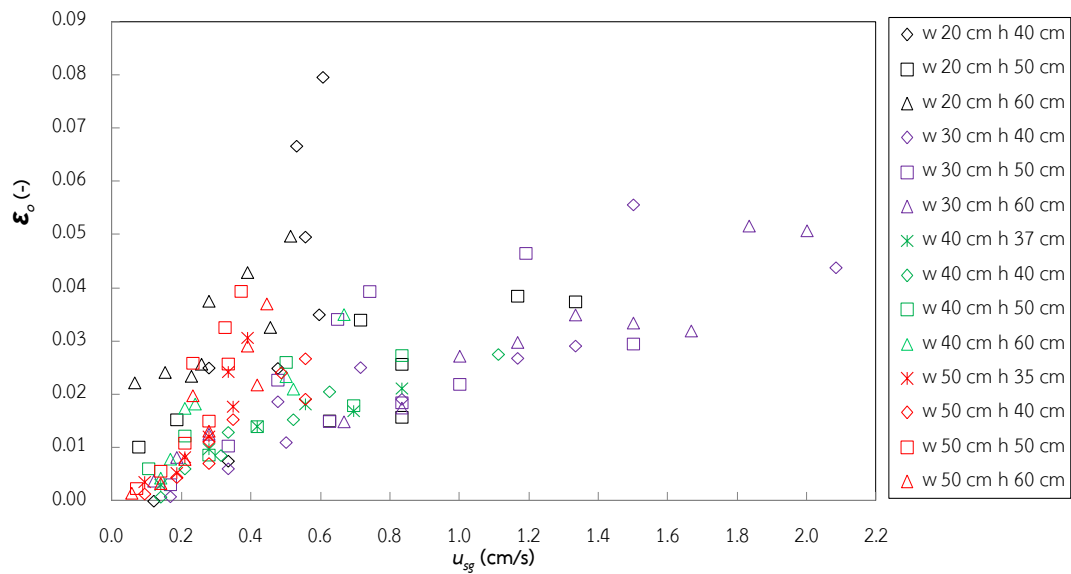


Figure 4.25 Overall gas-holdup in NB-FP-ALCs with different widths and unaerated liquid heights

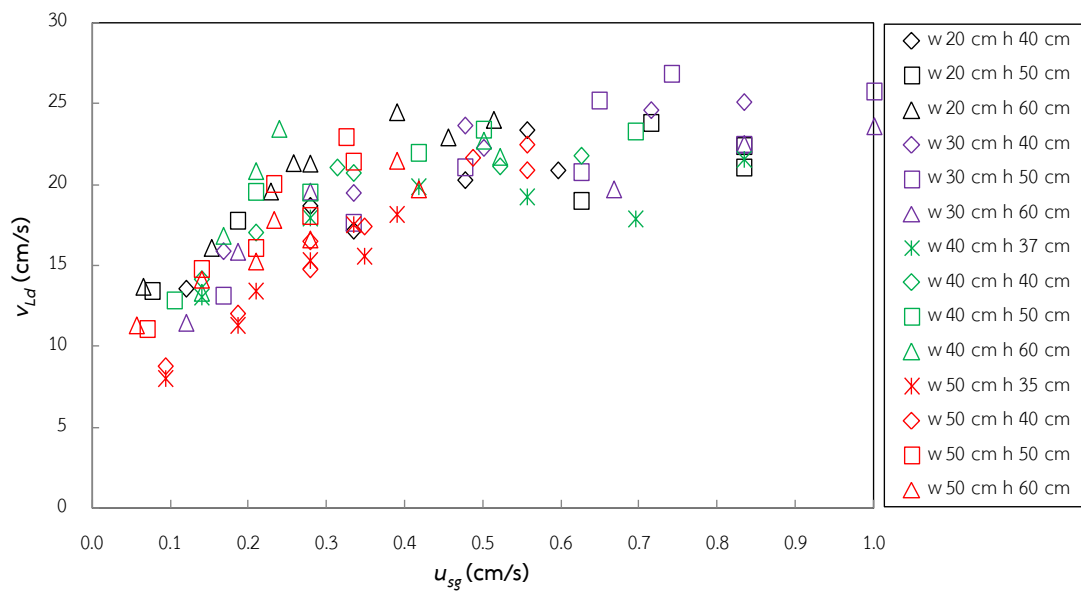


Figure 4.26 Downcomer liquid velocity in NB-FP-ALCs with different widths and unaerated liquid heights

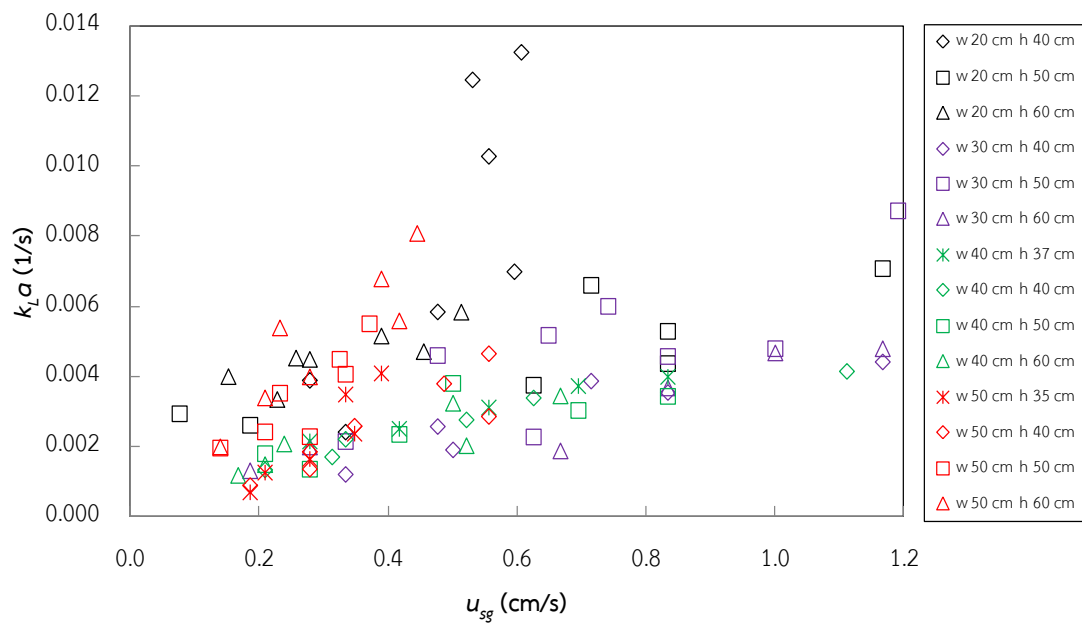


Figure 4.27 $k_L a$ in NB-FP-ALCs with different widths and un-aerated liquid heights

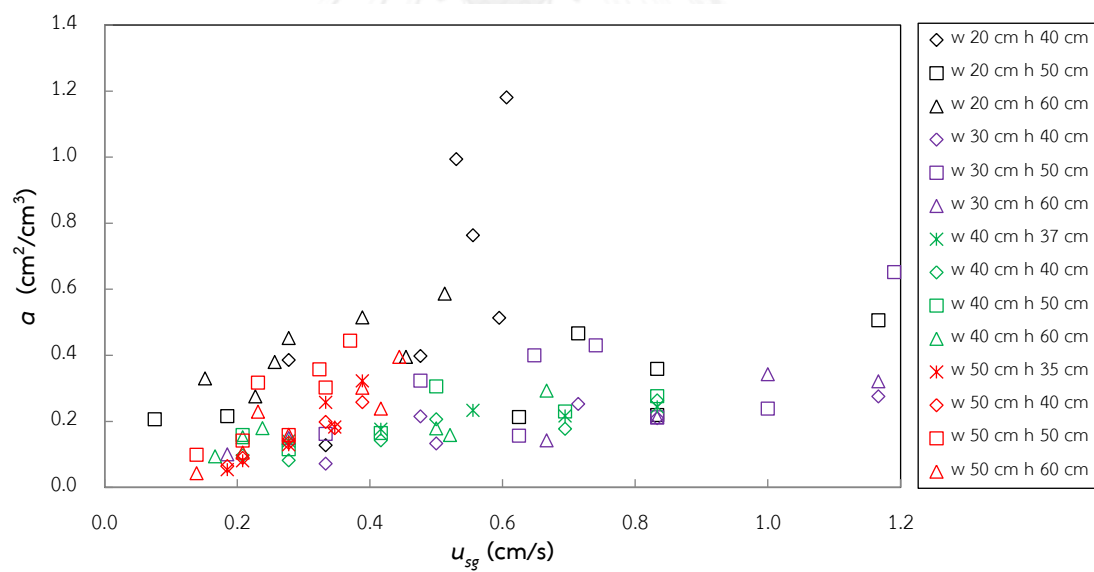


Figure 4.28 Specific interfacial area (a) in NB-FP-ALCs with different widths and un-aerated liquid heights

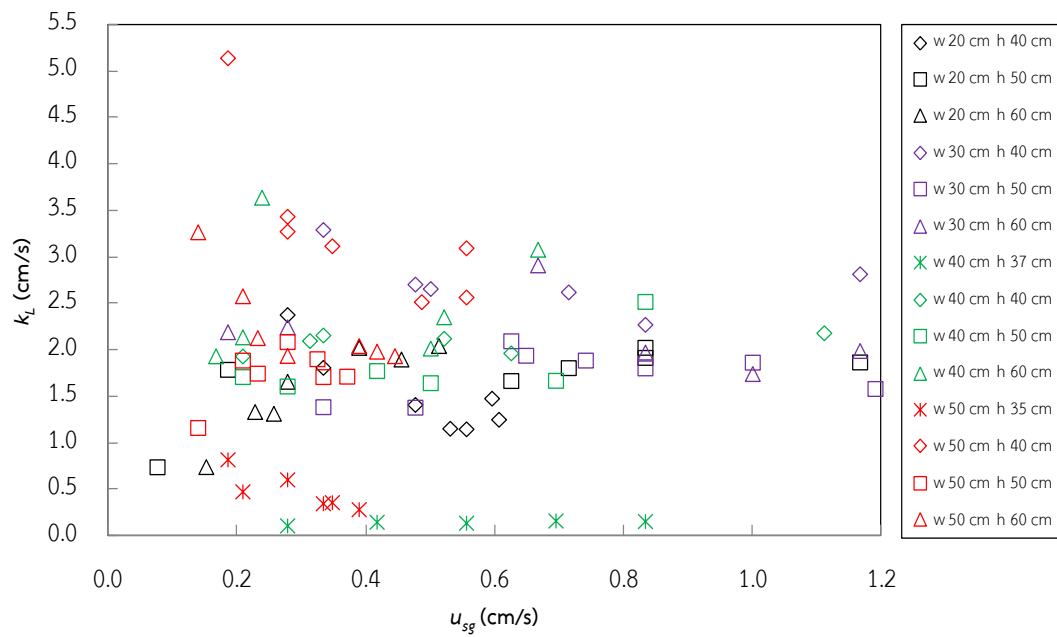


Figure 4.29 Overall gas-liquid mass transfer coefficient (k_L) in NB-FP-ALCs with different width of contactors and un-aerated liquid heights

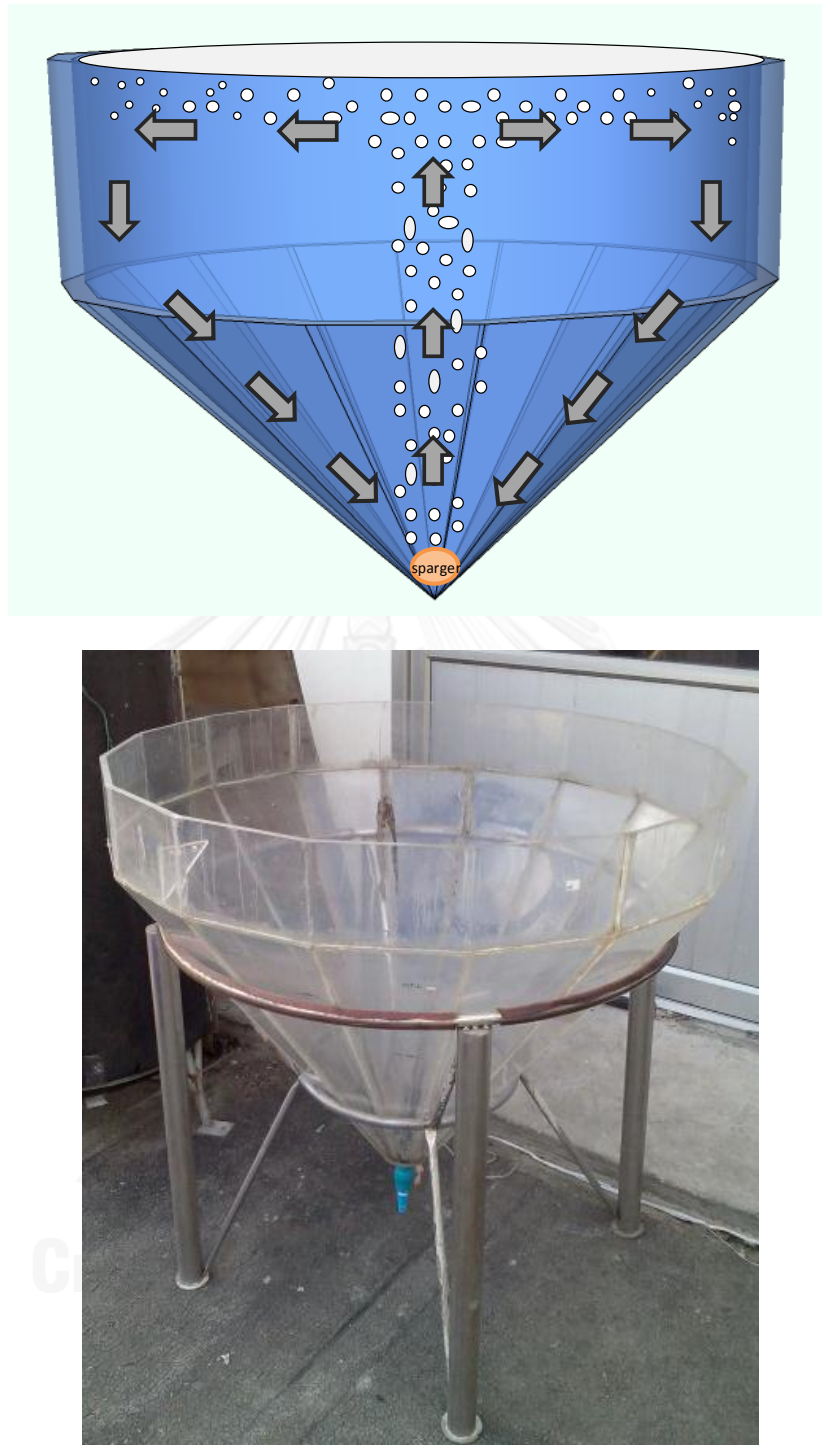


Figure 4.30 Flow directions in NB-C-ALCs

h \ w	3	6	9	12	15	18	21	24	27	30	33	36	39	42	45	48	50
3	↑	↑	→	→	→	→	→	→	→	→	→	→	→	→	↓	↓	↓
6	↑	↑	↑	→	↑	←	←	→	→	→	→	→	→	↓	↓	↓	↓
9	↑	↑	↑	↑	↑	←	←	→	→	→	→	→	↓	↓	↓	↓	↓
12	↑	↑	↑	↑	↑	←	←	←	→	→	←	↓	↓	↓	↓	↓	↓
15	↑	↑	↑	↑	↑	←	←	←	←	←	←	↓	↓	↓	↓	↓	↓
18	↑	↑	↑	↑	↑	←	←	←	←	←	←	↓	↓	↓	↓		
21	↑	↑	↑	↑	↑	←	←	←	←	←	←	←	←				
24	↑	↑	↑	↑	←	←	←	←	←	←	←	←					
27	↑	↑	↑	↑	←	←	←	←	←	←	←						
30	↑	↑	↑	←	←	←	←	←	←	←							
33	↑	↑	↑	←	←	←	←	←									
36	↑	↑	↑	←	←	←	←										
39	↑	↑	↑	←	←												
42	↑	↑	↑	←													
45	↑	↑	↑														
48	↑	↑															
50	↑																



Figure 4.31 Flow directions diagram of NB-C-ALC at the angle of bottom 30° with unaerated liquid height 50 cm and air flow rate 0.15 vvm

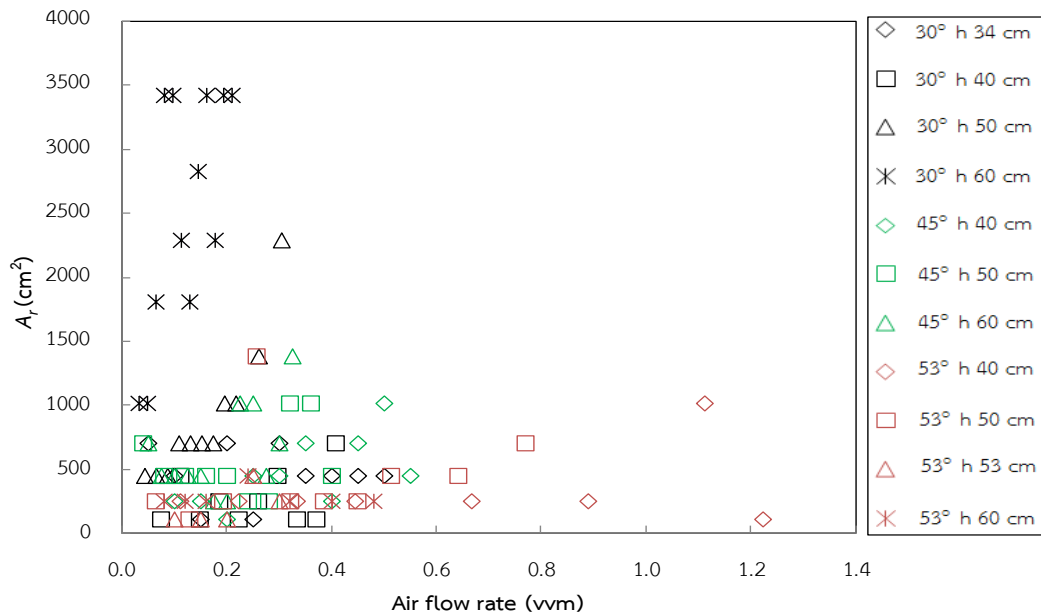


Figure 4.32 Area of riser in NB-C-ALCs with different the angles of bottom and un-aerated liquid heights

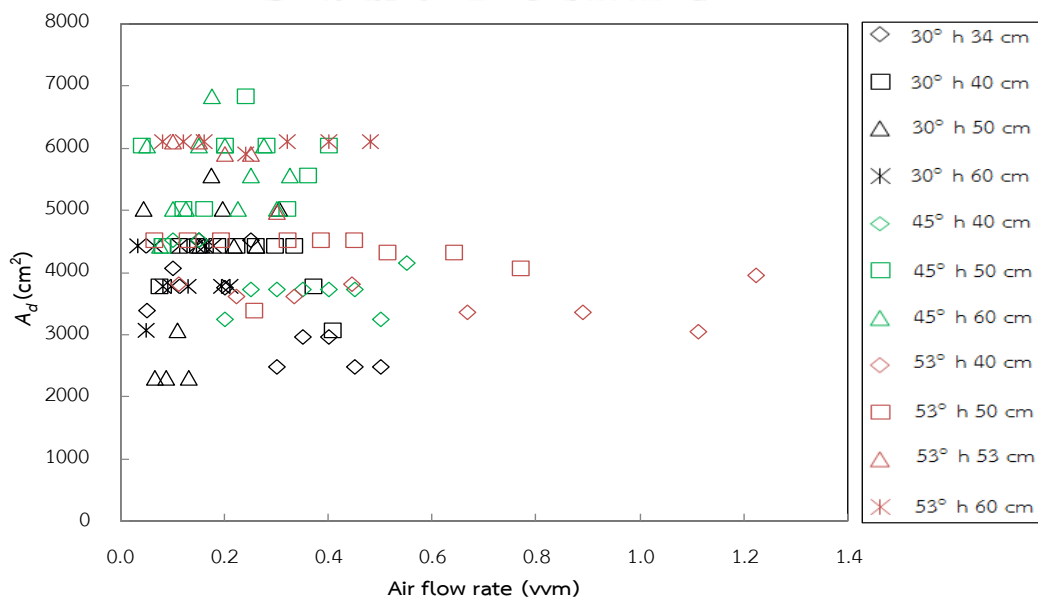


Figure 4.33 Area of downcomer in NB-C-ALCs with different the angles of bottom and un-aerated liquid heights

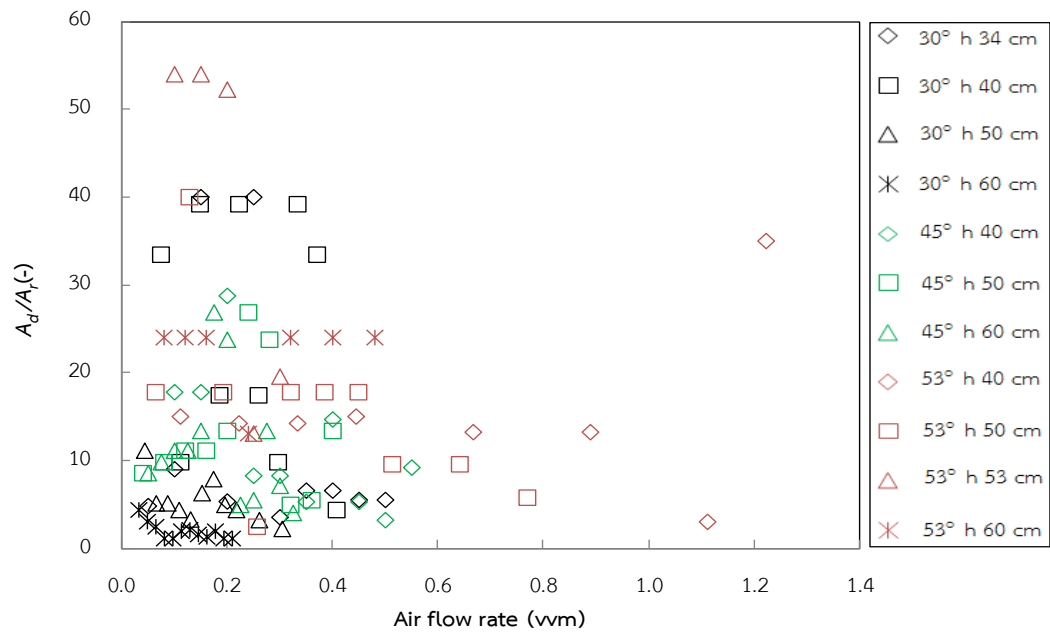


Figure 4.34 A_d/A_r ratio in NB-C-ALCs with different the angles of bottom and un-aerated liquid heights

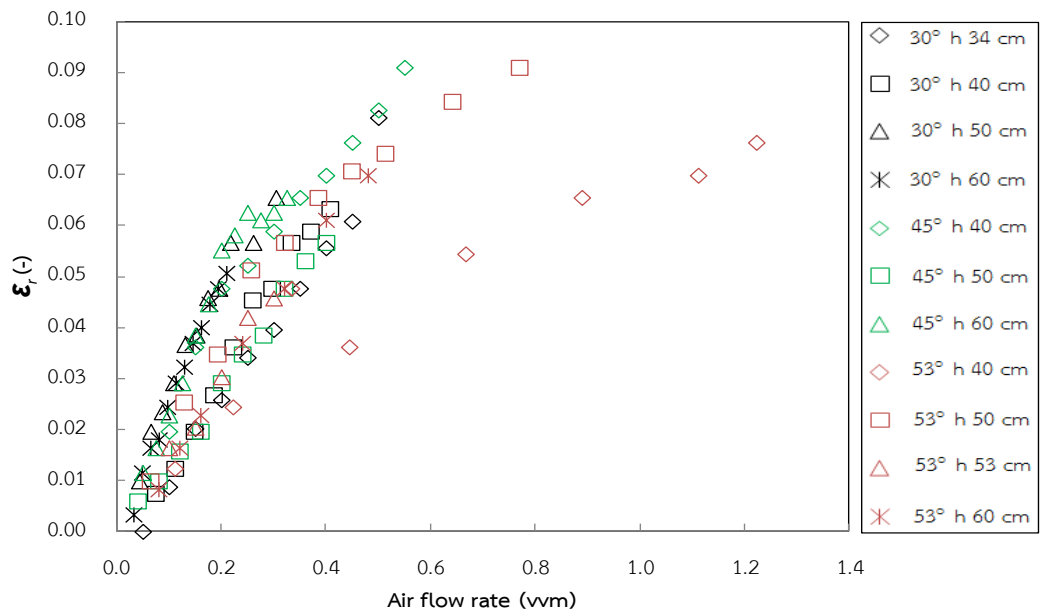


Figure 4.35 Riser gas-holdup in NB-C-ALCs with different the angles of bottom and un-aerated liquid heights

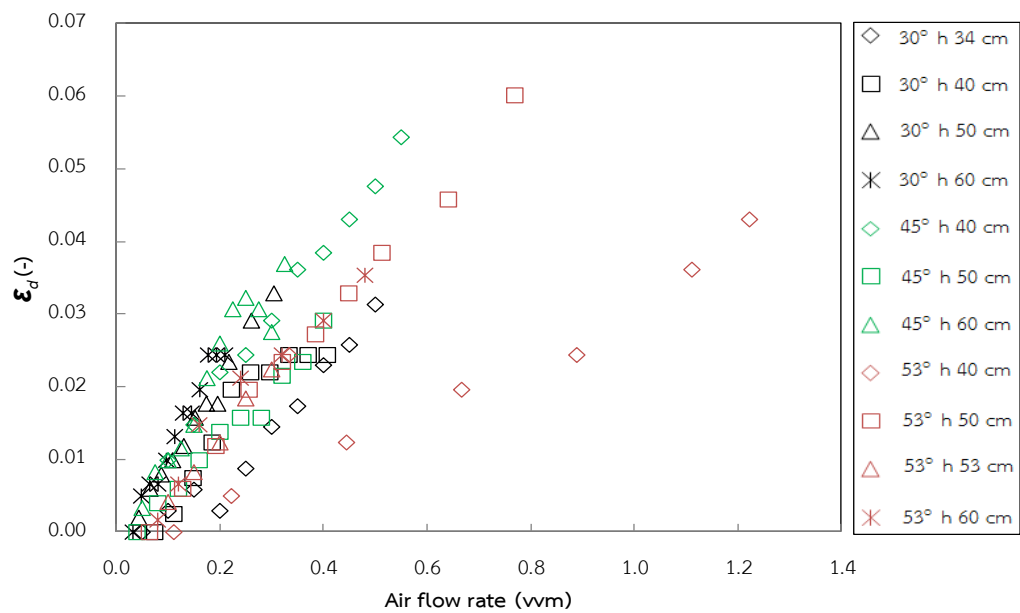


Figure 4.36 Downcomer gas-holdup in NB-C-ALCs with different the angles of bottom and un-aerated liquid heights

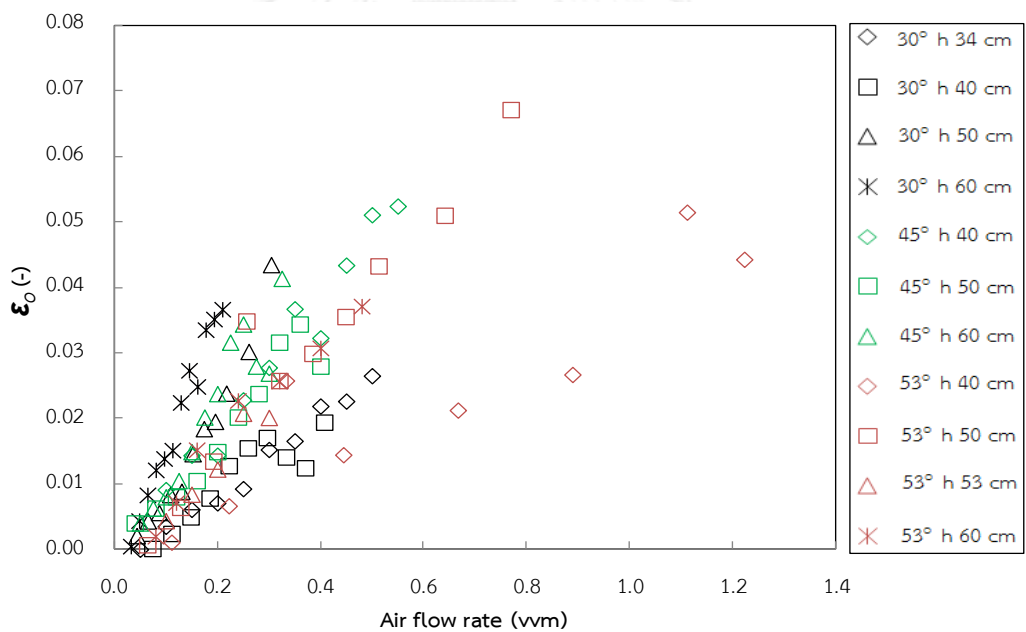


Figure 4.37 Overall gas-holdup in NB-C-ALCs with different the angles of bottom and un-aerated liquid heights

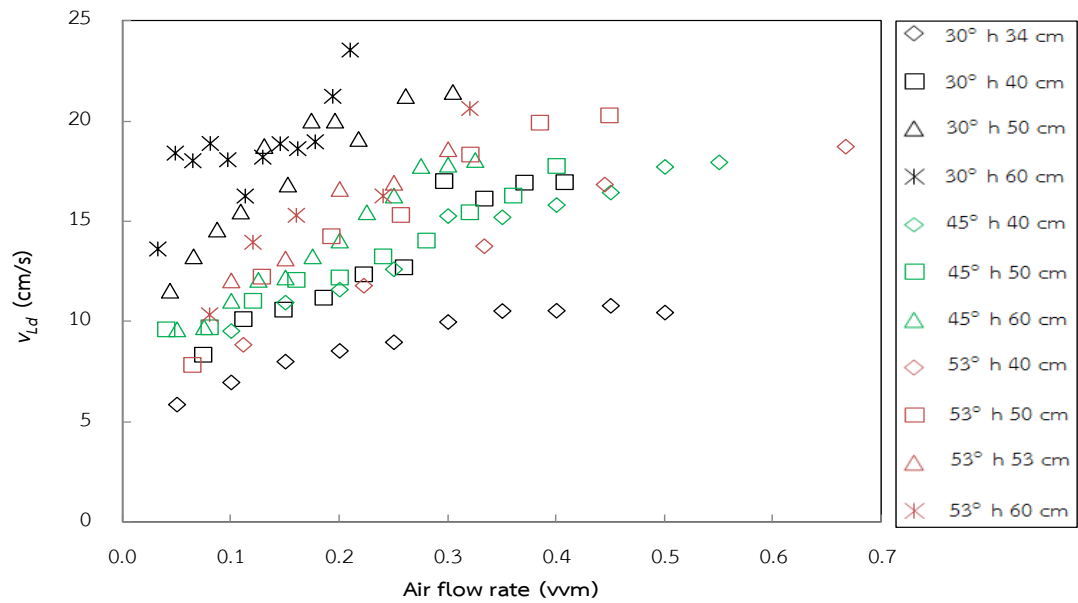


Figure 4.38 Downcomer liquid velocity in NB-C-ALCs with different the angles of bottom and un-aerated liquid heights

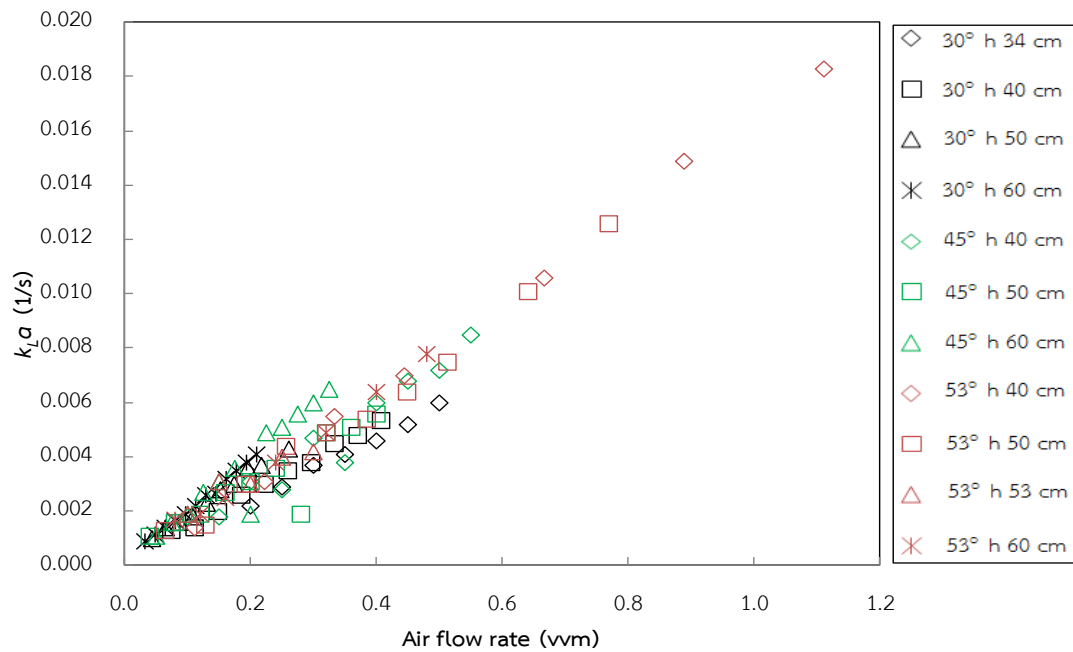


Figure 4.39 $k_L a$ in NB-C-ALCs with different the angles of bottom and un-aerated liquid heights

CHAPTER V

CONCLUSIONS & RECOMMENDATIONS

5.1 Conclusions

- Air flow rate has a strong effect on hydrodynamic and mass transfer both of NB-FP-ALCs and NB-C-ALCs.
- Most of A_d/A_r were constant and did not depend on air flow rate and unaerated liquid height.
- Hydrodynamic and mass transfer of NB-FP-ALCs except liquid velocity that increased with the width of the contactor from 30 to 50 cm. However, hydrodynamic and mass transfers of width of contactor 20 cm were high taking similar values with those from the contactor with 50 cm width. This was due to the differences in the riser and downcomer induced in the contactors of various widths.
- An increase in unaerated liquid height enhanced downcomer liquid velocity both in NB-FP-ALCs and NB-C-ALCs.
- Gas holdups in NB-C-ALCs were the highest when the angle of the cone bottom was 30° .
- The $k_L a$ of NB-C-ALCs depended on air flow rate but did not depend on the angles of the bottom of the contactor and unaerated liquid heights.

5.2 Contributions

Airlift contactor was developed to be an alternative reactor for the systems that do not need a very high mass transfer, but requires the cyclic fluid flow to promote a relatively high mixing. Typical of airlift contactors have a draft tube or a partition for the separation of riser and downcomer sections. This complicating arrangement causes problems at the installation and the maintenance of such systems. The systems also suffered from the lack of information when it comes to scale up to pilot or industrial scale. It was shown in our previous work that the flat panel airlift configuration allowed an easy scale up as this could be achieved by extending the length of the reactor, where the system behavior remained unaltered. By removing

the draft tube or separating plate, along with the design of the contactor, the novel contactor in this experiment could be installed, operated, and maintained with ease. The information regarding the behavior of the flat panel airlift from this work will be useful in the application of such reactors and the expansion of this reactor to a larger scale system. In the following table, the performance of the airlift contactors used in this work is compared with the reported value.

Table 5.1 Summary the hydrodynamic and mass transfer in airlift contactors

References	Type contactor	Hydrodynamics		$k_L a_L$ (1/s)
		Overall gas-holdup (-)	Liquid velocity (cm/s)	
This study	NB-FP-ALCs (u_{sg} 0.1 - 0.8 cm/s)	0 - 0.08	7 - 27	0.001 - 0.014
	NB-C-ALCs (u_{sg} 0.1 - 4 cm/s)	0 - 0.07	5 - 24	0.001 - 0.018
Issarapayup (2011)	FP-ALPBRs (u_{sg} 0.2 -3.0 cm/s)	-	2 - 10	0.0003 - 0.006
Linthong (2008)	Multiple draft tube of large scale airlift (u_{sg} 0.5 cm/s)	0.008	25	0.002

5.3 Recommendations

There are several limitations on the typical measurement techniques as employed in this work. A more accurate measure/monitor of various system parameters will allow a better prediction of the system performance. Future work might be directed towards the proposition of new measurement techniques as follows:

1. Gas-holdup: the volume expansion was very sensitive and could be easily misled.
2. The photographic technique of bubble size distribution should be taken in riser as this was the location where most gas-liquid mass transfer took place.

REFERENCES

- Al-Masry, W. and A. E. Abasaeed, 1998: On the scale-up of external loop airlift reactors: Newtonian systems. *Chemical engineering science*, **53**, 4085-4094.
- Bentifraouine, C., C. Xuereb and J.-P. Riba, 1997: Effect of gas liquid separator and liquid height on the global hydrodynamic parameters of an external loop airlift contactor. *Chemical Engineering Journal*, **66**, 91-95.
- Blažej, M., M. Kiša and J. Markoš, 2004: Scale influence on the hydrodynamics of an internal loop airlift reactor. *Chemical Engineering and Processing: Process Intensification*, **43**, 1519-1527.
- Cerri, M. and A. Badino, 2010: Oxygen transfer in three scales of concentric tube airlift bioreactors. *Biochemical Engineering Journal*, **51**, 40-47.
- Chisti, Y., 1989: *Airlift Bioreactors*. Elsevier, London and New York.
- Choi, K., Y. Chisti and M. Moo-Young, 1996: Comparative evaluation of hydrodynamic and gas—liquid mass transfer characteristics in bubble column and airlift slurry reactors. *The Chemical Engineering Journal and the Biochemical Engineering Journal*, **62**, 223-229.
- Deng, Z., T. Wang, N. Zhang and Z. Wang, 2010: Gas holdup, bubble behavior and mass transfer in a 5m high internal-loop airlift reactor with non-Newtonian fluid. *Chemical Engineering Journal*, **160**, 729-737.
- Freitas, C., M. Fialová, J. Zahradnik and J. A. Teixeira, 1999: Hydrodynamic model for three-phase internal-and external-loop airlift reactors. *Chemical engineering science*, **54**, 5253-5258.
- Gavrilescu, M. and R. Tudose, 1998: Concentric-tube airlift bioreactors. *Bioprocess Engineering*, **19**, 37-44.
- Heijnen, J., J. Hols, R. Van Der Lans, H. Van Leeuwen, A. Mulder and R. Weltevrede, 1997: A simple hydrodynamic model for the liquid circulation velocity in a full-scale two-and three-phase internal airlift reactor operating in the gas recirculation regime. *Chemical Engineering Science*, **52**, 2527-2540.
- Hsiun, D.-Y. and W.-T. Wu, 1995: Mass transfer and liquid mixing in an airlift reactor with a net draft tube. *Bioprocess Engineering*, **12**, 221-225.
- Juraščík, M., M. Blažej, J. Annus and J. Markoš, 2006: Experimental measurements of volumetric mass transfer coefficient by the dynamic pressure-step method in internal loop airlift reactors of different scale. *Chemical Engineering Journal*, **125**, 81-87.

- Kilonzo, P. M., A. Margaritis, M. Bergougnou, J. Yu and Q. Ye, 2007: Effects of geometrical design on hydrodynamic and mass transfer characteristics of a rectangular-column airlift bioreactor. *Biochemical Engineering Journal*, **34**, 279-288.
- Kochbeck, B. and D. C. Hempel, 1994: Liquid velocity and dispersion coefficient in an airlift reactor with inverse internal loop. *Chemical engineering & technology*, **17**, 401-405.
- Korpijarvi, J., P. Oinas and J. Reunanen, 1999: Hydrodynamics and mass transfer in an airlift reactor. *Chemical engineering science*, **54**, 2255-2262.
- Krichnavaruk, S., W. Loataweesup, S. Powtongsook and P. Pavasant, 2005: Optimal growth conditions and the cultivation of *Chaetoceros calcitrans* in airlift photobioreactor. *Chemical Engineering Journal*, **105**, 91-98.
- Lau, Y., K. T. Sujatha, M. Gaeini, N. Deen and J. Kuipers, 2013: Experimental study of the bubble size distribution in a pseudo-2D bubble column. *Chemical Engineering Science*, **98**, 203-211.
- Littlejohns, J. V. and A. J. Daugulis, 2009: Oxygen mass transfer and hydrodynamics in a multi-phase airlift bioscrubber system. *Chemical Engineering Science*, **64**, 4171-4177.
- Lu, X., J. Ding, Y. Wang and J. Shi, 2000: Comparison of the hydrodynamics and mass transfer characteristics of a modified square airlift reactor with common airlift reactors. *Chemical Engineering Science*, **55**, 2257-2263.
- Luo, L., F. Liu, Y. Xu and J. Yuan, 2011: Hydrodynamics and mass transfer characteristics in an internal loop airlift reactor with different spargers. *Chemical Engineering Journal*, **175**, 494-504.
- Merchuk, J. C., N. Ladwa, A. Cameron, M. Bulmer, I. Berzin and A. M. Pickett, 1996: Liquid flow and mixing in concentric tube air-lift reactors. *Journal of Chemical Technology and Biotechnology*, **66**, 174-182.
- Ruen-ngam, D., P. Wongsuchoto, A. Limpanuphap, T. Charinpanitkul and P. Pavasant, 2008: Influence of salinity on bubble size distribution and gas-liquid mass transfer in airlift contactors. *Chemical Engineering Journal*, **141**, 222-232.
- Šimčík, M., A. Mota, M. Ruzicka, A. Vicente and J. Teixeira, 2011: CFD simulation and experimental measurement of gas holdup and liquid interstitial velocity in internal loop airlift reactor. *Chemical Engineering Science*, **66**, 3268-3279.
- Wongsuchoto, P., 2002: Bubble Characteristics and Liquid Circulation in Internal Loop Airlift Contactor. *Chemical Engineering*. Chulalongkorn University, Bangkok, Thailand.

Wongsuchoto, P. and P. Pavasant, 2004: Internal liquid circulation in annulus sparged internal loop airlift contactors. *Chemical Engineering Journal*, **100**, 1-9.

Wu, W. T., J. Y. Wu and J. Z. Jong, 1992: Mass transfer in an airlift reactor with a net draft tube. *Biotechnology progress*, **8**, 465-468.

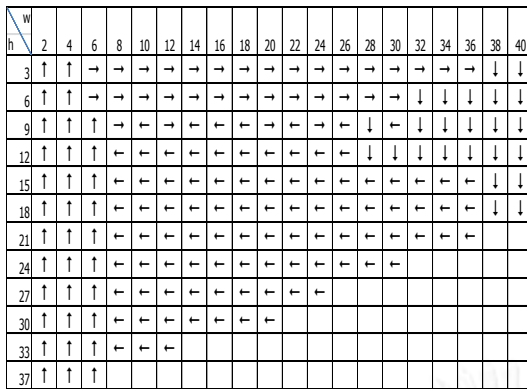


จุฬาลงกรณ์มหาวิทยาลัย
CHULALONGKORN UNIVERSITY

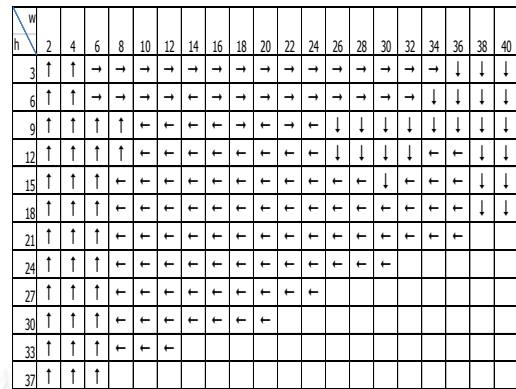


APPENDIX

จุฬาลงกรณ์มหาวิทยาลัย
CHULALONGKORN UNIVERSITY

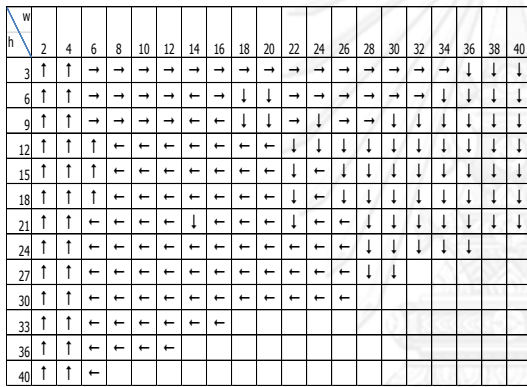


Air flow rate 0.59 vvm

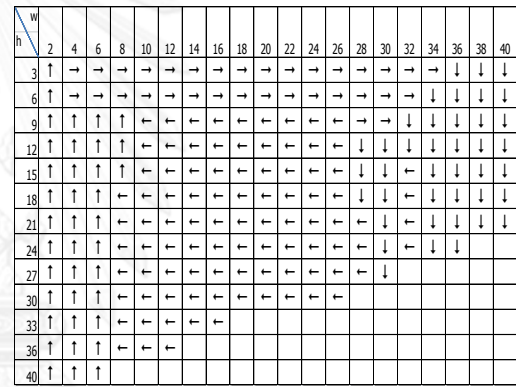


Air flow rate 0.71 vvm

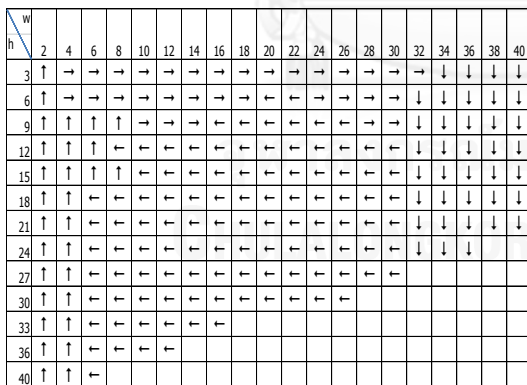
Flow diagram of NB-FP-ALC at w 40 cm h 40 cm



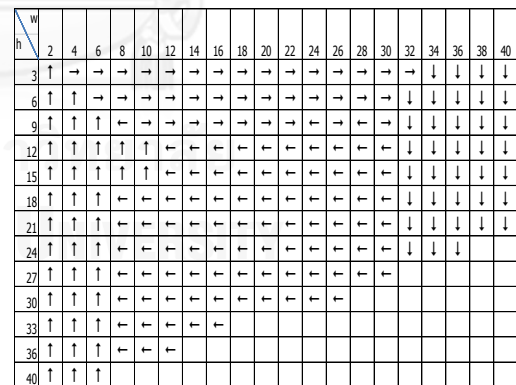
Air flow rate 0.10 vvm



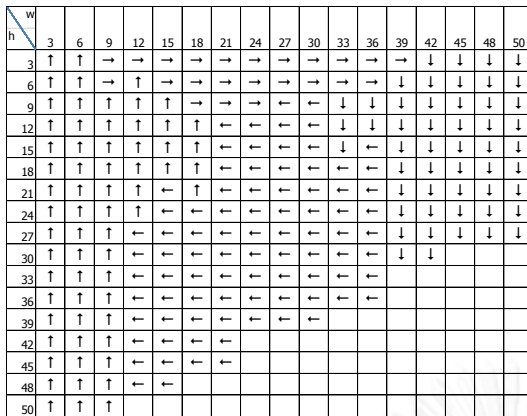
Air flow rate 0.21 vvm



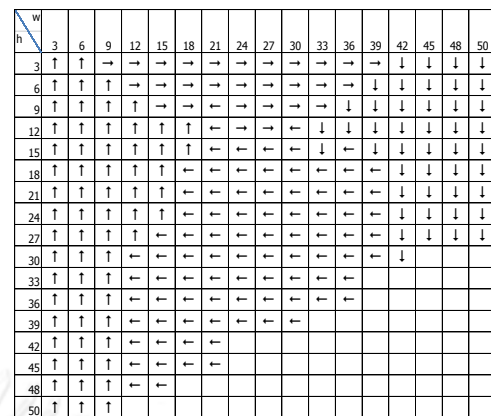
Air flow rate 0.31 vvm



Air flow rate 0.42 vvm

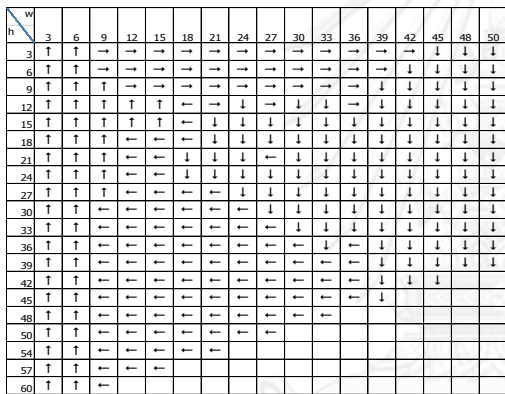


Air flow rate 0.49 vvm

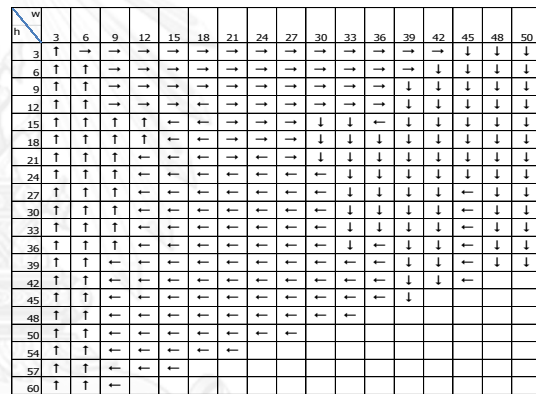


Air flow rate 0.56 vvm

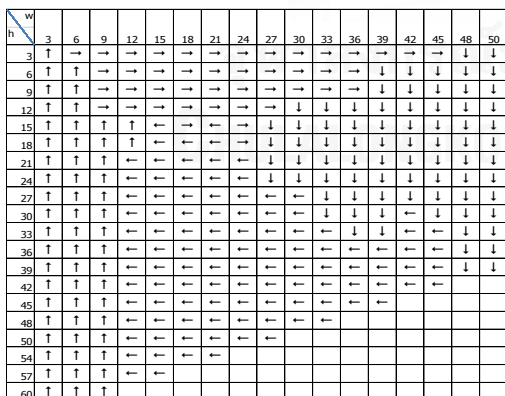
Flow diagram of NB-FP-ALC at w 50 cm h 60 cm



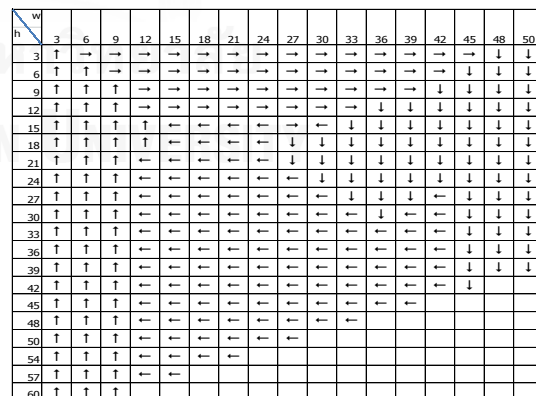
Air flow rate 0.05 vvm



Air flow rate 0.12 vvm



Air flow rate 0.16 vvm



Air flow rate 0.21 vvm

Flow diagram of NB-C-ALC 45° h 40 cm

h \ w	3	6	9	12	15	18	21	24	27	30	33	36	39
3	↑	→	→	→	→	→	→	→	→	→	→	↓	↓
6	↑	↑	→	→	→	→	→	←	↓	↓	↓	↓	
9	↑	↑	↑	←	←	←	↓	←	↓	↓	↓		
12	↑	↑	↑	←	←	←	↓	↓	↓	↓			
15	↑	↑	↑	←	←	←	↓	↓	↓				
18	↑	↑	←	←	←	←	↓	↓					
21	↑	↑	←	←	←	←	↓						
24	↑	↑	←	←	←	←							
27	↑	↑	←	←	←								
30	↑	↑	←	←									
33	↑	↑	←										
36	↑	↑											
40	↑												

h \ w	3	6	9	12	15	18	21	24	27	30	33	36	39
3	→	→	→	→	→	→	→	→	→	→	↓	↓	↓
6	↑	↑	→	←	←	←	←	←	→	↓	↓	↓	
9	↑	↑	←	←	←	←	←	←	←	←	↓		
12	↑	↑	←	←	←	←	←	←	←	←			
15	↑	↑	←	←	←	←	←	←	←				
18	↑	↑	←	←	←	←	←	←					
21	↑	↑	←	←	←	←	←						
24	↑	↑	←	←	←	←							
27	↑	↑	←	←	←								
30	↑	↑	←	←									
33	↑	↑	←										
36	↑	↑											
40	↑												

Air flow rate 0.10 vvm

h \ w	3	6	9	12	15	18	21	24	27	30	33	36	39
3	→	→	→	→	→	→	→	→	→	→	↓	↓	↓
6	→	→	→	→	←	←	→	→	←	↓	↓	↓	
9	↑	↑	↑	↑	←	←	←	←	←	←	↓		
12	↑	↑	↑	↑	←	←	←	←	←				
15	↑	↑	↑	←	←	←	←	←	←				
18	↑	↑	↑	←	←	←	←	←					
21	↑	↑	←	←	←	←	←						
24	↑	↑	←	←	←	←							
27	↑	↑	←	←	←								
30	↑	↑	←	←									
33	↑	↑	←										
36	↑	↑											
40	↑												

Air flow rate 0.15 vvm

h \ w	3	6	9	12	15	18	21	24	27	30	33	36	39
3	→	→	→	→	→	→	→	→	→	→	↓	↓	↓
6	↑	↑	→	→	→	→	→	←	↓	↓	↓	↓	
9	↑	↑	↑	↑	→	→	→	→	↓	↓	↓		
12	↑	↑	↑	↑	←	←	←	←	←	↓			
15	↑	↑	↑	←	←	←	←	←	←				
18	↑	↑	↑	←	←	←	←	←					
21	↑	↑	←	←	←	←	←						
24	↑	↑	←	←	←	←							
27	↑	↑	←	←	←								
30	↑	↑	←	←									
33	↑	↑	←										
36	↑	↑											
40	↑												

Air flow rate 0.20 vvm

h \ w	3	6	9	12	15	18	21	24	27	30	33	36	39
3	→	→	→	→	→	→	→	→	→	→	↓	↓	↓
6	→	→	↑	→	→	→	→	→	→	↓	↓	↓	
9	↑	↑	↑	↑	↑	←	←	←	←	←	↓		
12	↑	↑	↑	↑	↑	←	←	←	←	↓			
15	↑	↑	↑	←	←	←	←	←	←	↓			
18	↑	↑	↑	←	←	←	←	←					
21	↑	←	←	←	←	←	←						
24	↑	←	←	←	←	←							
27	↑	←	←	←	←								
30	↑	←	←	←									
33	↑	←	←										
36	↑	←											
40	↑												

Air flow rate 0.25 vvm

h \ w	3	6	9	12	15	18	21	24	27	30	33	36	39
3	→	→	→	→	→	→	→	→	→	→	↓	↓	↓
6	↑	↑	↑	→	→	→	→	→	→	↓	↓	↓	
9	↑	↑	↑	↑	→	→	→	→	→	↓	↓	↓	
12	↑	↑	←	←	←	←	←	←	←	↓	↓		
15	↑	↑	←	←	←	←	←	←	←	↓			
18	↑	←	←	←	←	←	←	←					
21	↑	←	←	←	←	←	←						
24	↑	←	←	←	←	←							
27	↑	←	←	←	←								
30	↑	←	←	←									
33	↑	←	←										
36	↑	←											
40	↑												

Air flow rate 0.30 vvm

h \ w	3	6	9	12	15	18	21	24	27	30	33	36	39
3	↑	→	→	→	→	→	→	→	→	→	↓	↓	↓
6	↑	→	↑	↑	↑	→	←	→	→	↓	↓	↓	
9	↑	↑	↑	↑	↑	←	←	←	←	↓	↓		
12	↑	↑	↑	↑	↑	←	←	←	←	↓	↓		
15	↑	↑	↑	←	←	←	←	←	←	↓			
18	↑	↑	←	←	←	←	←	←					
21	↑	↑	←	←	←	←	←						
24	↑	↑	←	←	←	←							
27	↑	↑	←	←	←								
30	↑	↑	←	←									
33	↑	↑	←										
36	↑	↑											
40	↑												

Air flow rate 0.35 vvm

h \ w	3	6	9	12	15	18	21	24	27	30	33	36	39
3	→	→	→	→	↑	→	→	→	→	→	↓	↓	↓
6	↑	→	↑	↑	↑	→	→	→	→	↓	↓	↓	
9	↑	↑	↑	↑	↑	↑	←	←	←	↓	↓		
12	↑	↑	↑	↑	↑	←	←	←	←	↓			
15	↑	↑	↑	↑	←	←	←	←	←				
18	↑	↑	↑	←	←	←	←	←					
21	↑	↑	↑	←	←	←	←						
24	↑	↑	↑	←	←	←							
27	↑	↑	↑	←	←								
30	↑	↑	←	←									
33	↑	↑	←										
36	↑	↑											
40	↑												

Air flow rate 0.40 vvm

Air flow rate 0.45 vvm

h \ w	3	6	9	12	15	18	21	24	27	30	33	36	39
3	↑	→	→	→	→	→	→	→	→	→	↓	↓	↓
6	↑	↑	↑	→	→	→	→	→	↓	↓	↓	↓	
9	↑	↑	↑	↑	←	←	→	↓	↓	↓	↓		
12	↑	↑	↑	↑	←	←	←	↓	↓	↓			
15	↑	↑	↑	←	←	←	←	↓	↓				
18	↑	↑	↑	←	←	←	←	↓					
21	↑	↑	↑	←	←	←	←						
24	↑	↑	↑	←	←	←							
27	↑	↑	↑	←	←								
30	↑	↑	↑	←									
33	↑	↑	↑										
36	↑	↑											
40	↑												

Air flow rate 0.50 vvm

h \ w	3	6	9	12	15	18	21	24	27	30	33	36	39
3	→	→	→	→	→	→	→	→	→	→	↓	↓	↓
6	↑	↑	→	→	→	→	→	→	↓	↓	↓	↓	
9	↑	↑	↑	←	←	←	→	←	↓	↓	↓		
12	↑	↑	↑	←	←	←	←	←	↓	↓			
15	↑	↑	↑	←	←	←	←	←	↓				
18	↑	↑	↑	←	←	←	←	←					
21	↑	↑	↑	←	←	←	←						
24	↑	↑	↑	←	←	←							
27	↑	↑	←	←	←								
30	↑	↑	←	←									
33	↑	↑	←										
36	↑	↑											
40	↑												

Air flow rate 0.55 vvm

Flow diagram of NB-C-ALC 45° h 50 cm

h \ w	3	6	9	12	15	18	21	24	27	30	33	36	39	42	45	48	50
3	→	→	↑	→	→	→	→	→	→	↓	↓	↓	↓	↓	↓	↓	↓
6	→	↑	↑	↑	↑	↑	←	←	←	↓	↓	↓	↓	↓	↓	↓	
9	↑	↑	↑	↑	↑	↑	←	←	←	↓	↓	↓	↓	↓	↓		
12	↑	↑	↑	←	↑	↑	←	←	←	↓	↓	↓	↓	↓			
15	↑	↑	←	←	↑	↑	←	←	←	↓	↓	↓	↓				
18	↑	↑	←	←	←	←	←	←	←	↓	↓	↓					
21	↑	↑	←	←	←	←	←	←	←	↓	↓						
24	↑	↑	←	←	←	←	←	←	←	↓							
27	↑	↑	←	←	←	←	←	←									
30	↑	↑	←	←	←	←	←										
33	↑	↑	←	←	←	←											
36	↑	↑	←	←													
39	↑	↑	←	←													
42	↑	↑	←														
45	↑	↑															
48	↑																
50	↑																

Air flow rate 0.04 vvm

h \ w	3	6	9	12	15	18	21	24	27	30	33	36	39	42	45	48	50
3	→	→	→	→	→	→	→	→	→	→	→	↓	↓	↓	↓	↓	↓
6	→	↑	↑	←	←	←	←	←	←	←	←	↓	↓	↓	↓	↓	
9	↑	↑	↑	←	←	←	←	←	←	←	←	↓	↓	↓	↓		
12	↑	↑	↑	←	←	←	←	←	←	←	←	↓	↓				
15	↑	↑	↑	←	←	←	←	←	←	←	←	↓	↓				
18	↑	↑	↑	←	←	←	←	←	←	←	←	↓					
21	↑	↑	↑	←	←	←	←	←	←	←							
24	↑	↑	←	←	←	←	←	←	←								
27	↑	↑	←	←	←	←	←	←									
30	↑	↑	←	←	←	←	←										
33	↑	↑	←	←	←	←											
36	↑	↑	←	←													
39	↑	↑	←	←													
42	↑	↑	←														
45	↑	↑															
48	↑																
50	↑																

Air flow rate 0.08 vvm

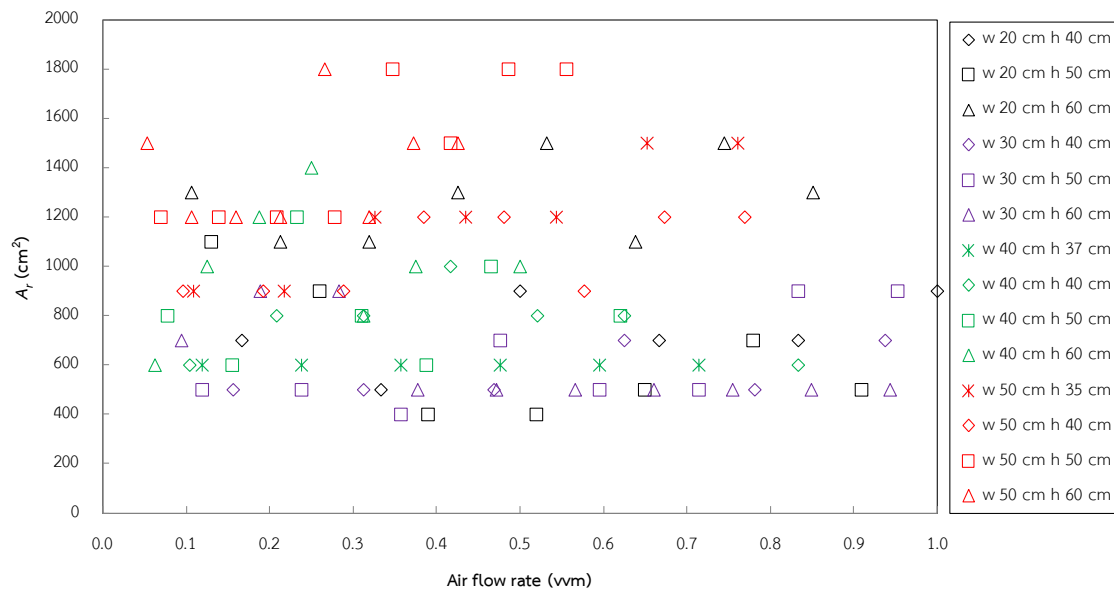
h \ w	3	6	9	12	15	18	21	24	27	30	33	36	39	42	45	48	50
3	→	→	↑	→	→	→	→	→	→	→	→	↓	↓	↓	↓	↓	↓
6	→	↑	↑	↑	←	←	←	←	←	←	←	↓	↓	↓	↓	↓	
9	↑	↑	↑	↑	←	←	←	←	←	←	←	↓	↓	↓	↓		
12	↑	↑	↑	←	←	←	←	←	←	←	←	↓	↓	↓			
15	↑	↑	↑	←	←	←	←	←	←	←	←	↓	↓	↓			
18	↑	↑	↑	←	←	←	←	←	←	←	←	↓	↓	↓			
21	↑	↑	↑	←	←	←	←	←	←	←	←	↓	↓				
24	↑	↑	↑	←	←	←	←	←	←								
27	↑	↑	←	←	←	←	←	←									
30	↑	↑	←	←	←	←	←										
33	↑	↑	←	←	←	←											
36	↑	↑	←	←													
39	↑	↑	←	←													
42	↑	↑	←														
45	↑	↑															
48	↑																
50	↑																

Air flow rate 0.12 vvm

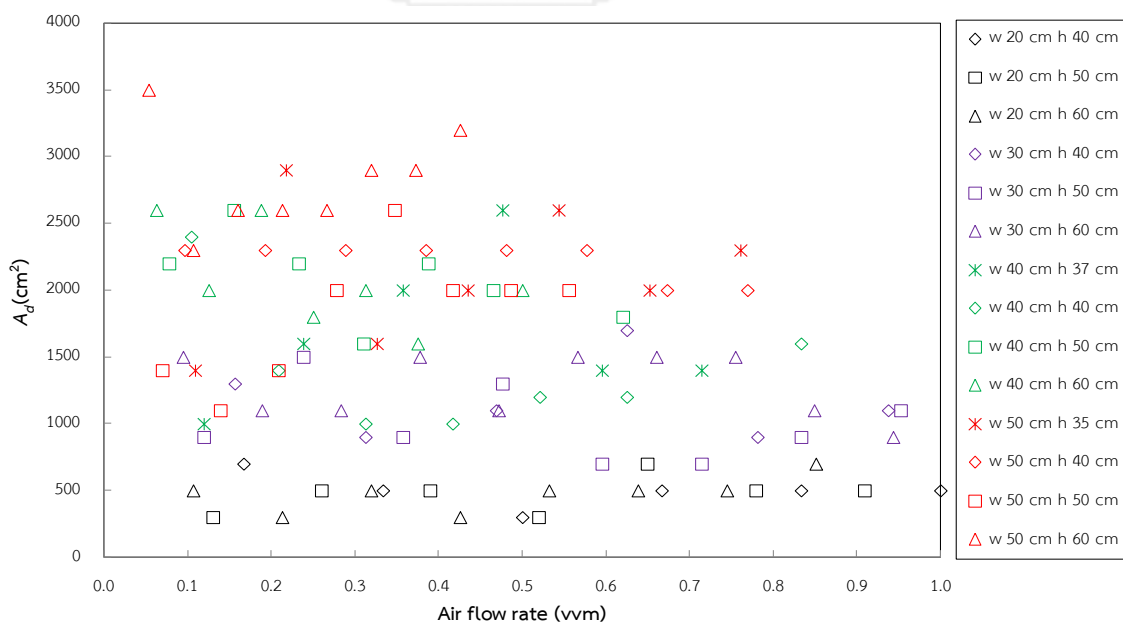
h \ w	3	6	9	12	15	18	21	24	27	30	33	36	39	42	45	48	50
3	→	→	↑	→	→	→	→	→	→	→	→	↓	↓	↓	↓	↓	↓
6	→	↑	↑	↑	←	←	←	←	←	←	←	↓	↓	↓	↓	↓	
9	↑	↑	↑	↑	←	←	←	←	←	←	←	↓	↓	↓	↓		
12	↑	↑	↑	↑	←	←	←	←	←	←	←	↓	↓	↓	↓		
15	↑	↑	↑	←	←	←	←	←	←	←	←	↓	↓	↓			
18	↑	↑	↑	←	←	←	←	←	←	←	←	↓	↓	↓			
21	↑	↑	↑	←	←	←	←	←	←	←	←	↓	↓				
24	↑	↑	↑	←	←	←	←	←	←	←	←	↓					
27	↑	↑	←	←	←	←	←	←									
30	↑	↑	←	←	←	←	←										
33	↑	↑	←	←	←	←											
36	↑	↑	←	←													
39	↑	↑	←	←													
42	↑	↑	←														
45	↑	↑															
48	↑																
50	↑																

Air flow rate 0.16 vvm

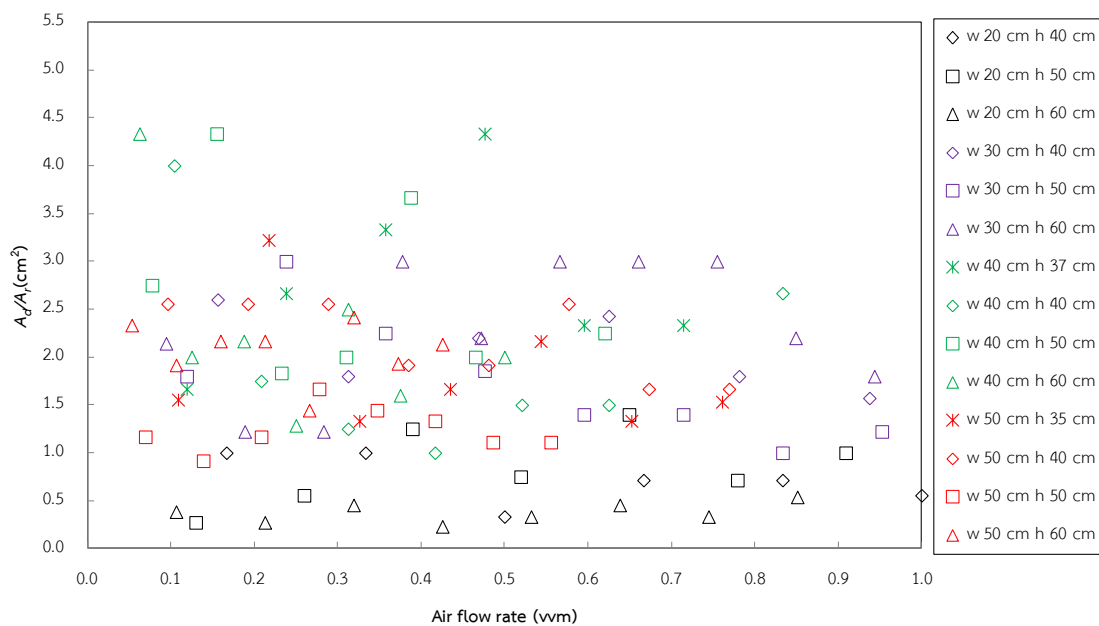
Appendix B



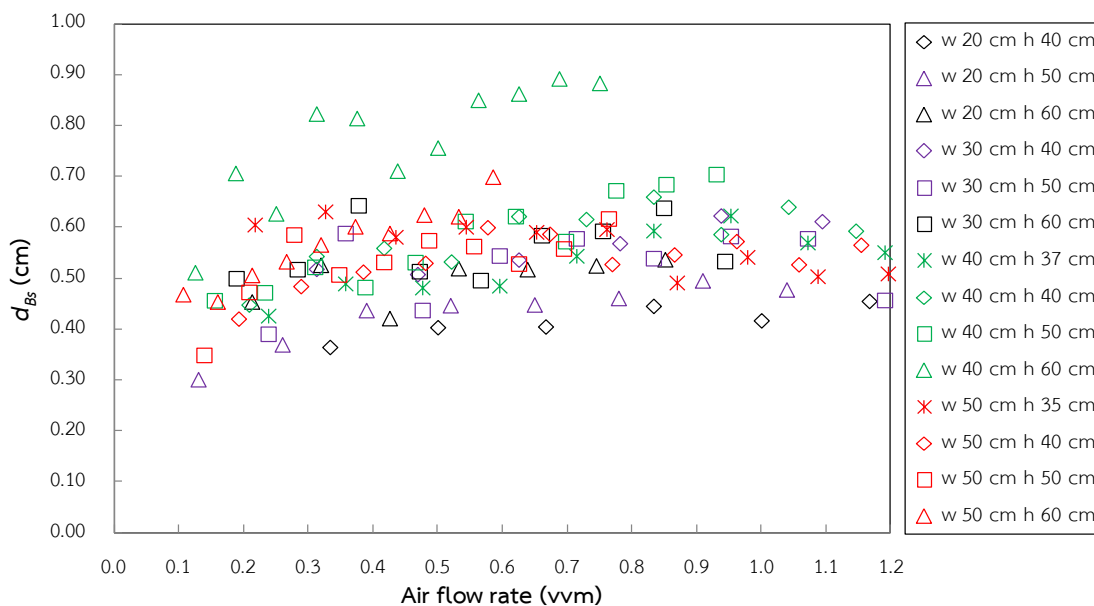
B-4.1 Area of riser in NB-FP-ALCs with different widths and unaerated liquid heights



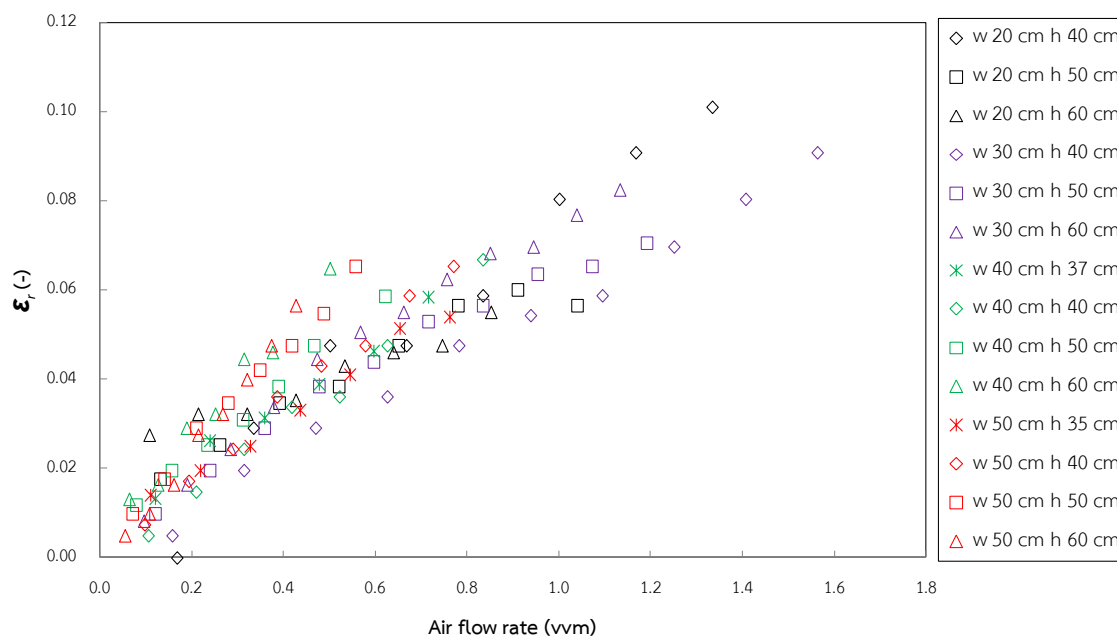
B-4.2 Area of downcomer in NB-FP-ALCs with different widths and unaerated liquid heights



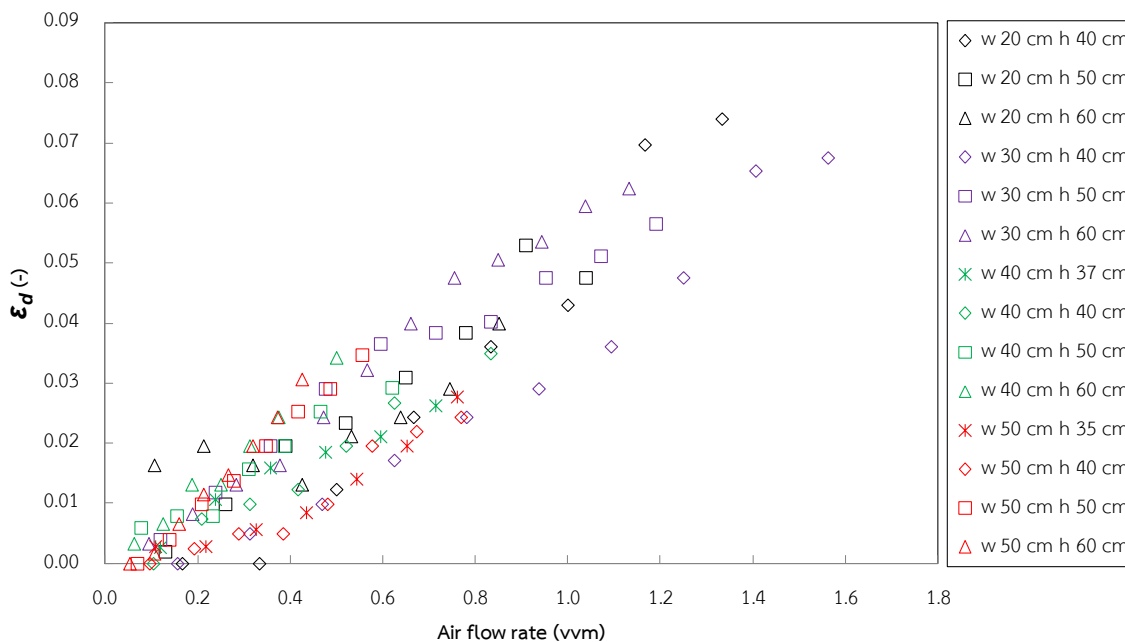
B-4.3 Downcomer to riser cross sectional area ratios in NB-FP-ALCs with different widths and unaerated liquid heights



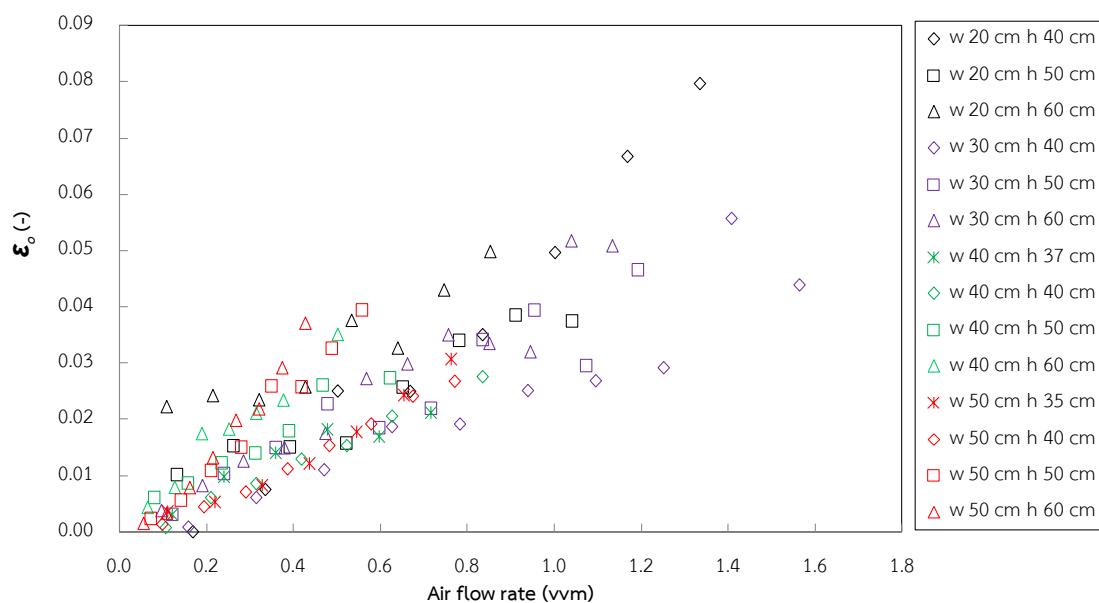
B-4.4 Average bubble size diameter (d_{BS}) in NB-FP-ALCs with different widths and unaerated liquid heights



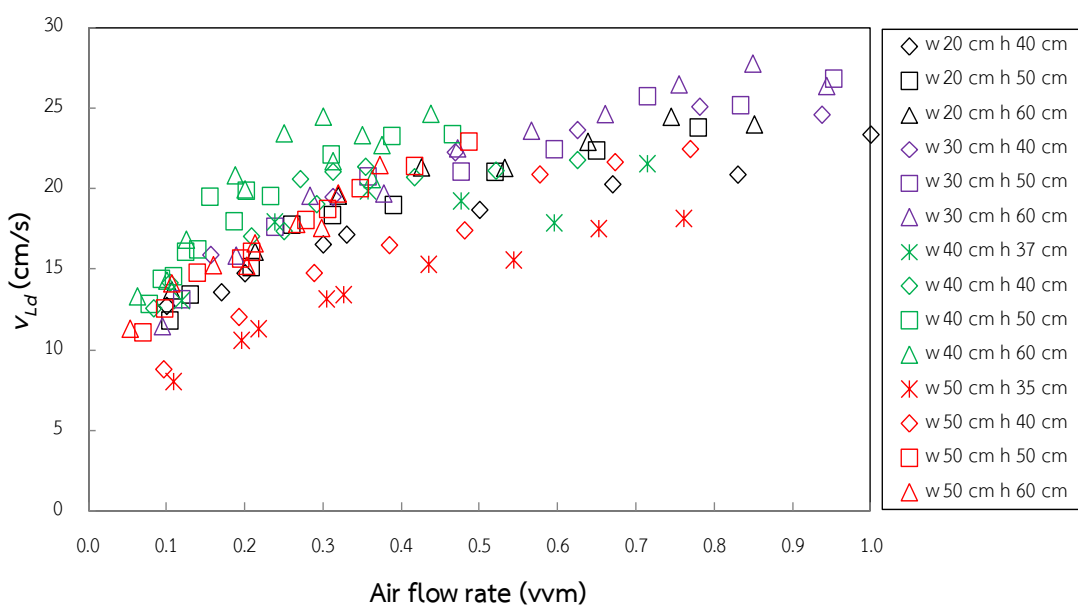
B-4.5 Gas-holdup in riser of NB-FP-ALCs with different widths and unaerated liquid heights



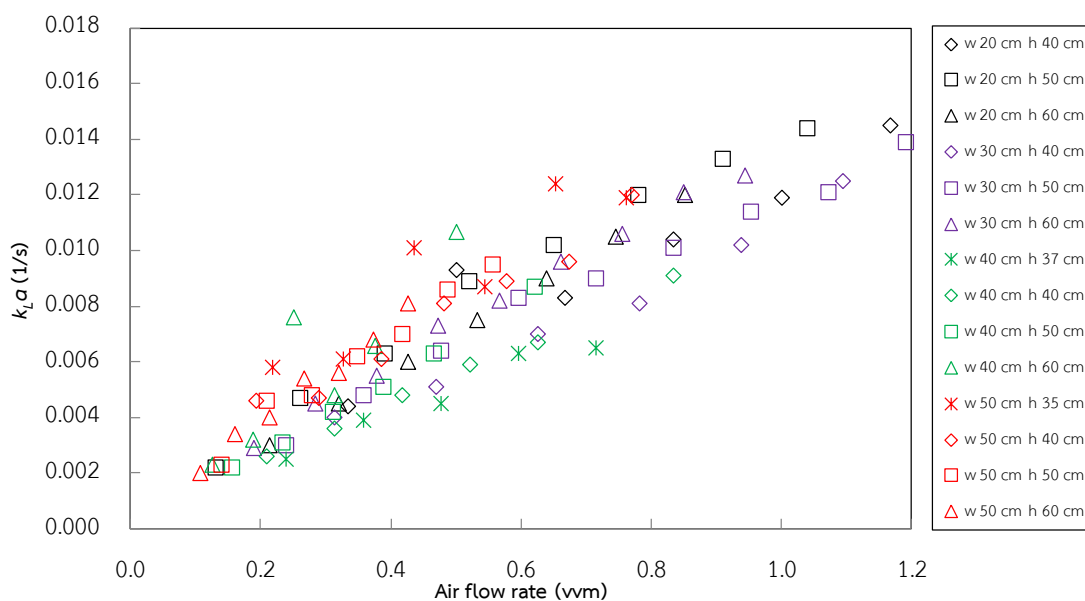
B-4.6 Gas-holdup in downcomer of NB-FP-ALCs with different widths and unaerated liquid heights



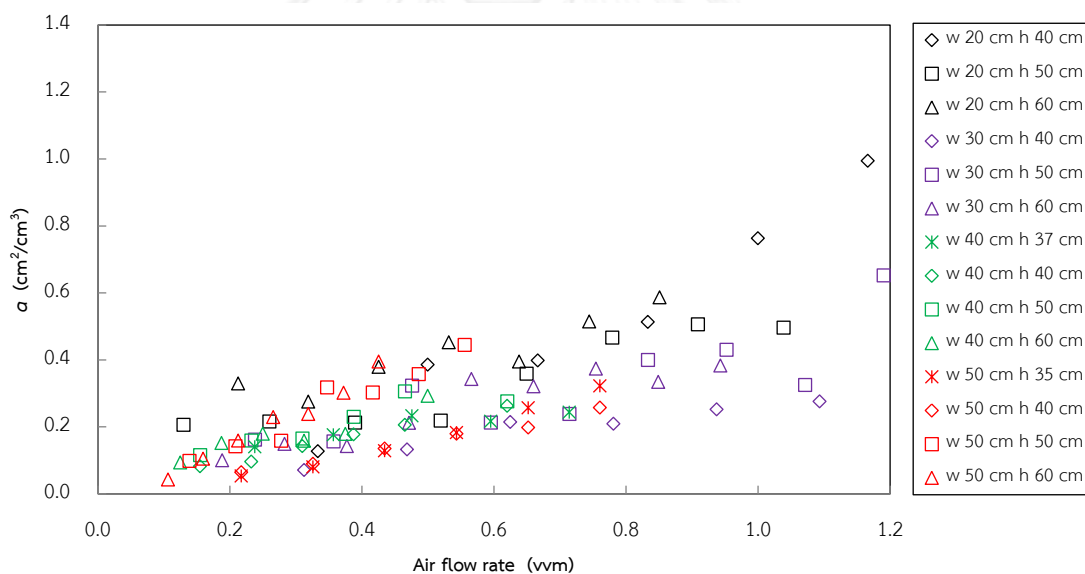
B-4.7 Overall gas holdup in NB-FP-ALCs with different widths and unaerated liquid heights



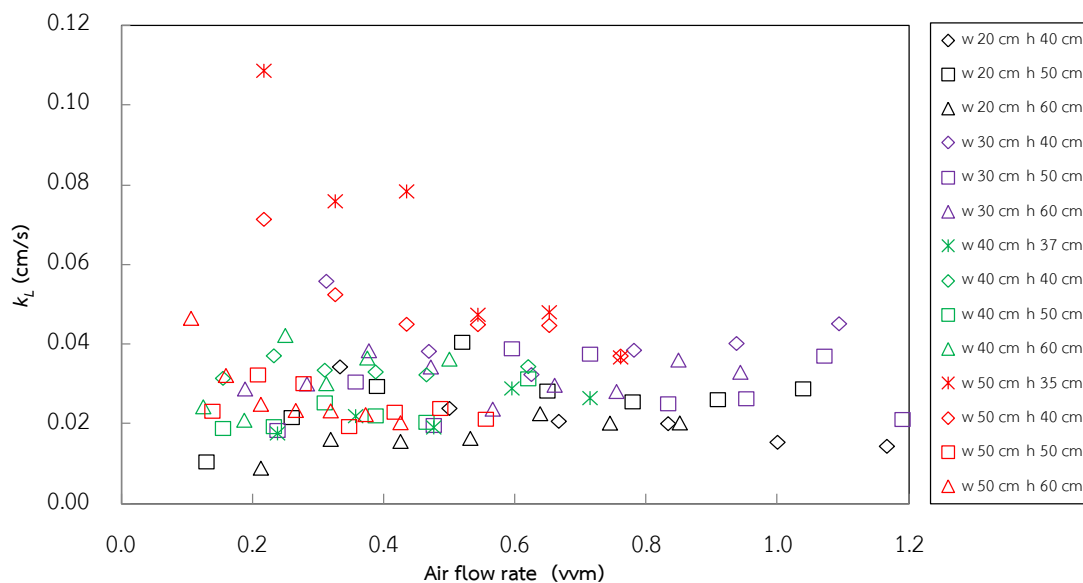
B-4.8 Downcomer liquid velocity in NB-FP-ALCs with different widths and unaerated liquid heights



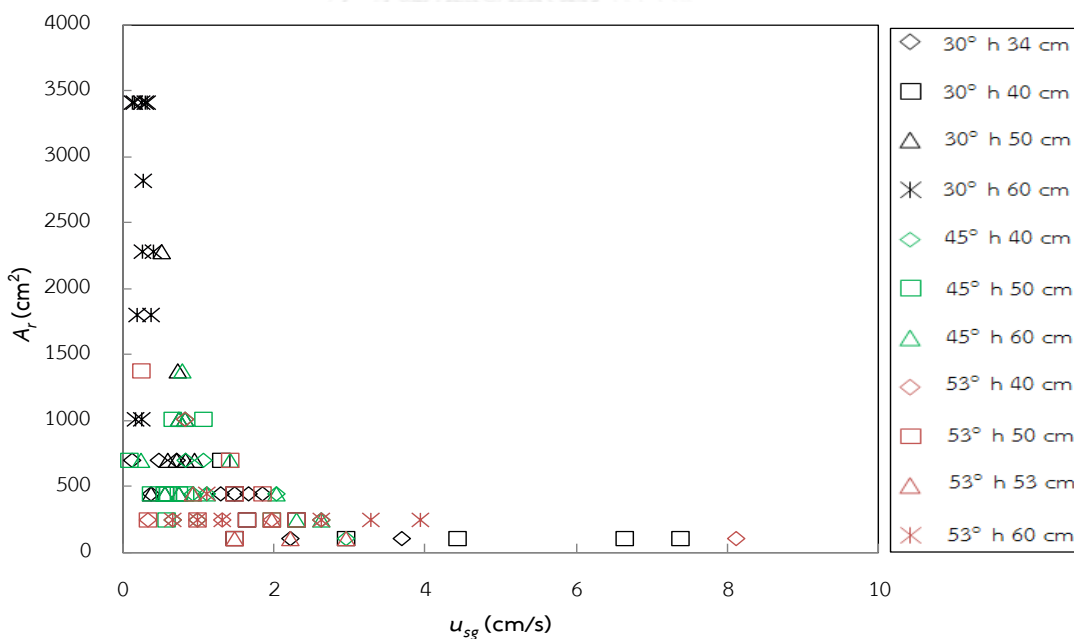
B-4.9 $k_L a$ in NB-FP-ALCs with different widths and unaerated liquid heights



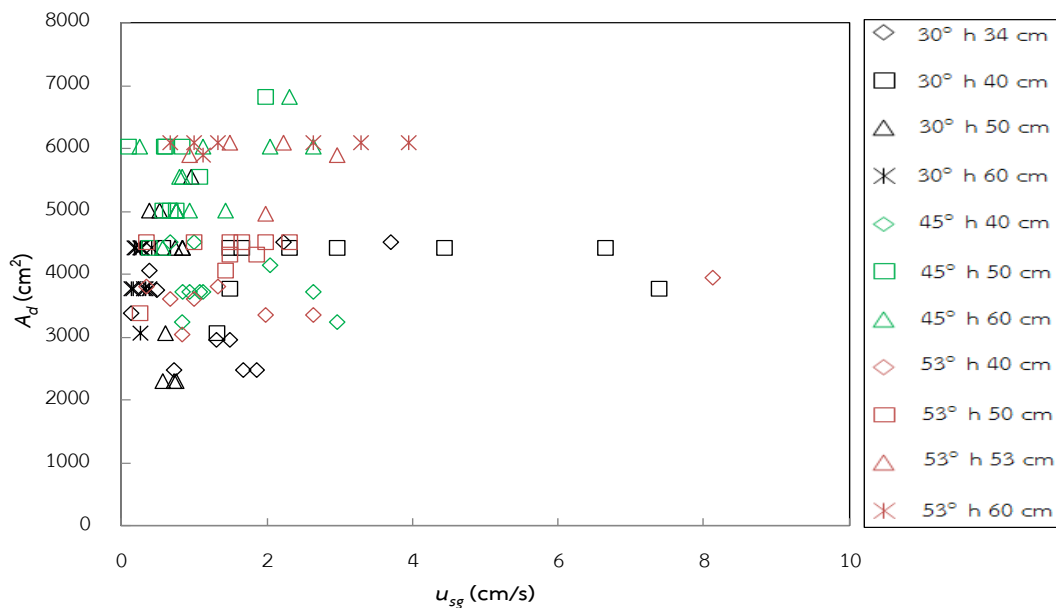
B-4.10 Specific interfacial area (a) in NB-FP-ALCs with different widths and unaerated liquid heights



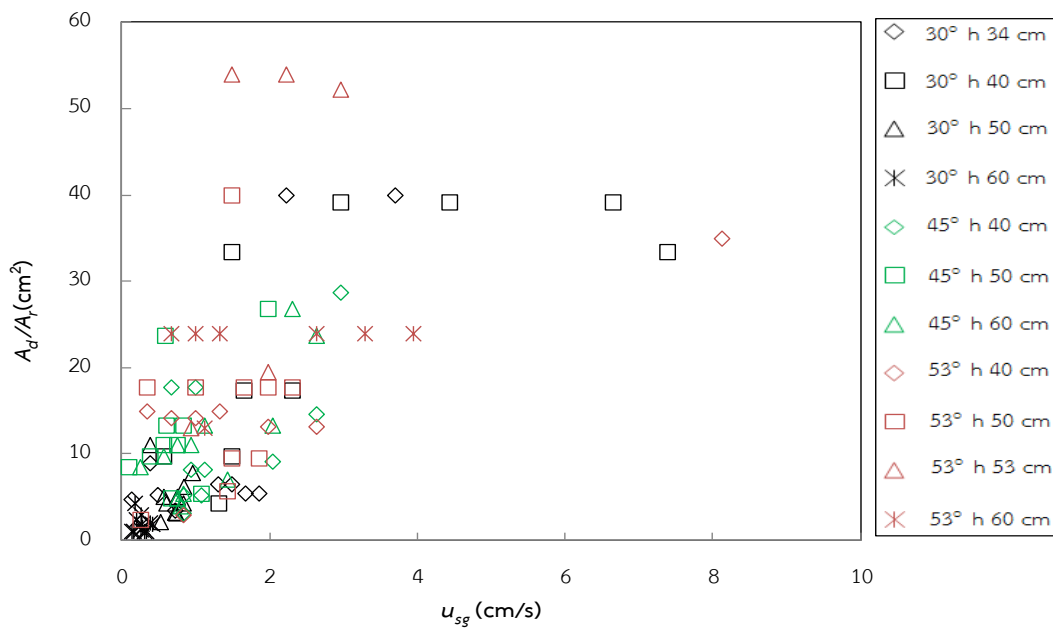
B-4.11 Overall gas-liquid mass transfer coefficient (k_L) with different widths of contactor and un-aerated liquid heights in NB-FP-ALCs



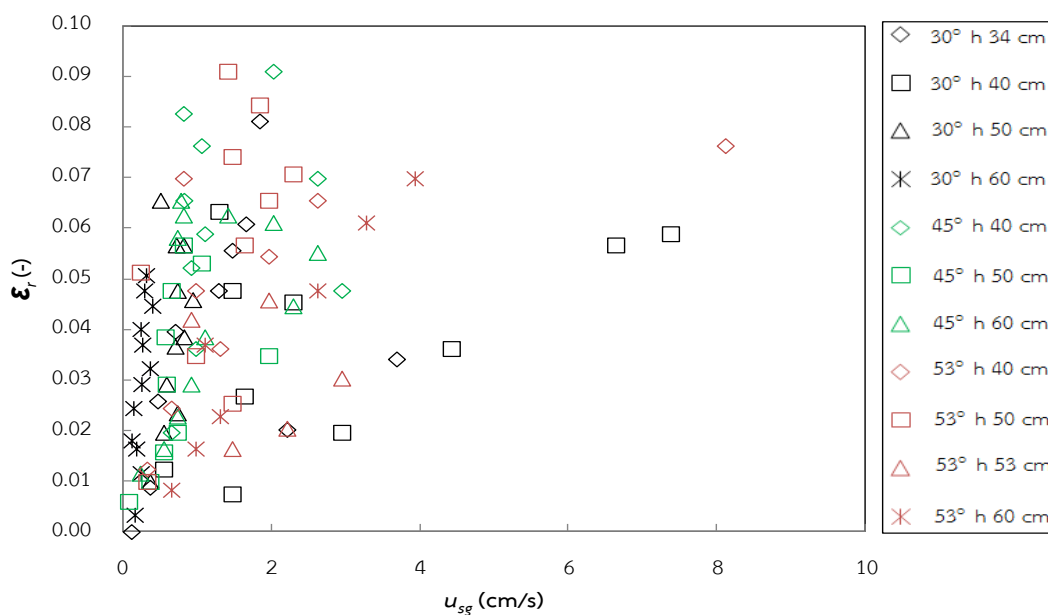
B-4.12 Area of riser in NB-C-ALCs with different the angles of the cone bottom and un-aerated liquid heights



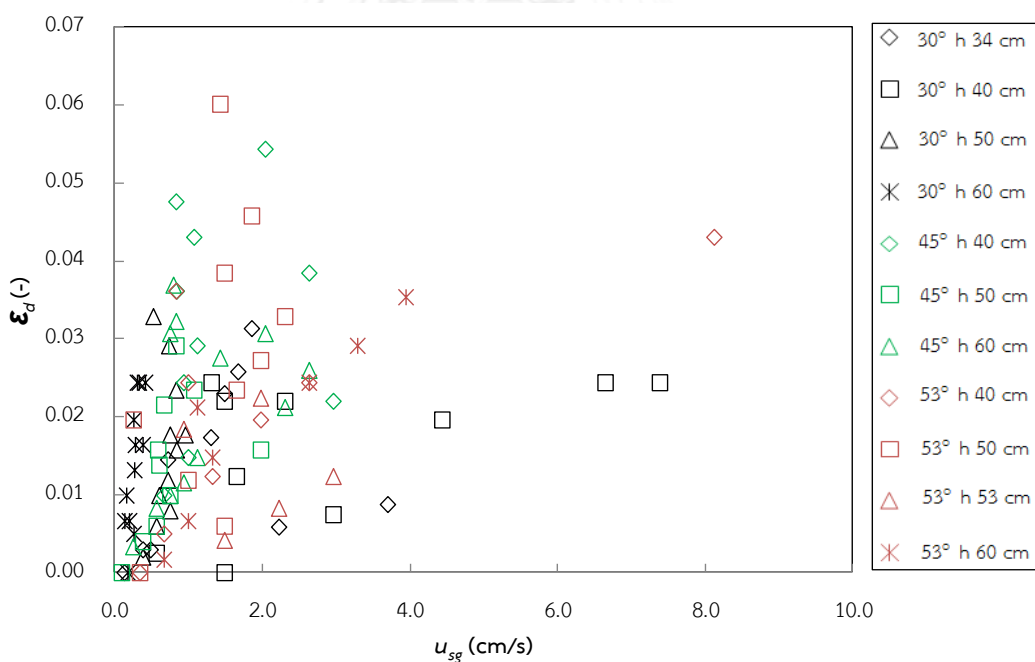
B-4.13 Area of downcomer in NB-C-ALCs with different the angles of the cone bottom and unaerated liquid heights



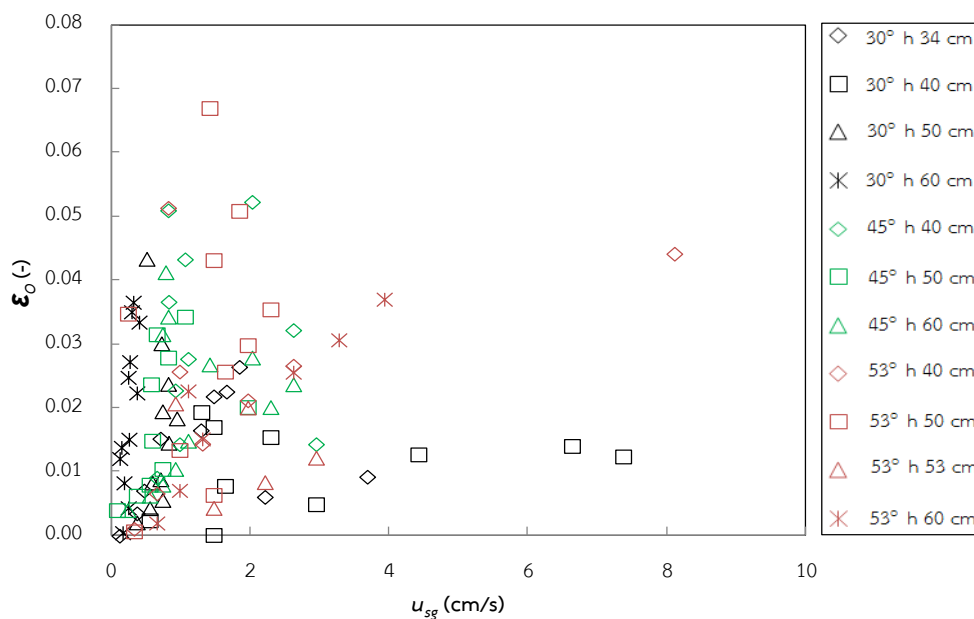
B-4.14 A_d/A_r ratio in NB-C-ALCs with different the angles of the cone bottom and unaerated liquid heights



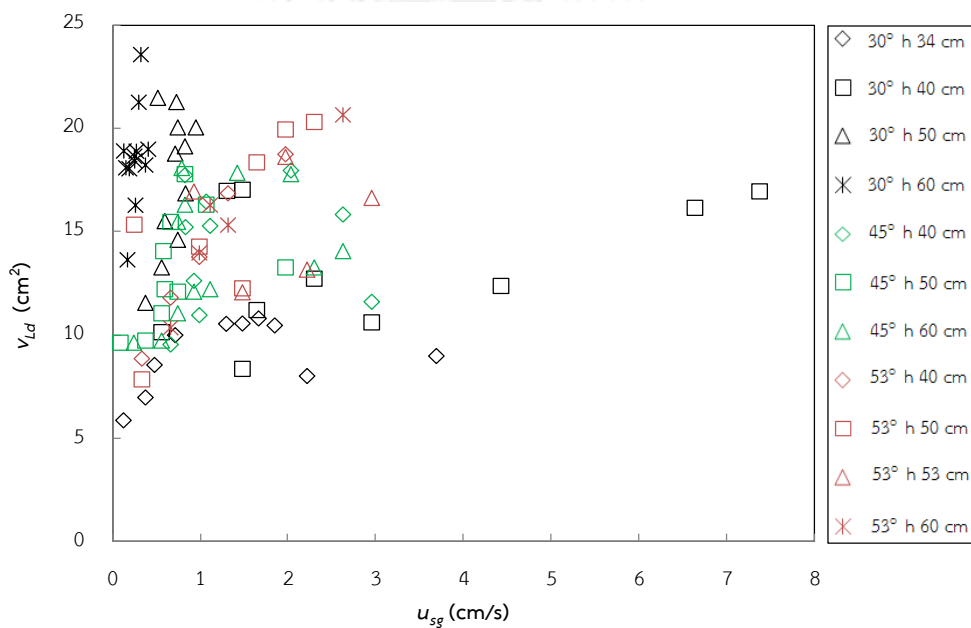
B-4.15 Riser gas-holdup in NB-C-ALCs with different the angles of the cone bottom and unaerated liquid heights



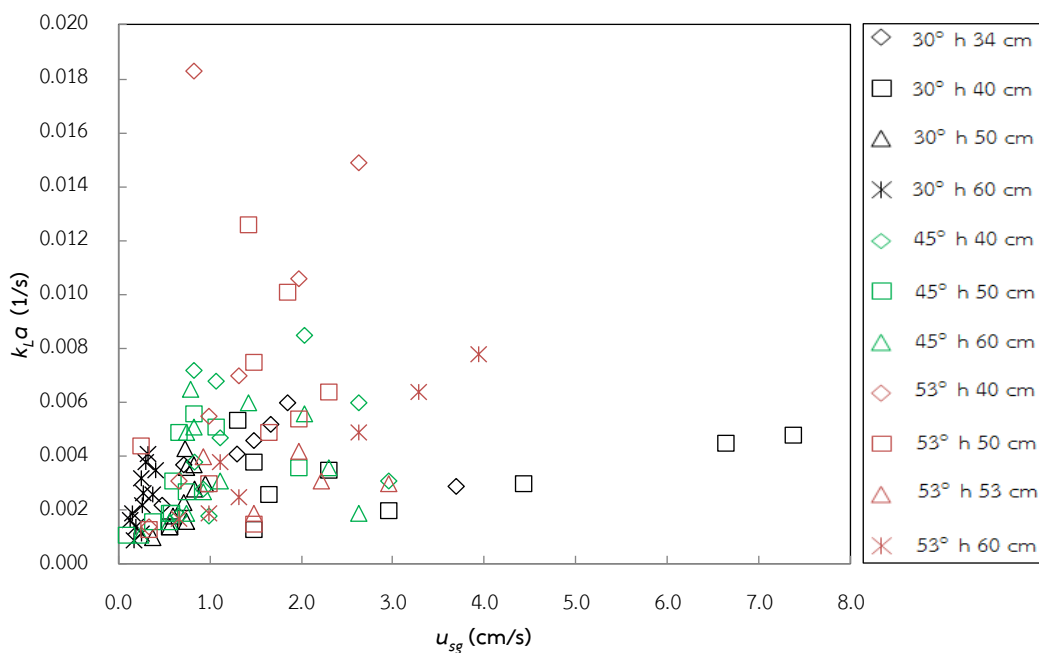
B-4.16 Downcomer gas-holdup in NB-C-ALCs with different the angles of the cone bottom and unaerated liquid heights



B-4.17 Overall gas holdup in NB-C-ALCs with different the angles of the cone bottom and un-aerated liquid heights

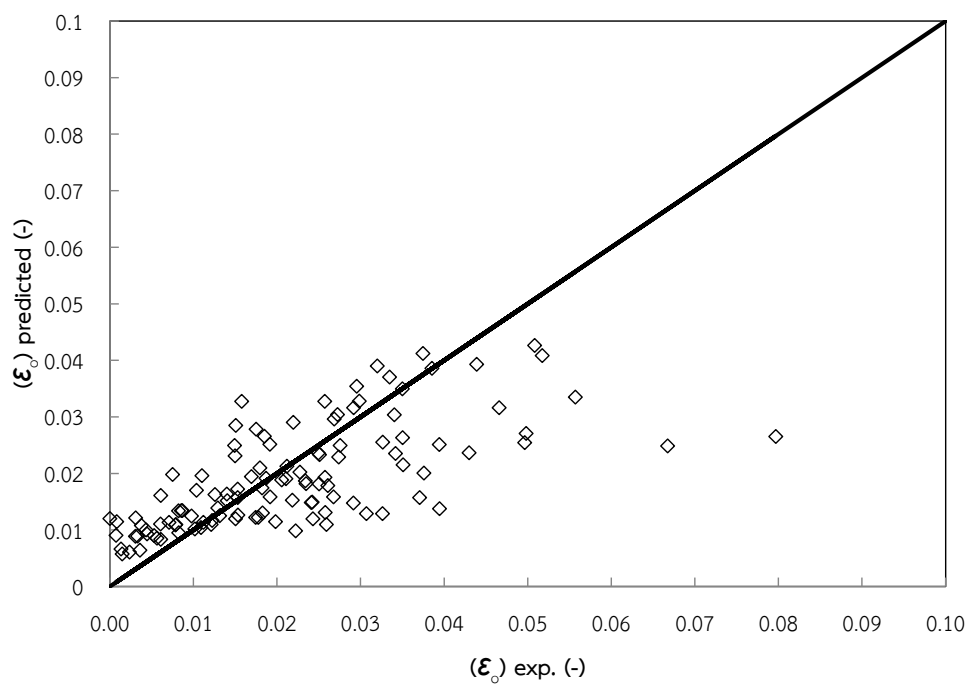


B-4.18 Downcomer liquid velocity in NB-C-ALCs with different the angles of the cone bottom and un-aerated liquid heights

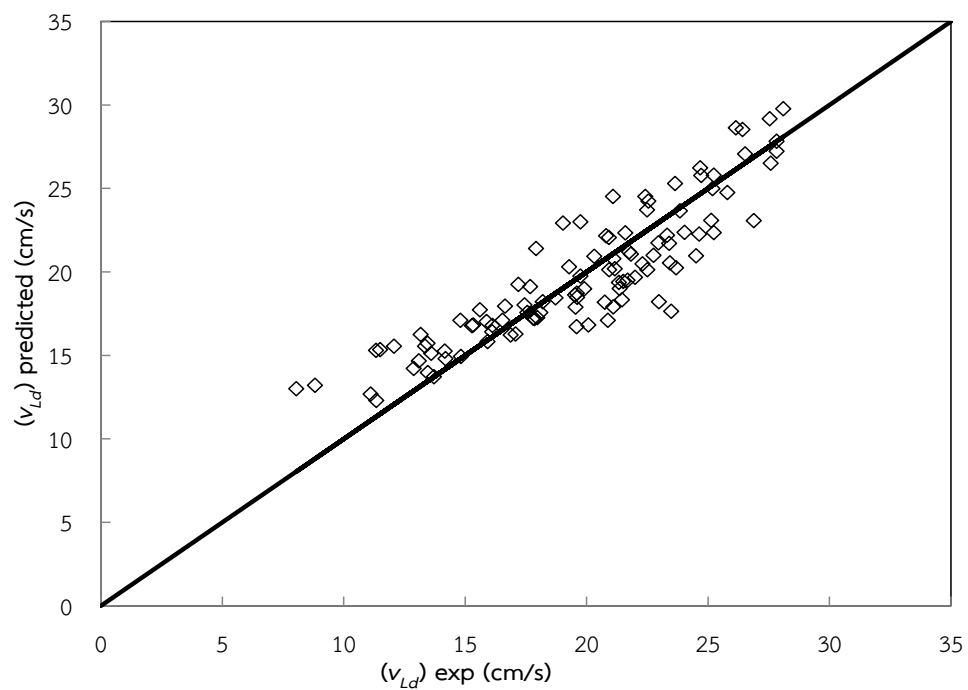


B-4.19 $k_L a$ in NB-C-ALCs with different the angles of the cone bottom and unaerated liquid heights

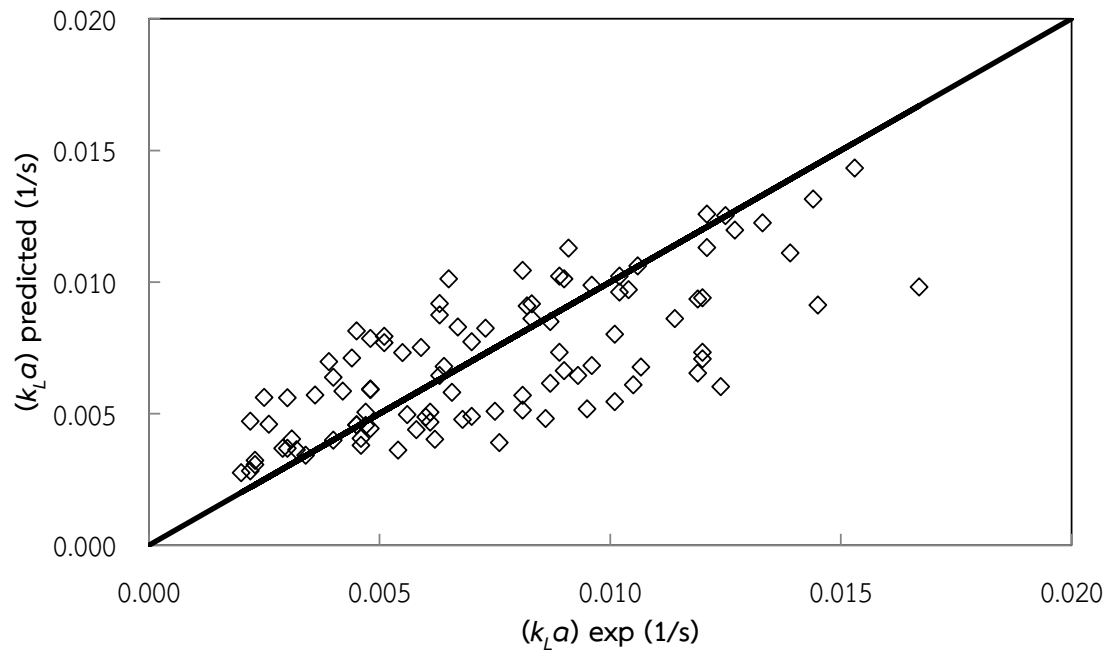
Appendix C



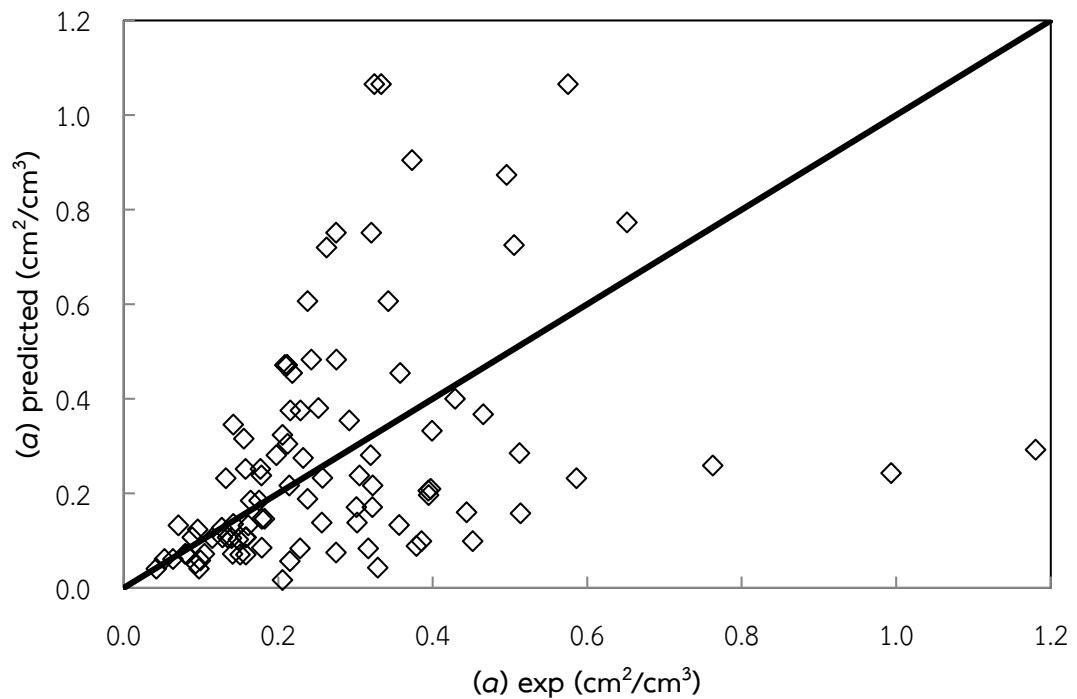
C- 1 Comparison of overall gas holdup of NB-FP-ALCs estimated by Eq. 4.10 with values observed in this work



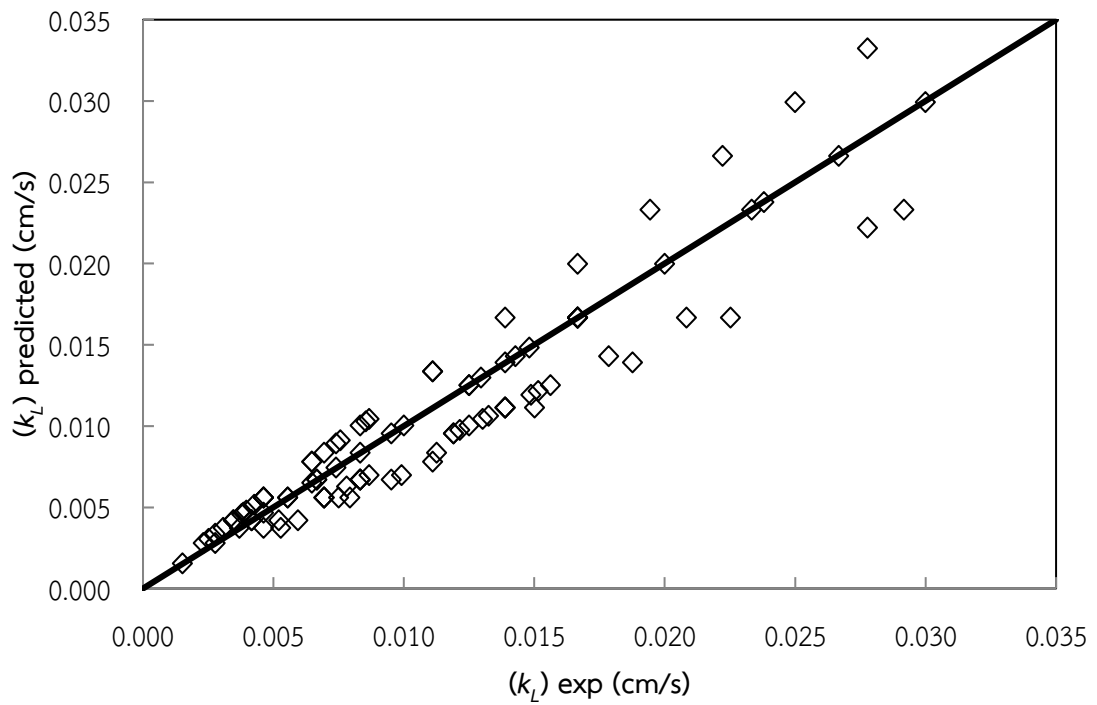
C- 2 Comparison of downcomer liquid velocity of NB-FP-ALCs estimated by Eq. 4.11 with values observed in this work



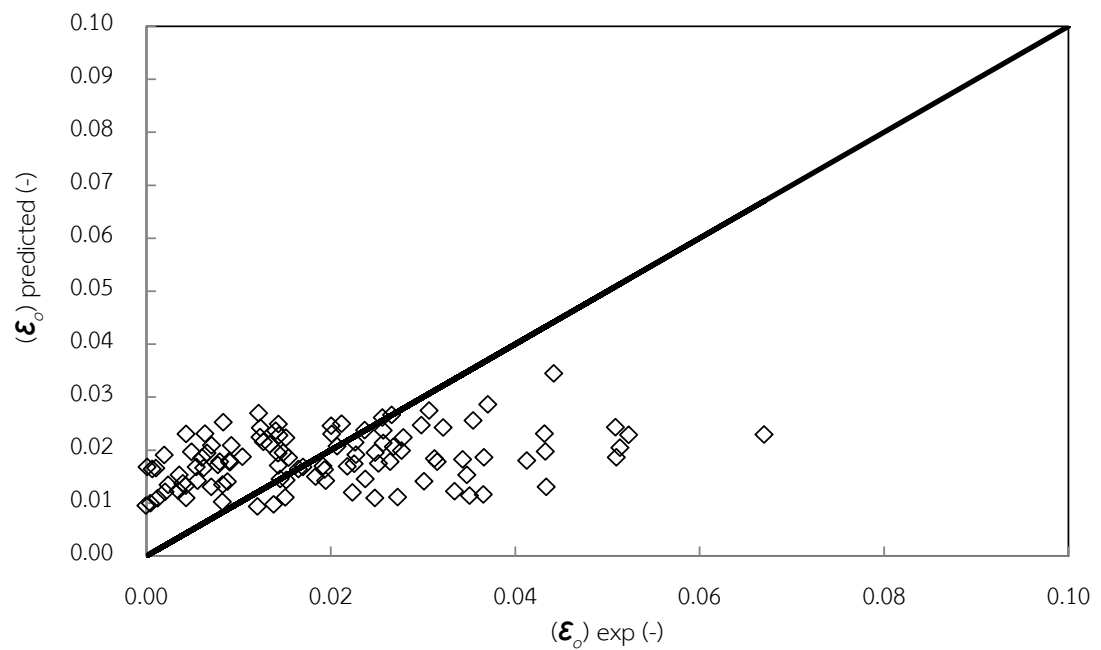
C- 3 Comparison of $k_L a$ of NB-FP-ALCs estimated by Eq. 4.12 with values observed in this work



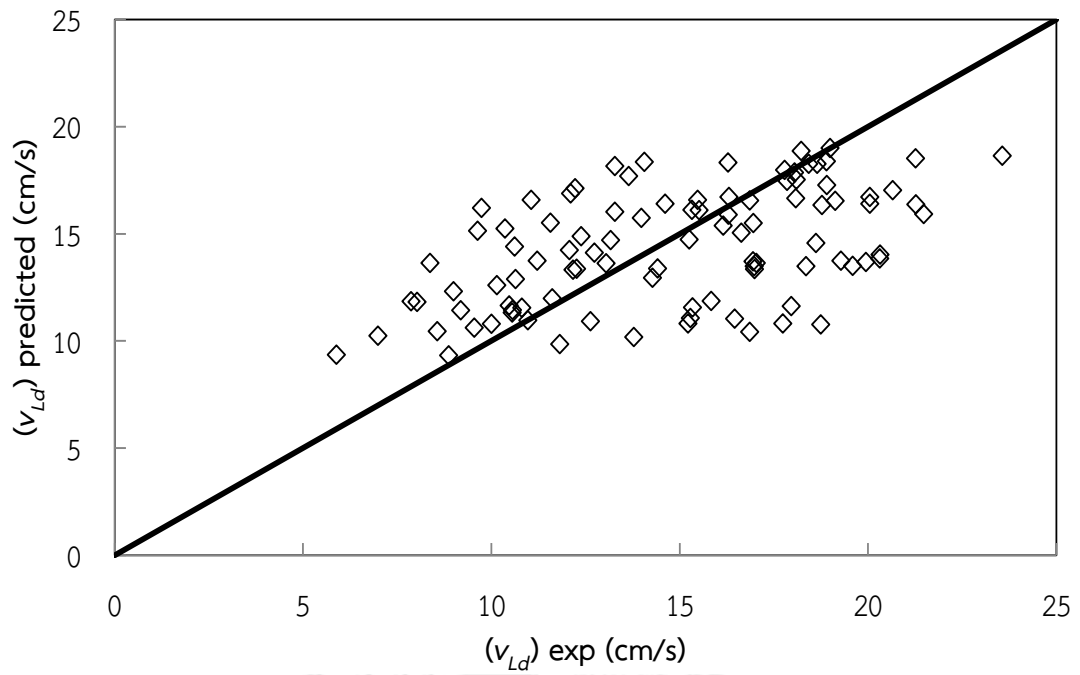
C- 4 Comparison of specific gas-liquid interfacial area of NB-FP-ALCs estimated by Eq. 4.13 with values observed in this work



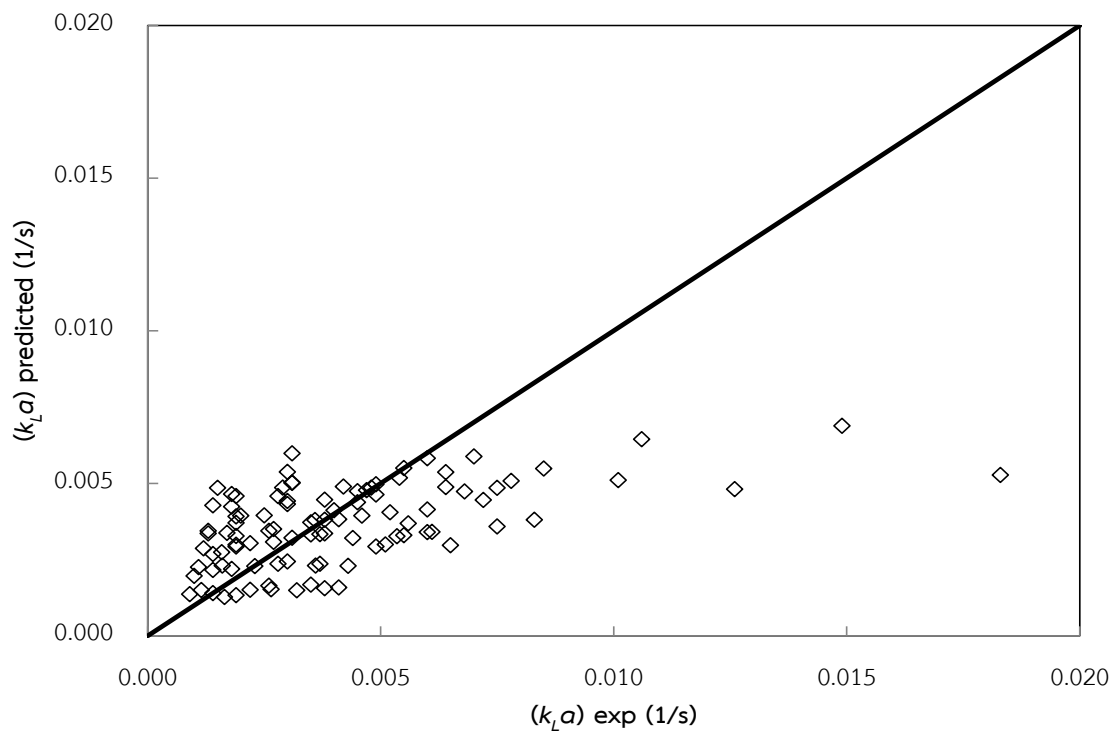
C- 5 Comparison of liquid phase mass transfer coefficient of NB-FP-ALCs estimated by Eq. 4.14 with values observed in this work



C- 6 Comparison of overall gas holdup of NB-C-ALCs estimated by Eq. 4.15 with values observed in this work



C- 7 Comparison of downcomer liquid velocity of NB-C-ALCs estimated by Eq. 4.16 with values observed in this work



C- 8 Comparison of $k_L a$ of NB-C-ALCs estimated by Eq. 4.17 with values observed in this work

VITA

Miss Praewpakun Sintharm was born on 2nd November, 1988 in Ayutthaya. She graduated her higher secondary school from Laboratory School of Phranakhon Si Ayutthaya Rajabhat University in March, 2006. Bachelor's degree, she studied in the major of Chemical Engineering in Faculty of Engineering at King Mongkut's Institute of Technology Ladkrabang. She continued her study for Master's degree in Chemical Engineering at Chulalongkorn University. She contributed in the Safety and Environment Engineering research group and graduated her Master's degree in April, 2014.





จุฬาลงกรณ์มหาวิทยาลัย
CHULALONGKORN UNIVERSITY